PhD

PROGRAM IN TRANSLATIONAL
AND MOLECULAR MEDICINE

DIMET

UNIVERSITY OF MILANO - BICOCCA
SCHOOL OF MEDICINE AND FACULTY OF SCIENCE

# Tumor infiltrating myeloid cells: modulators of the tumor microenvironment and novel therapeutic targets

Coordinator: Prof. Andrea Biondi
Tutor: Prof. Giuliana Ferrari
Co-Tutor: Prof. Luigi Naldini

Dr. Erika Zonari
Matr. No. 033032

XXIII CYCLE
ACADEMIC YEAR
2010-2011

The research presented in this thesis was performed at the San Raffaele Telethon Institute for Gene therapy (HSR-TIGET), Department of Regenerative Medicine, Stem Cells and Gene Therapy, San Raffaele Scientific Institute, in the laboratory directed by Prof. Luigi Naldini and with the supervision of Dr. Bernhard Gentner and Dr. Roberta Mazzieri.

*A Sofia*

# TABLE OF CONTENTS

# Abbreviations

| | |
|---|---|
| ADAMS | A disintegrin and metalloproteinase |
| AID | Activation Induced cytidine Diamine |
| AML | Acute Myeloid Leukemia |
| ANG1 | Angiopoietin-1 |
| ANG2 | Angiopoietin-2 |
| APC | Antigen Presenting Cell |
| BIC | B-cell Integration Cluster |
| BM | Bone Marrow |
| BMDC | Bone Marrow Dendritic Cell |
| C/EBPβ | CCAAT/Enhancer-Binding Protein-β |
| CCL | CC chemokine Ligand |
| CCR | CC chemokine Receptor |
| CSF-1 | Colony-Stimulating Factor-1 |
| CSF-1R | Colony-Stimulating Factor-1 Receptor |
| CXCL | Chemokine (C-X-C motif) Ligand |
| DC | Dendritic Cell |
| DGCR8 | DiGeorge syndrome critical region gene 8 |
| dsRNA | double strand RNA |
| EC | Endothelial Cell |
| ECM | Extracellular Matrix |
| EGF | Endhotelial Growth Factor |
| ErbB2/Neu | v-erb-b2 erythroblastic leukemia viral oncogene homolog 2, neuro/glioblastoma |
| FGF | Fibroblast Growth Factor |

| | |
|---|---|
| FoxP3 | Forkhead box P3 |
| GFI1 | Growth Factor Independent 1 |
| GFP | Green Fluorescent Protein |
| HC | Hematopoietic Cell |
| HSC | Hematopoietic Stem Cell |
| IFN | Inteferon |
| IgG | Immunoglobulin |
| IL | Interleukin |
| IL-R | Interleukin Receptor |
| Let-7a | Lethal-7 |
| LLC | Lewis Lung Carcinoma |
| LPS | Lypopolisaccaryde |
| MEF2C | Myocyte-specific Enhancer Factor 2C |
| MHC II | Major Histocompatibility Complex Class II |
| miRNA | microRNA |
| MMP | Matrix Metalloproteinase |
| MMTV/PyMT | Mouse Mammary Tumor Virus/ Polyoma middle T antigen |
| MRC1 | Mannose Receptor, C thype 1 |
| mRNA | messenger RNA |
| ncRNA | non coding RNA |
| NFIA | Nuclear Factor I-A |
| NF-kB | Nuclear Factor-kB |
| NK | Natural Killer |
| NOS2 | Nitric Oxyde Synthase-2 |
| OFP | Orange Fluoresecent Protein |

| | |
|---|---|
| PAMP | Phatogen-Associated Molecular Pattern |
| PDGF | Platelet-Derivated Growth Factor |
| PGE2 | Prostaglandin E2 |
| PI3K | Phosphoinositide 3-Kinase |
| PlGF | Placental Growth Factor |
| Pre-miRNA | Precursor-miRNA |
| Pri-miRNA | Primary-miRNA |
| PTGS2/COX2 | Prostaglandin-endoperoxide synthase2/ Cyclooxigenase-2 |
| RISC | RNA-Induced Silencing Complex |
| RNAPII | DNA-dependent RNA Polymerase II |
| ROS | Reactive Oxygen Species |
| RUNX1 | Runt-related transcrition factor 1 |
| SDF1 | Stromal-cell Derived Factor-1, |
| SFFV | Spleen Focus-Forming Virus |
| SHIP1 | Src homology 2 (SH2) domain-containing inositol-5′-phosphatase 1 |
| SOCS1 | Soppressor of Cytokines Signaling-1 |
| SV40 | Simian Virus 40 |
| TAM | Tumor Assocyated Macrophages |
| TEM | Tie2 Expressing Monocytes |
| TF | Transcription Factor |
| TGF | Tumor Growth Factor |
| TLR | Toll-Like Receptor |
| TNF | Tumor Necrosis Factor |
| TRBP | TAR (HIV) RNA binding protein 2 |

| | |
|---|---|
| Treg | Regulatory T cell |
| UTR | Untraslated Region |
| VEGF | Vaacular Endothelial Growth Factor |

# CHAPTER 1.

# General Introduction

## The Hallmarks of Cancer

Several lines of evidence indicate that tumorigenesis in humans is a multistep process and that these steps reflect genetic alterations that drive the progressive transformation of normal human cells into malignant ones. Observations in human cancers and animal models argue that tumor development follows a process formally analogous to Darwinian evolution, in which a succession of genetic changes, each conferring one or another type of growth advantage, leads to cumulative selection of genetic alterations and the progressive conversion of normal human cells into cancer cells. The vast catalog of cancer cell genotypes is believed to be a manifestation at least of six essential alterations in cell physiology that collectively dictate malignant growth (Figure 1). These six capabilities are shared in common by most and perhaps all types of human tumors (Hanahan and Weinberg, 2000). Whereas acquired capabilities such as evading apoptosis, insensitivity to anti-growth signals and limitless replicative potential are cell autonomous (Hanahan and Weinberg, 2000), the remaining three, i.e. self-sufficiency in growth signals, tissue invasion and metastasis as well as sustained angiogenesis can receive a variable contribution from the microenvironment. More recently, inflammation has been proposed to represent a 7th hallmark of cancer (Colotta et al., 2009).

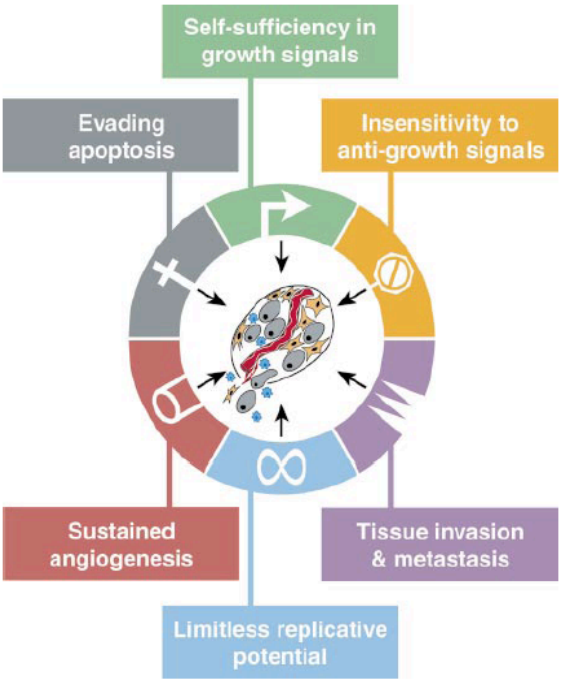


***Figure 1. The Hallmarks of Cancer***.
*(Adapted from Hanahan and Weinberg 2000).*

*Enabling Characteristics and Emerging Hallmarks*

The hallmarks of cancer are defined as acquired functional capabilities that allow cancer cells to survive, proliferate, and disseminate; these functions are acquired in different tumor types by distinct mechanisms and at various times during the course of multistep tumorigenesis. Their acquisition is made possible by two enabling characteristics. Most obvious is the development of genomic instability in cancer

cells, which generates random mutations including chromosomal rearrangements driving a process of clonal selection. A second enabling characteristic involves the inflammatory state of premalignant lesions that is driven by cells of the immune system, some of which serve to promote tumor progression by supplying bioactive molecules to the tumor microenvironment, including growth factors, survival and proangiogenic factors (DeNardo et al., 2010; Grivennikov et al., 2010; Qian and Pollard, 2010). Inflammatory cells can also release reactive oxygen species (ROS), which are actively mutagenic for close cancer cells, accelerating their genetic evolution toward states of malignancy (Grivennikov et al., 2010). Two other distinctive features of cancer cells have been proposed to be functionally important for the development of cancer and might therefore be added to the list of core hallmarks (Colotta et al., 2009; Luo et al., 2009; Negrini et al., 2010). The first involves reprogramming of cellular energy metabolism in order to support continuous cell growth and proliferation. The second involves evasion of cancer cells from the surveillance of immune cells. Thus, the immune cells that may exert a dual role in cancer, as they can either antagonize or enhance tumor development and progression (Figure 2).

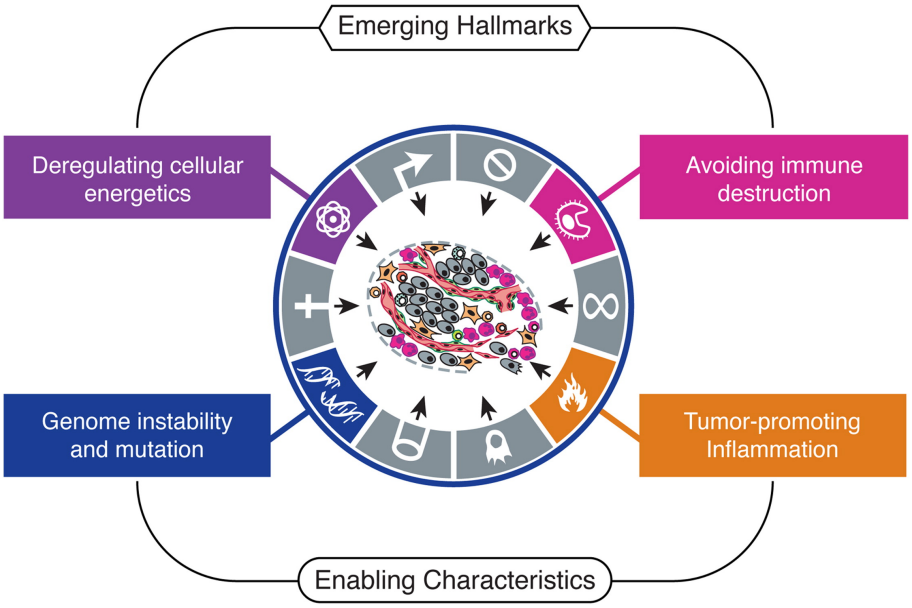


***Figure 2. Emerging Hallmarks and Enabling Characteristics.*** *Two additional hallmarks of cancer are involved in the pathogenesis of some cancers. One involves the capability to modify, or reprogram, cellular metabolism in order to most effectively support neoplastic proliferation. The second allows cancer cells to evade immunological destruction, in particularly by T and B-lymphocytes, macrophages, and natural killer cells. Because neither capability is yet generalized and fully validated, they are labeled as emerging hallmarks. Additionally, two consequential characteristics of neoplasia facilitate acquisition of both core and emerging hallmarks. Genomic instability and thus mutability endow cancer cells with genetic alterations that drive tumor progression. Inflammation by innate immune cells designed to fight infections and heal wounds can instead result in*

*their inadvertent support of multiple hallmark capabilities, thereby manifesting the now widely appreciated tumor-promoting consequences of inflammatory responses (from Hanahan and Weinberg 2011).*

**Inflammation and cancer**

Back in 1863, Rudolph Virchow documented the association between the *lymphoreticular infiltrate* present in chronically inflamed tissues and the site of origin of human cancer (Plytycz and Seljelid, 2003). Such an observation was revisited in recent years with the now popular concept that inflammation and cancer are causally linked (Balkwill and Mantovani, 2001). Indeed, when tissues are chronically injured or exposed to irritants, damaged cells are removed by induction of cell-death pathways while cell proliferation is enhanced to facilitate tissue regeneration (Vakkila and Lotze, 2004). These processes are often associated with, or even promoted by, the recruitment of a variety of leukocytes. Whereas infiltrating leukocytes may represent an attempt to remove the damaging/irritating agent and re-establish tissue homeostasis, they also generate an "inflammatory microenvironment" that can trigger tumorigenesis. Leukocytes, such as macrophages and granulocytes, can induce DNA damage in proliferating cells, through their generation of reactive oxygen and nitrogen species that are produced normally by these cells to fight infection (Maeda and Akaike, 1998). When inflammation persists over time (like "chronic inflammation"), sustained cycles of cell death

and proliferation in environments rich in leukocytes and their bioactive, mutagenic products may accelerate the accumulation of genetic and epigenetic alterations that affect the expression or function of proto-oncogenes and tumor suppressor genes in somatic cells (Hussain et al., 2003).

It has been estimated that more than 15% of malignancies worldwide can be attributed to chronic inflammatory diseases (Coussens and Werb, 2002; Finch and Crimmins, 2004; Mantovani et al., 2008). In established tumors, leukocytes represent a large proportion of the tumor-associated stromal cells (de Visser and Coussens, 2006). These include both innate and adaptive immune cells. Subsets of these cells, such as $CD8^+$ cytotoxic T-cells and natural killer (NK) cells, may play roles in restricting tumor development and progressive growth (de Visser and Coussens, 2006). On the other hand, myeloid cells, such as granulocytes and macrophages, may promote tumor growth and progression. In particular, it is increasingly appreciated that, among myeloid cells, tumor-associated macrophages (TAMs) are important drivers of tumor growth and progression to malignancy, at least in mouse models of cancer (Qian and Pollard, 2010).

**Role of TAMs in promoting tumor growth and progression**

TAMs support tumor progression in mouse models of cancer by accomplishing several protumoral functions (Qian and Pollard, 2010). The protumoral activities of TAMs may depend, at least in part, on their production of growth and proangiogenic factors, such as members of the epidermal (EGF), fibroblast (FGF) and vascular

growth factors families (VEGFs and PlGF) (Fischer et al., 2008; Halin et al., 2009; Lin et al., 2006b; Lin and Pollard, 2007; Mantovani et al., 2008; Wyckoff et al., 2007). TAMs also secrete TGF-β, a pleiotropic cytokine that stimulates tumor-associated fibroblasts to synthesize extracellular matrix (ECM) molecules (Barrientos et al., 2008; Wynn and Barron, 2010) and induces tumor cells to acquire a proinvasive phenotype. Moreover, TAMs are an important source of several proteolytic and tissue-remodelling enzymes, such as matrix-metalloproteinase (MMPs), Cathepsins and A disintegrin and metalloproteinase (ADAMs) (Bergers et al., 2000; Gocheva et al., 2010; Wagsater et al., 2008). By facilitating remodelling of the ECM, these TAM-derived proteases support mobilization of proangiogenic factors, e.g. vascular endothelial growth factor (VEGF), making them available for interaction on related receptors expressed on endothelial cells (Bergers et al., 2000). Overall, TAMs produce a large number of cytokines and growth factors that regulate the biology of both tumor and stromal cells; some of these cytokines exert immunomodulatory activities on other components of the immune system (Sica et al., 2008a).

The first clear evidence for the ability of macrophages to promote tumor progression was provided using a mouse model of macrophage deficiency. Pollard and colleagues crossed mice carrying a homozygous mutation in the colony-stimulating factor 1 (*Csf1*) gene with mice that develop oncogene-induced mammary tumors ($Csf1^{op/op}$/MMTV-PyMT). The authors found that the tumors developing in these macrophage-deficient mice had delayed

progression to malignancy (Lin et al., 2001). Following this pioneering study which demonstrated the involvement of macrophages in tumor progression, many other studies investigated the protumoral activity of macrophages and established their relevance in this process as discussed below (Qian and Pollard, 2010).

***TAMs and angiogenesis***

In order to grow over a few millimeters in size, emerging tumors need to generate their own vasculature to support oxygen and nutrition delivery to the growing tumor cells. However, due to their excessive production of proangiogenic factors, tumors generally induce poorly organized and dysfunctional vasculature (Bergers and Benjamin, 2003; Carmeliet and Jain, 2011). It is now well established that tumor-associated stromal cells such as macrophages and fibroblasts cooperate with tumor cells to generate a fine vasculature in experimental mouse tumors (Coffelt et al., 2010a; Egeblad et al., 2010; Murdoch et al., 2008).

The finding that, in breast carcinoma and other tumor types, high macrophage counts correlate with higher microvessel densities (Leek et al., 1996) suggested that these cells exert a direct proangiogenic function in tumors. However, clear evidence for the ability of macrophages to promote tumor angiogenesis was only provided using mouse models of *in vivo* monocyte/macrophage deficiency or adoptive transfer. De Palma and colleagues, in our lab, identified a subset of circulating and tumor-infiltrating monocytes expressing the angiopoietin receptor Tie2, the Tie2-expressing monocytes (TEMs).

Our previous studies indicated that TEMs are proangiogenic when isolated from either tumors or peripheral blood, suggesting their commitment to a proangiogenic function already in the circulation. Moreover, the selective elimination of TEMs by a conditional suicide gene approach inhibited angiogenesis and tumor growth in several mouse tumor models (De Palma et al., 2005; De Palma et al., 2003b). In the macrophage-deficient Csf1$^{op/op}$/MMTV-PyMT mice the delayed progression to malignancy was associated with reduced angiogenesis (Lin et al., 2006b). Conversely, the enforced generation and tumor recruitment of monocyte/macrophages mediated by genetic overexpression of colony-stimulating factor-1 (CSF-1) in the mammary epithelium accelerated the angiogenic switch (i.e., the transition from a quiescent to a growing vasculature (Bergers and Benjamin, 2003) and accelerated progression to malignancy in MMTV-PyMT mice (Lin et al., 2006b). Together, these studies have highlighted the important proangiogenic role played by macrophages in mouse models of cancer.

Macrophages can stimulate tumor angiogenesis by several mechanisms. For instance, they secrete a plethora of proangiogenic factors, including endothelial cell mitogens and proteases that mobilize endothelial growth factors entrapped in the tumor ECM. Furthermore, recent data have suggested that macrophages may physically “guide” the extension and fusion of endothelial tip cells (i.e., cells at the fore-front of growing blood vessels). Fantin and colleagues showed that, during all phases of vascular networking, TEMs appear to interact with the endothelial-tip cells; in some cases,

TEMs were found to bridge neighboring endothelial-tip cells belonging to distinct vascular sprouts. These observations suggest that macrophages adopt strategic positions around the developing vasculature that are consistent with a role in promoting blood vessel fusion (Fantin et al., 2010).

***TAMs and tumor progression***

In addition to promoting ECM remodeling and angiogenesis, macrophages have been shown to favor tumor progression and metastasis. For instance, Lin and colleagues found that genetic macrophage deficiency in MMTV-PyMT tumors (*Csf1*$^{op/op}$/MMTV-PyMT) resulted in reduced tumor cell invasion and decreased number of pulmonary metastases (Lin et al., 2001).

During the adenoma-to-carcinoma transition, macrophages are found at points of basement-membrane breakdown; in locally invasive carcinomas, macrophages are then most abundant at the invasive front of the tumor. These observations suggest that tumors may exploit the ECM remodeling capabilities of TAMs to escape into and migrate through the peritumoral stroma (Condeelis and Pollard, 2006).

TAMs, likely through their pro-tissue remodeling activity, can enhance tumor cell dissemination at distant sites by promoting tumor cell intravasation (i.e., invasion of blood vessels). Wyckoff and colleagues used dynamic intravital imaging to demonstrate that tumor cell intravasation almost consistently occurs in close proximity to macrophages (Wyckoff et al., 2007). Interestingly, by using a CSF-1 receptor-blocking antibody, the authors could reduce the occurrence

of tumor cell intravasation (Wyckoff et al., 2007). Qian and colleagues showed that macrophages assist tumor cell extravasation and subsequent growth at the metastatic site. These metastasis-promoting macrophages express a distinctive cell surface marker profile (Qian et al., 2009) and originate from circulating inflammatory monocytes (Qian et al., 2011). Genetic ablation of these metastasis-associated macrophages limits metastatic growth, even when it is performed after metastatic lesions had been established. The observation of a physical interaction between macrophages and metastatic tumor cells suggests the occurrence of short-range transmission of growth and survival signals from the macrophages to the disseminated tumor cells (Qian et al., 2009). DeNardo and colleagues proposed that the prometastatic activities of macrophages are regulated in part by interleukin 4 (IL4), which is mainly produced by $CD4^+$ T cells in tumors. Indeed, either IL4 blockade by anti-IL4 antibodies or genetic deficiency of interleukin 4 receptor alpha (IL4Rα) reduced the number of metastatic foci in MMTV-PyMT mice (DeNardo et al., 2009). It appears that IL4, in concert with CSF-1, stimulates *ex vivo* cultured TAMs to express the proinvasive growth factor, EGF; consistent with this finding, inhibition of IL4 reduced the expression of the *Egf* mRNA by cultured TAMs (DeNardo et al., 2009).

***TAMs and immunosuppression***

Macrophages represent an important cellular component of the innate arm of the immune system, and are essential for the clearance of

pathogens and other foreign agents (Akira et al., 2006). There is also evidence that macrophages can directly kill tumor cells; for example, early studies showed that activated macrophages could efficiently recognize and eliminate tumor cells (Adams et al., 1982; Fidler and Schroit, 1988). In regressing tumors or specific tumor areas, macrophages can express an activated phenotype characterized by elevated production of ROS and molecules with cytotoxic or even cytolytic activity (Grivennikov et al., 2010). However, such activated, tumoricidal macrophage phenotype is often subverted by the tumor microenvironment (Sica et al., 2008b).

In patho-physiological conditions such as infection and inflammation, macrophages are also able to present antigens to T lymphocytes and activate adaptive immune responses. However, in the vast majority of solid tumors, the immunosuppressive microenvironment limits the activation of macrophages, thus blocking their antitumor activity (Swann et al., 2008). Gene expression profiling of TAMs indeed showed that these cells downregulate genes that promote immunological responses, while they upregulate genes with immunosuppressive activity, such as arginase I (Biswas et al., 2006; Mills et al., 1992; Pucci et al., 2009; Sharda et al., 2011; Stein et al., 1992). Enhanced arginase I activity in TAMs and other myeloid cells impairs T cell proliferation and activation by depleting L-arginine from the tumor microenvironment (Sica and Bronte, 2007). TAMs further inhibit the activation of adaptive immune responses through several other mechanisms. For instance, TAMs may suppress cytotoxic T cell responses against mammary tumor xenografts by

releasing prostaglandin E2 (PGE2) and tumor growth factor beta (TGF-β) (Torroella-Kouri et al., 2009). Among its many activities, TGF-β signaling inhibits T and B cell proliferation; impairs both helper and cytotoxic T cell differentiation; induces regulatory T cell (Treg) differentiation; and limits the classical activation of macrophages (Li et al., 2006). In human ovarian cancer, TAMs also produce chemokine (C-C motif) ligand 22 (CCL22), a cytokine that increases the recruitment of regulatory Tregs (Balkwill, 2012; Hagemann et al., 2006); Tregs block the activation of effector T cells, and high Treg numbers in human cancers are generally associated with a poor survival (Curiel et al., 2004). Together, these studies indicate that, in tumors, macrophages display reduced antigen-presentation activity and express genetic programs that promote immunosuppression, leading to enhanced tumor progression (Kuang et al., 2009).

**Macrophage polarization: the proposed M1-M2 paradigm**

Tissue macrophages can display different activation states according to the stimuli present in the local microenvironment. It has been shown in several microbial infections and other inflammatory conditions performed *in vitro*, the products (e.g., IFNγ) of activated T helper-1 (Th1) lymphocytes and NK cells can induce macrophages to undergo a "classical activation" (or "M1") program that enhances their cytotoxic and antimicrobial activity. Conversely, signals produced by Th2 polarized lymphocytes (e.g., IL4, IL10 or IL13) can induce macrophages to acquire an "alternative activation" (or "M2")

status in various pathophysiological conditions, such as wound healing and granuloma formation, or in certain disease conditions, such as fibrosis, atherosclerosis and stroke (Chinetti-Gbaguidi and Staels, 2011; Gordon and Martinez, 2010; Nucera et al., 2011).

Stein and colleagues first described in 1992 that IL4 induces the alternative activation of macrophages (Stein et al., 1992). It was found that IL4 stimulates macrophages to upregulate the macrophage mannose receptor C type 1 (MRC1) (Stein et al., 1992), which is involved in the clearance of glycoproteins and plays an important role in the regulation of glycoprotein homeostasis in tissues and serum (Lee et al., 2002). Orlikowsky and colleagues, who introduced for the first time the terms "M1" and "M2" macrophages in 1999, described differential effects of interferon gamma (IFNγ) and interleukin 10 (IL10) on macrophages: whereas IFNγ-stimulated macrophages (M1) promoted T cell activation and expansion, IL10-stimulated macrophages (M2) induced T cell destruction (Orlikowsky et al., 1999). One year later, Mills and colleagues showed that IFNγ and IL4 influence the metabolic features of macrophages and their ability to stimulate Th1 or Th2 immune responses (Mills et al., 2000).

The widely adopted M1/M2 paradigm best describes the modulation of macrophages characterized *in vitro* under diverse stimuli. Weather it can be applied to *in vivo* setting remains to be clarified. Indeed, TAMs appeared to mostly represent an M2 phenotype, possibly related to the elevated tumor production of cytokines such as IL4, IL13, IL10 and TFG-β (Mantovani et al., 2008; Mantovani et al., 2002).

**Identification of distinct TAM subsets**

It is increasingly appreciated that the diverse protumoral functions of macrophages are executed by phenotypically distinct subsets. Although it is well established that several tumor-derived factors – or specific tumor microenvironments – can modulate the phenotype of TAMs at the tumor site (Coffelt et al., 2010a; Murdoch et al., 2008; Pollard, 2004; Sica et al., 2008b), recent reports also support the notion that certain TAM subsets may derive from distinct circulating monocyte precursors (De Palma et al., 2005; De Palma et al., 2003b; MacDonald et al., 2010; Pucci et al., 2009; Qian et al., 2011; Qian and Pollard, 2010). Studies from our group showed that $TIE2^+$ TAMs (TEMs), which mostly localize at the tumor periphery and/or associate with small blood vessels dispersed within the tumor parenchyma (Figure 3), display enhanced proangiogenic activity in mouse tumor models compared with other TAM subsets (De Palma et al., 2005).

We then went on to perform gene expression profiling of TEMs and TAMs isolated from mammary tumors implanted subcutaneously. We found that many genes involved in tissue remodeling and angiogenesis were upregulated in TEMs, including *Lyve1*, *Nrp1*, *Cxcl12/Sdf1*, *Cd163*, *Mrc1*, *Msr2*, *Stab1*, *Igf1*, *Edg1* and *Efnb2*. On the other hand, proinflammatory or antiangiogenic molecules were downregulated, including *Il1b*, *Ptgs2/Cox2*, *Tnfα*, *Il12a*, *Cxcl10*, *Nos2* and *Cxcl11*. The "TEM gene signature" also distinguishes resident from inflammatory monocytes in the peripheral blood and identifies a population of $TIE2^+$ embryonic/fetal macrophages that appear early

during mouse development (starting from E8.5) and are preferentially associated with areas of active tissue remodeling and angiogenesis (Pucci et al., 2009).

In most mouse tumor models, TEMs express a $MRC1^{+}CD11c^{-}$ surface marker profile; this distinguishes them from other TAMs, which conversely express a $MRC1^{low}CD11c^{+}$ phenotype (Mazzieri et al., 2011; Pucci et al., 2009; Squadrito and De Palma, 2011). Recently, the gene expression signatures of distinct TAM subsets have been profiled. It was found that macrophages that promote tumor cell invasion and metastasis differ, for example, from those that promote angiogenesis (Qian and Pollard, 2010).

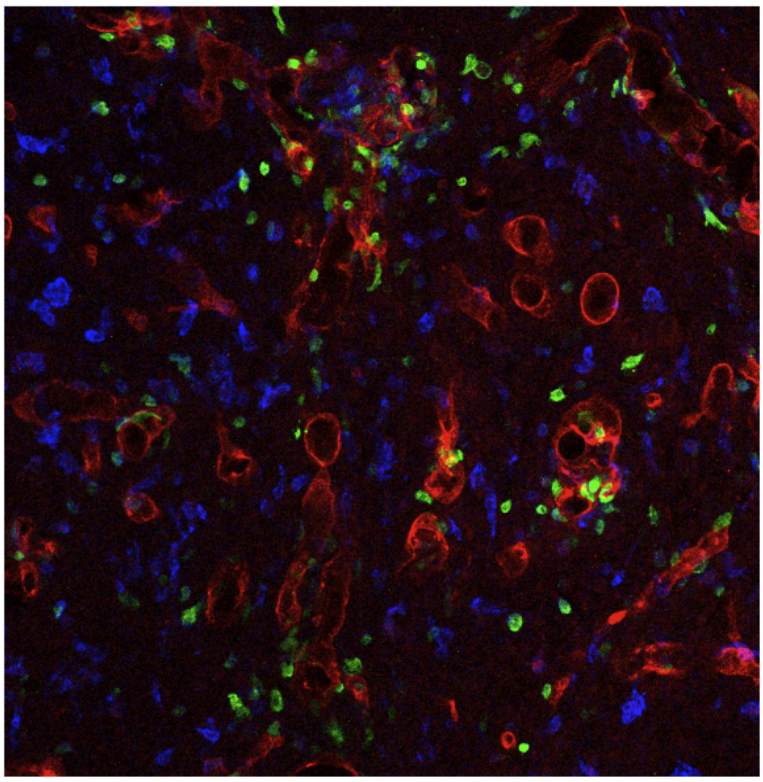

***Figure 3. Perivascular localization of TEMs in tumors.*** *Immunofluorescence staining of N202 tumor sections from a Tie2p/e-GFP BM chimera mouse. Of note, the perivascular position of Tie2p/e-GFP$^+$ TEMs, which contrast to the widespread distribution of CD11b$^+$ myeloid cells (in blue). Blood vessels are in red. (De Palma et al., 2008).*

Movahedi and colleagues identified multiple subsets of tumor-infiltrating, CD11b$^+$ myeloid cells by analyzing the expression of Ly6C and major histocompatibility complex class II (MHC II) (Movahedi et al., 2010). The authors implanted TS/A mammary carcinomas subcutaneously in Balb/c mice and identified three main macrophage subsets in these tumors: (i) CD11b$^+$ MHC IIhigh Ly6C$^{int}$; (ii) CD11b$^+$ MHC II$^{high}$ Ly6C$^{low}$; (iii) CD11b$^+$ MHC IIlow Ly6C$^{low}$. Similar TAM subsets were observed also in 4T1 mammary carcinomas and Lewis lung carcinoma (LLC) implanted in Balb/c and C57Bl/6 mice, respectively (Movahedi et al., 2010). The authors analyzed the expression of a panel of genes of interest in TAMs sorted from TS/A tumors and found that the gene expression signature of MHC II$^{low}$ TAMs (Movahedi et al., 2010) was strikingly similar to that of TEMs (Pucci et al., 2009); on the other hand, MHC II$^{high}$ TAMs (Movahedi et al., 2010) were highly related to TIE2$^-$ TAMs (Pucci et al., 2009). Similar to TEMs, MHC II$^{low}$ TAMs display enhanced proangiogenic activity compared to other TAM subsets (Movahedi et al., 2010). Hence, a unifying marker signature of

different TAM subsets is still lacking. Yet, recent data point to a significant heterogeneity within the macrophage lineage rather than simple modulation of macrophage within the tumor microenvironment.

**Tie2 receptor**

Our group has identified the $Tie2^{+}$ TAM (TEMs) subpopulation endowed with pro-tumoral and pro-angiogenic activity, and characterized, among other markers, by the expression of the Tie2 receptor (De Palma et al., 2005; De Palma et al., 2003b).

In the mouse and human system, the TIE2 receptor is expressed by endothelial cells (ECs), hematopoietic stem cells (HSCs) and TEMs. The *Tek* gene encodes for the TIE2 protein. TIE2 is a receptor tyrosine kinase which possesses a unique extracellular domain containing 3 immunoglobulin-like loops which fold together with 3 epidermal growth factor-like repeats and three fibronectin type III repeats (Figure 4) (Barton et al., 2006). Studies with dominant-negative and null mice reveal that loss of *Tie2* gene function results in embryonic death at 9.5 day post coitum as a consequence of an underdeveloped vasculature (Dumont et al., 1994; Sato et al., 1995). TIE2 is expressed at the highest levels in ECs and at lower levels in TEMs and HSCs.

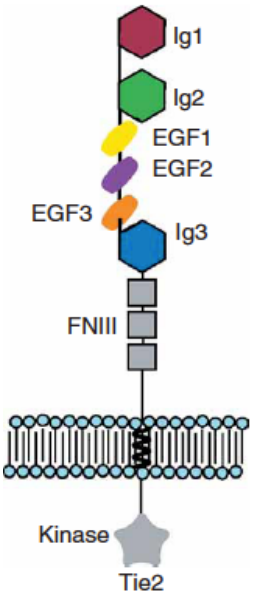


***Figure 4. Schematic representation of the domain organization of the TIE receptors.***

***Signaling mechanism***

Initially described as an orphan receptor (Dumont et al., 1992), TIE2 was subsequently shown to interact with all four of the angiopoietins (ANG1 – ANG4) (Valenzuela et al., 1999). The different angiopoietins, although having high sequence homology, elicit different responses from the TIE2 receptor. Indeed, ANG1 is a constitutive receptor agonist, while ANG2 is a context-dependent one (Ward and Dumont, 2002). The four known angiopoietins each

contain an N terminus that modulates angiopoietin clustering and a C terminus that mediates the interaction with TIE2 (Davis et al., 2003). Ligand oligomerization is necessary for receptor activation. Indeed, all angiopoietins exist primarily as tetramers, hexamers and higher order oligomers in solution (Seegar et al., 2010; Ward and Dumont, 2002). Ligand-induced oligomerization of the extracellular regions of TIE2 leads to activation of the intracellular tyrosine kinase domain, which creates binding sites for Src homology 2 and phosphotyrosine binding domain containing proteins (Lemmon and Schlessinger, 2010). TIE1, although a close homolog of TIE2, does not interact directly with the angiopoietins, and its in vivo ligands are yet to be identified. A recent study using catalytically inactive TIE2 demonstrated that TIE1 phosphorylation is dependent on a functional TIE2 (Yuan et al., 2007). Recently, it has been proposed that TIE1 is an inhibitory co-receptor. Specifically, in cells expressing both TIE1 and TIE2, the receptors form heterodimers that inhibit Tie2 activation and clustering. Binding of ANG1 to TIE2 promotes heterodimer dissociation, TIE2 clustering, and signalling initiation. On the other hand, ANG2 is unable to dissociate the inhibitory TIE2-TIE1 complexes upon binding TIE2 and, therefore, does not induce TIE2 clustering and signaling, yet behaves as a competitive antagonist by blocking further binding of ANG1. Indeed, both ANG1 and ANG2 bind to the same region of Tie2 (Barton et al., 2006). Alternatively, in cells that do not express TIE1, all angiopoietins promote TIE2 clustering and activation (Seegar et al., 2010). This model proposes that the balance of TIE1 and TIE2 expression modulates the

functional potential of ANG2, and by analogy, vascular homeostasis (Figure 5). However, this model is based on studies performed in ECs and it is not known if it holds true also in hematopoietic cells (HCs).

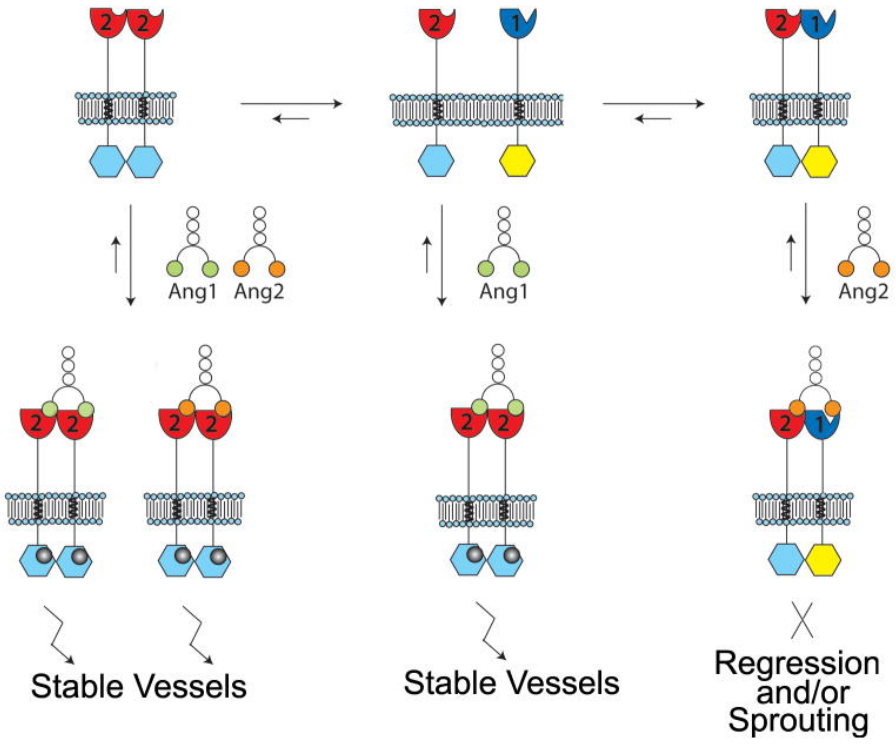


***Figure 5. Model for Angiopoietin-Mediated TIE2 Signaling***.

*Left: expression of TIE2 in the absence of TIE1 at sites of vessel quiescence and maturity. In the absence of TIE1, TIE2 can be activated with either ANG1 or ANG2. Both ligands stimulate receptor clustering, tyrosine kinase activity, and downstream signaling events, effectively become unresponsive to vessel sprouting and branching*

*cues. Middle and right: within sites of active angiogenesis, TIE1 and TIE2 associate to form a complex prior to ligand stimulation. Upon addition of ANG2 (right), TIE1 and TIE2 association and localization remain unchanged. Under these conditions, ANG2 fails to activate the TIE2 receptor and opposes the activation of downstream signaling generated by ANG1. However, upon addition of ANG1 (middle), the opposite is observed. ANG1 stimulates TIE2 clustering, tyrosine kinase activity, and downstream signaling events similar to those observed in the absence of Tie1. Angiopoietins are depicted as dimers for illustration purposes, although they are known to exist as higher-order clusters. (from Seegar et al., 2010).*

***Regulation of vascular homeostasis***

ANG1 is constitutively expressed by many different cell types such as pericytes, smooth muscle cells and fibroblasts (Sundberg et al., 2002). Constitutive ANG1 expression and low level TIE2 phosphorylation in the adult vasculature suggest that ANG1-mediated TIE2 signaling functions as the default pathway to control vascular quiescence. ANG1 exerts a protective effect on the endothelium, limits its ability to be activated by exogenous cytokines and growth factors and inhibits vascular leakage. For these reasons, it has an anti-inflammatory action.

On the other hand, ANG2 is almost exclusively expressed by ECs (Fiedler et al., 2004). *Angpt2* mRNA is almost undetectable in the quiescent vasculature and dramatically upregulated in tumor blood

vessels (Stratmann et al., 1998). ANG2 expression is regulated by several different cytokines (FGF2, VEGFs and TNF) and environmental cues (hypoxia, high glucose levels and superoxides) (Fiedler and Augustin, 2006). ANG2 protein is stored in EC Weibel-Palade bodies and thus is readily available following endothelial stimulation. The release of ANG2 results in rapid destabilization of the endothelium, suggesting that ANG2 functions as an autocrine negative regulator of the quiescent resting endothelium (Scharpfenecker et al., 2005). In contrast to ANG1, ANG2 triggers an inflammatory response by activating the endothelium and inducing vascular permeability (Roviezzo et al., 2005).

***Regulation of TEM biology***

Although it has been shown that TIE2 mediates quiescence in HSCs (Arai et al., 2004; De Palma et al., 2005), in TEMs TIE2 appears to drive the recruitment to tumors via ANG2/TIE2 interaction. Of note, expression of ANG2 is known to be upregulated in tumors and inflamed tissues as compared to normal, quiescent tissues (Nasarre et al., 2009a), and activated ECs appear to be a major source of ANG2, at least in the mouse (Fiedler et al., 2004). In support of a putative chemoattractant role of ANG2, Lewis and colleagues showed that human peripheral blood-derived monocytes respond to ANG2 with both chemotaxis and altered cytokine release (Murdoch et al., 2007b). Similarly, work that I performed in our laboratory suggests that human peripheral blood mononuclear cells enriched in $TIE2^{+}$ monocytes migrate towards ANG2 in vitro. Because ANG2-induced

chemoattraction of monocytes is inhibited by anti-TIE2 neutralizing antibodies (Venneri et al., 2007), it is likely that this response is mediated by engagement of the TIE2 receptor. Recently, to investigate the effects of ANG2 on the phenotype and function of TEMs in tumors, Lewis and co-workers (Coffelt et al., 2010b) used a transgenic mouse model in which ANG2 was specifically over-expressed by endothelial cells. Syngeneic tumors grown in these ANG2 transgenic mice were more vascularized and contained greater numbers of TEMs than those in wild-type mice. In this thesis work, we investigated whether ANG2 directly regulates TEM homing/function in tumors, and whether targeting ANG2 or its receptor, TIE2, could represent a therapeutic strategy to impair TEM activity in mammary tumor models (see below, chapter 2) (Mazzieri et al., 2011).

## Mouse Models to Study the Tumor Microenvironment

Breast cancer is the most frequently diagnosed form of cancer and the second principal cause of death in Western women (Weigelt et al., 2005). Recently, the development of genetically modified mouse models and advanced transplantation techniques, have allowed the rapid improvement of our knowledge on the role played by the tumor microenvironment in breast cancer progression and metastasis.

### *Genetically modified mice*

Several promoters can be used to drive the expression of transgenes in the mammary epithelium, and many known oncogenes have been

expressed under their control to initiate or modulate breast carcinogenesis in mice, including ErbB2/Neu (v-erb-b2 erythroblastic leukemia viral oncogene homolog 2, neuro/glioblastoma), polyoma middle T antigen (PyMT), simian virus 40 (SV40) T antigen, Ha-Ras, Wnt-1, TGF-α, and c-Myc. Comparisons of gene expression profiles obtained from mammary gland tumor models initiated by different oncogenes have allowed the identification of several common and oncogene-specific targets and similarities with human molecular breast cancer pathology (Desai et al., 2002).

In particular, the mammary gland-specific expression of PyMT under the control of the mammary epithelium MMTV promoter/enhancer in transgenic mice (**MMTV-PyMT**) results in widespread transformation of the mammary epithelium and in the development of multifocal mammary adenocarcinomas and metastatic lesions in the lymph nodes and in the lungs (Guy et al., 1992). Tumor formation and progression in these mice is characterized by four stages: hyperplasia, adenoma/mammary intra-epithelial neoplasia, and early and late carcinoma (Lin et al., 2003). The close similarity of this model to human breast cancer is also represented by the fact that in these mice a gradual loss of steroid hormone receptors (estrogen and progesterone) and β1-integrin is associated with overexpression of ErbB2 and cyclin D1 in late-stage metastatic cancer (Maglione et al., 2001).

In MMTV-PyMT transgenic mice, increased metastatic potential has been shown to depend on the presence of macrophages in primary tumors and on the establishment of a chemoattractant paracrine loop of CSF-1 and EGF ligands between macrophages and tumor cells (Lin

et al., 2001; Wyckoff et al., 2004). In MMTV-PyMT/CSF-1$^{-/-}$ mice, tumor progression and metastasis are significantly delayed, but they are restored upon overexpression of CSF-1 in the mammary gland (Gouon-Evans et al., 2000; Lin et al., 2001). Taken together, these data highlight the utility of transgenic mouse models of breast cancer metastasis to understand the role of several stromal components in modulating key steps during malignant progression.

***Tumor transplantation***

In addition to spontaneous transgenic models of multistage breast carcinogenesis, there are various ways to mimic the late stages of breast cancer growth including metastasis formation. Primary mammary adenocarcinoma cells or breast tumor cells lines can be ectopically or orthotopically implanted in the skin or mammary fat pad resulting in the formation of primary tumors and the subsequent dissemination and growth of spontaneous metastasis, in part resembles the multiple stages involved in malignant breast cancer progression in patients (Khanna and Hunter, 2005). Alternatively, primary tumor cells or tumor cell lines can be directly injected into the tail vein mainly resulting in lung metastasis, or into the portal vein provoking colonization of the liver. Finally, intracardiac infusion gives rise to a broader target organ spectrum, including bone.

To investigate the growth and metastasis of human breast cancer cell lines *in vivo*, xenograft transplantation experiments can be performed in immunocompromised mice (Hurst et al., 1993). Human breast cancer cells can be injected subcutaneously, intravenously,

intracardially, or orthotopically into the fat pad of the mouse (Kim et al., 2004). However, there are clear limitations to xenograft models. First, immune responses, which have a key role during tumor development, are impaired in immunocompromised mice. Second, stromal components are not of human origin as the tumor cells. Last, human cells are apparently not fully adapted to grow in a murine environment.

## Regulation of innate immune cells by microRNAs

Given the accumulating amount of data underlining the relevant role of TAMs in tumor biology, it is of key interest to understand the regulatory molecules which control their pro- and anti-tumoral genetic program. While many transcription factors (TFs) regulating the protumoral activities of TAMs have been characterized, little is known about biologically relevant miRNAs expressed by these cells. During the past decade, scientists found that miRNAs which are a class of non-coding RNAs (ncRNAs) of approximately 20-25 nucleotide length, regulate gene expression at the posttranscriptional level. miRNAs participate in virtually all biological processes by inducing posttranscriptional gene silencing; in order to do so, miRNAs bind to the 3'-untranslated region (UTR) of a target mRNA and induce mRNA decay and/or translational repression.

Immature miRNAs are transcribed from the nucleus as long precursors, which are then finely processed to give rise to mature and active miRNAs. Eukaryotic cells, including both plants and animals, express the miRNA processing machinery, and many miRNAs are highly conserved throughout evolution. This indicates that miRNA regulation of gene expression is a widespread phenomenon playing a fundamental role in most biological processes, including development, cell cycle, differentiation, apoptosis, and metabolism.

**microRNA biology**

The majority of animal primary miRNAs (pri-miRNAs) are typically contained within intronic or exonic regions of either non-coding or coding transcripts. In other cases, polycistronic clusters containing multiple miRNAs are encoded by individual transcripts. Most of miRNAs are transcribed by DNA-dependent RNA polymerase II (RNAPII). Once transcribed, Drosha, an RNAse III enzyme, catalyzes the first cleavage of the pri-miRNA hairpin structure (Yang and Lai, 2011). DiGeorge syndrome critical region gene 8 (DGCR8) is a RNA binding protein that forms an heterodimer with Drosha and binds to 10 nt of the pri-miRNA hairpin, positioning the catalytic domain of Drosha for RNA cleavage (Han et al., 2006). Drosha processing produces a precursor-miRNA (pre-miRNA) that is typically 55–70 nt long (Yang and Lai, 2011). Exportin-5 recognizes 2 or 3 overhanging nucleotides at the 3' of the pre-miRNA, and transports it to the cell cytoplasm. Dicer, an RNAse III enzyme, catalyzes the second step in the maturation of miRNAs. Similar to DGCR8, TAR (HIV) RNA binding protein 2 (TRBP) forms a protein complex with Dicer and guides its catalytic domain to cleave the dsRNA. Dicer cleaves the pre-miRNAs close to the loop structure of the hairpin, thus generating 22 nt-long small RNA duplexes. Then, one of the two strands of the RNA duplex, called *guide strand*, is incorporated together with argonaute proteins (AGO 1–4) to generate the RNA-induced silencing complex (RISC). The other miRNA strand, termed *passenger strand* is degraded (Czech and Hannon, 2011) (Figure 6). For some miRs,

either strand of the duplex can be incorporated into RISC. In these cases, the less frequently found strand is referred to as miR*.

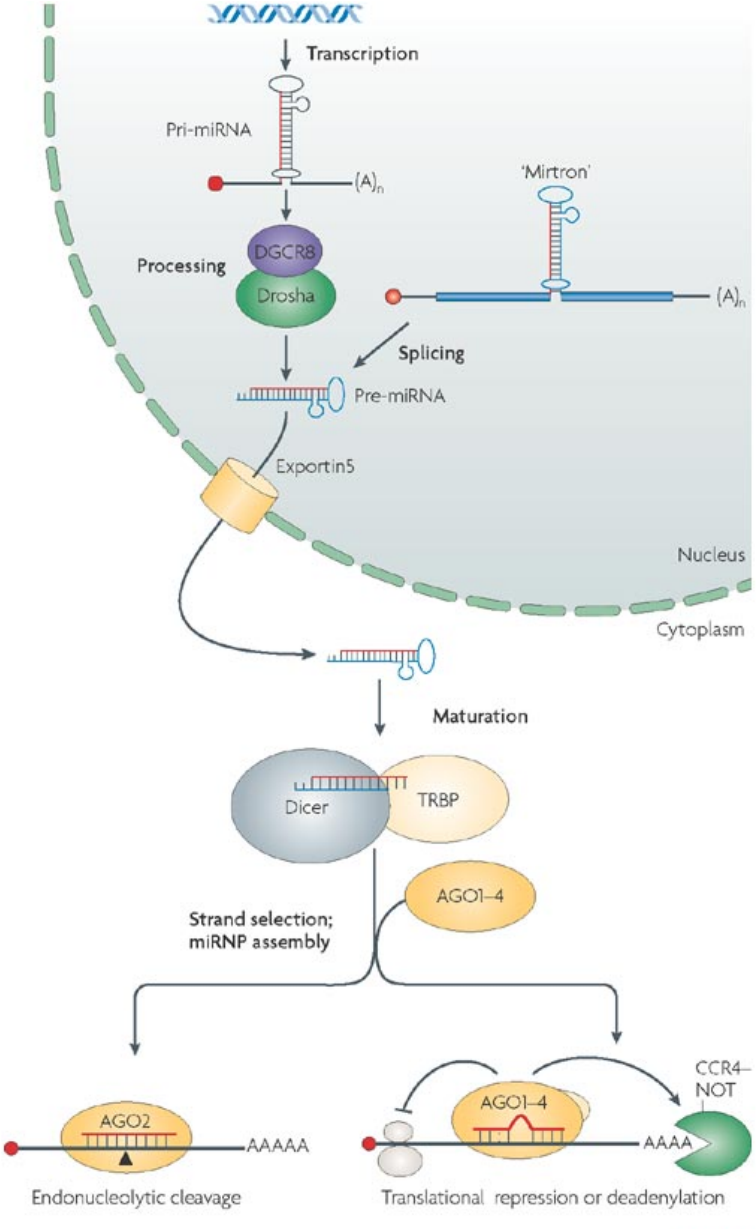

***Figure 6. MicroRNA biogenesis***.

*miRNA genes encode long primary mRNA transcripts that in turn produce mature miRNAs through a series of endonucleolytic maturation steps that are thought to be essential for the production of functional miRNAs. Primary miRNA transcripts are processed into pre-miRNA, stem-loops of approximately 60 nucleotides in length, by the nuclear RNase III enzyme Drosha. The pre-miRNA is then actively transported to the cytoplasm by Exportin-5 and further processed into an approximately 21-nucleotide long duplex. The final step of miRNA maturation is the selective loading of the functional strand of the small RNA duplex into the RISC. DGRC8 and TRBP are double-stranded RNA-binding proteins that facilitate mature miRNA biogenesis by Drosha and Dicer RNase III enzymes, respectively. The guide strand of the miRNA duplex gets incorporated into the effector complex RISC, which recognizes specific targets through imperfect base-pairing and induces post-transcriptional gene silencing. Several mechanisms have been proposed for this mode of regulation: miRNAs can induce the repression of translation initiation, mark target mRNAs for degradation by deadenylation, or sequester targets into the cytoplasmic P-body. (Adapted from He et al., 2007).*

**microRNAs in the innate immune system**

Some miRNAs show cell-type specific expression patterns among innate immune cells such as granulocytes, monocytes/macrophages, dendritic cells (DCs) and NK cells, and adaptive immune cells, which

mostly include B and T-cell lineages. For example, miR-223 is preferentially expressed by myeloid cells and controls granulocyte differentiation and proliferation (Fazi et al., 2005; Gentner et al., 2009; Johnnidis et al., 2008). miR-155 is expressed in activated T or B cells but is also highly upregulated in activated DCs/macrophages (Tili et al., 2009). On the other hand, miR-142 is broadly expressed in all types of leukocytes (Brown et al., 2007). These observations suggest that, in the immune system, miRNAs may directly regulate the expression of several genes and thus provide intrinsic signals that control immune cell differentiation, proliferation and function.

***The role of miRNAs in myeloid cell differentiation***

It is increasingly appreciated that the differentiation of the myeloid lineage is finely controlled by both TFs and miRNAs (El Gazzar and McCall, 2011). The expression of the miR-17-92 and miR-106a-92a clusters, encoding for miR-17-5p, miR-20a and miR-106a among others, is down regulated during the differentiation of progenitor cells into mature monocytes, while their direct targets, including runt-related transcription factor 1 (RUNX1) (also known as Acute Myeloid Leukemia, AML1), are upregulated (Fontana et al., 2007). RUNX1 activation, as a consequence of miR-17-5p/20a/106a downregulation, enhances the expression of CSF-1 receptor (CSF-1R; also known as CD115), which promotes monocyte differentiation (Fontana et al., 2007). Thus, miR-17-5p/20a/106a downregulation stimulates monocyte differentiation via RUNX1/CSF-1R. Moreover, RUNX1 may reduce the expression of the miR-17-92 and miR-106a-92

clusters by directly interacting with its promoter region. Thus, miR-17-5p/20a/106a and the transcription factor RUNX1 may be involved in a mutual negative feedback loop (Fontana et al., 2007).

Some miRNAs are under the control of TFs that regulate cell commitment to the myeloid lineage. For example, PU.1, a transcription factor that induces the maturation of monocytes and macrophages (El Gazzar and McCall, 2011), increases the expression of miR-424. In turn, miR-424 decreases the expression of its direct target, nuclear factor I-A (NFIA) (Rosa et al., 2007). NFIA is an inhibitor of the monocytic/macrophage maturation (Starnes et al., 2009). Thus, miR-424, activated by the transcription factor PU.1, induces monocyte/macrophage differentiation by silencing the expression of NFIA (Rosa et al., 2007). Growth factor independent 1 (GFI1) is a transcription factor that induces the differentiation of granulocyte/monocyte progenitors to mature granulocytes. miR-21 and miR-196 overexpression reduce the expression of GFI1, leading to decreased granulopoiesis (Velu et al., 2009). Thus, endogenous miR-21/miR-196 expression may finely balance the differentiation of myeloid precursor cells into monocytes or granulocytes. GFI1 can bind to the promoter region of miR-21/miR-196 and decrease their transcription rate. Thus, miR-21/miR-196, and the transcription factor GFI1, may be involved in a mutual negative feedback loop (Velu et al., 2009).

The TFs PU.1 and CCAAT/enhancer-binding protein-β (C/EBPβ) induce the expression of miR-223, which negatively regulates both the proliferation and activation of granulocytes (Fazi et al., 2005; Fukao

et al., 2007). miR-223 was found to target NFIA and myocyte-specific enhancer factor 2C (MEF2C), which control the differentiation and proliferation of myeloid lineages. This was shown in miR-223-deficient mice (Johnnidis et al., 2008), or mice in which miR-223 was specifically knocked-down in the hematopoietic cell compartment (Gentner et al., 2009). Thus, miR-223 expression may control the proliferation and activation of granulocytes by directly down regulating the expression of both NFIA and MEF2C (Gentner et al., 2009; Johnnidis et al., 2008). Altogether, these observations indicate that, even if miR-223 is broadly expressed in leukocytes, it controls specific aspects of granulocyte biology (Figure 7).

Recently, O'Connell and colleagues showed that sustained expression of miR-155 in hematopoietic cells induced myeloproliferative disorder by increasing immature granulocytes (O'Connell et al., 2008).

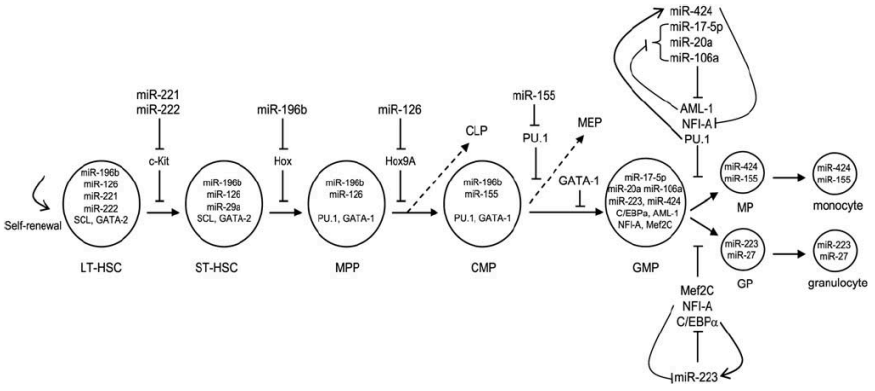

***Figure 7. Overview of miRNA- and TF-mediated regulation of normal hematopoiesis, differentiation and maturation of innate immune cells.***

*This scheme emphasizes the interplay between individual miRNAs and TFs and its effects on repressing hematopoietic and progenitor relevant genes to produce lineage restricted innate immune cells. HSC gradually loses self-renewal capacity and gives rise to multipotent progenitor (MPP), which in turns gives rise to common lymphoid progenitor (CLP) and common myeloid progenitor (CMP). Under cross-antagonism between PU.1 and GATA-1, CMP gives rise to megakaryocyte-erythrocyte progenitor (MEP) and granulocyte-monocyte progenitor (GMP). Note that miR-221 and miR-222 also inhibit c-Kit at progenitor level (that is, CMP) and thus inhibit erythrocyte differentiation. All these branch points are controlled by the interplay between miRNAs and TFs. MP, macrophages progenitor; GP, granulocytes progenitors; LT-HSC, long-term hematopoietic stem cell; ST-HSC, short-term hematopoietic stem cell (El Gazzar and McCall, 2011).*

***The role of miRNAs in macrophage and dendritic cell function***

Several studies demonstrated that miRNAs finely regulate the activation state of macrophages and DCs. Stimulation of Toll-like receptors (TLRs) induces the expression of many miRNAs including miR-155, miR-146a, miR-125b, miR-132, miR-21, miR-147, let-7e, miR-27b, miR-466l, among others (Ma et al., 2010; O'Neill et al.,

2011). While many miRNAs were found to be upregulated by TLR signaling, miR-125b is down regulated (Ma et al., 2010; O'Neill et al., 2011). However, there are contradictory data regarding the expression of miR-125b upon TLR activation (O'Neill et al., 2011), indicating the complexity of miRNA regulation in macrophages. miRNAs that are upregulated by pro-inflammatory signals (e.g. miR-155, miR-146, miR-21 and miR-147) can negatively regulate the activation of inflammatory pathways (Liu et al., 2009; Ruggiero et al., 2009; Sheedy et al., 2010; Taganov et al., 2006). Thus, to prevent overwhelming inflammation, miRNAs may finely contain the activation state of macrophages. Interestingly, in several inflammatory conditions, such as psoriasis or rheumatoid arthritis, miRNA expression is deregulated. For instance, psoriasis-affected skin shows increased expression of miR-203, miR-146a and miR-21, while showing reduced expression of miR-125b (Sonkoly et al., 2007); of note, miR-146a is also highly upregulated in the synovial tissue of rheumatoid arthritis patients (Nakasa et al., 2008).

***miR-155***

One of the most studied miRNAs involved in macrophage biology is miR-155. The gene-encoding miR-155 is located on chromosome 21 in the B-cell integration cluster (BIC) (Tam, 2001). BIC is highly conserved between humans and mice and is highly expressed in lymphoid organs. miR-155 plays key roles in both innate and adaptive immune responses (Lindsay, 2008; Tili et al., 2008; Xiao and Rajewsky, 2009). miR-155 expression is strongly induced in response

to lipopolysaccharide (LPS) or type I interferons, in both monocytes and macrophages of human or mouse origin, suggesting that this miRNA participates in the innate immune response to both bacterial and viral infection (O'Connell et al., 2009; O'Connell et al., 2007; Tili et al., 2007). Moreover, miR-155 is highly expressed in activated B and T cells and has been shown to play a role in regulating cytokine expression in the germinal center (Thai et al., 2007).

miR-155 function indicates that it is likely to be pro-inflammatory. In dendritic cells, miR-155 is necessary for activation of responder T cells in the context of antigen presentation (Rodriguez et al., 2007). In macrophages its activity allows the translation of tumor necrosis factor (TNF), a key pro-inflammatory cytokine (Bala et al., 2011; Tili et al., 2007). In resting macrophages, the 3' UTR of TNF induces a self-repression, which is released upon LPS stimulation via the binding of miR-155. This has been shown in macrophages, where miR-155 overexpression results in increased TNF production and miR-155 deficiency results in lower levels of TNF (Bala et al., 2011). Targeting miR-155 in macrophages would therefore limit TNF production suggesting important therapeutic application in the contest of TNF-mediated disorders. Another relevant target of miR-155 in antigen presenting cells is represented by SHIP1 (Androulidaki et al., 2009; O'Connell et al., 2010a). Src homology 2 (SH2) domain-containing inositol-5′-phosphatase 1 (SHIP1) is a negative regulator of TLR-induced responses (An et al., 2005; Gabhann et al., 2010). Many studies have shown that increased miR-155 expression in response to LPS stimulation or pathogen infection in macrophages can

lead to decreased SHIP1 expression (Cremer et al., 2009; McCoy et al., 2010; O'Connell et al., 2009). This might represent an important mechanism that is required for the propagation of a pro-inflammatory response. McCoy and colleagues showed that the inhibition of miR-155 expression by IL-10, an anti-inflammatory cytokine, led to an increase in SHIP1 expression, identifying a new target for IL-10-mediated anti-inflammatory responses (McCoy et al., 2010). Furthermore, the serine/threonine protein kinase AKT has been shown to negatively regulate miR-155, which indicates that a negative feedback loop might exist whereby sustained AKT expression can switch off miR-155 expression, allowing SHIP1 levels to increase and subsequently inhibit the AKT signaling pathway (Androulidaki et al., 2009) (Figure 8).

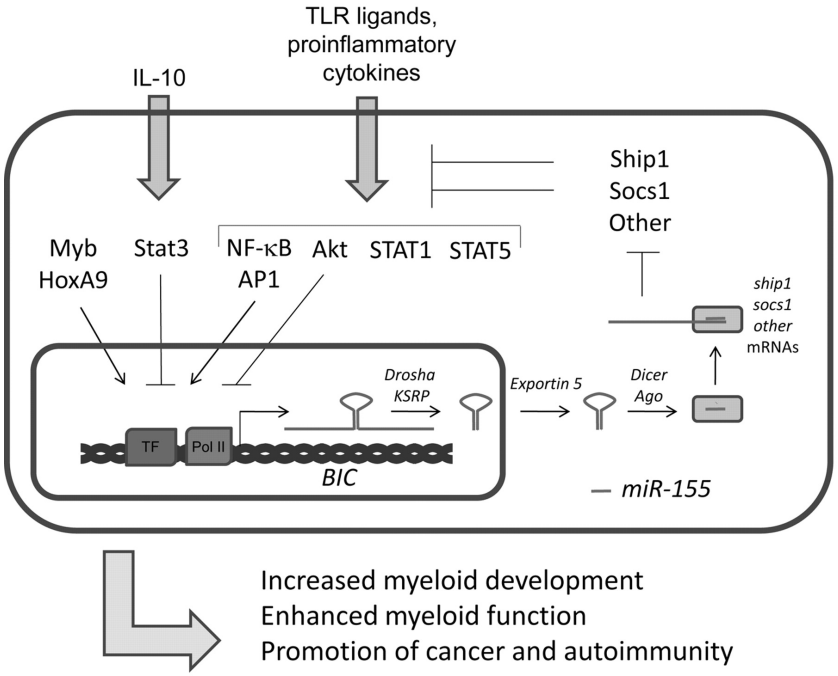


***Figure 8. Summary of miR-155 regulation and functions****. Transcription of miR-155 is up-regulated by the TFs NF-κB, AP-1, Myb, and HoxA9 and inhibited by Stat3- and Akt-dependent pathways. miR-155 targets mRNAs encoding Ship1, Socs1, as well as other proteins. Inhibition of Ship1 and Socs1 by miR-155, which themselves normally inhibit inflammatory responses, leads to enhanced activation of pro-inflammatory pathways. Functionally speaking, miR-155 has been shown to promote myeloid development and function and play a positive role in the promotion of cancer and autoimmunity. (O'Connell et al., 2011).*

miR-155 deficient T cells exhibit a Th2 bias (Rodriguez et al., 2007; Thai et al., 2007). In T lymphocytes, miR-155 promotes the development of inflammatory T cells including the T helper 17 (Th17) cell and Th1 cell subsets (O'Connell et al., 2010a). Moreover, miR-155 is shown to be involved in nTreg cell mediated tolerance by decreasing the susceptibility of conventional human as well as murine $CD4^+$ Th cells to nTreg cell-mediated suppression (Stahl et al., 2009). miR-155 is also important for nTreg fitness: it is induced by the nTreg master regulator forkhead box P3 (FoxP3) and increases their competitiveness, at least in part by targeting suppressor of cytokine signaling 1 (SOCS1) protein (Lu et al., 2009).

miR-155 is also important in B-cell-mediated antibody production and immunity (Rodriguez et al., 2007; Thai et al., 2007). miR-155 knockout mice exhibit reduced numbers of germinal centre (GC) B cells, and failed to develop an immune response to pathogens upon immunostimulation (Thai et al., 2007). These defective responses appear to be mediated through the involvement of miR-155 in B cell production of high affinity immunoglobulin-1 (IgG1) antibodies, the development of B cell memory and the production of TNFalpha (Thai et al., 2007; Vigorito et al., 2007). Recent studies with miR-155-deficient mice revealed elevated levels of activation induced cytidine diamine (AID) (Teng et al., 2008). This enzyme catalyses the deamination of cytosine residues and introduction of U:G mismatches, that is required for the generation of the secondary antibody repertoire through somatic hypermutation, gene conversion and class switching form IgM to IgG1 (Dorsett et al., 2008; Teng et al., 2008). The gene-

encoding AID contains a miR-155 binding site in its 3' UTR (Thai et al., 2007). Genetically modified mice with a mutation in the 3' UTR binding site for miR-155 in the AID gene that blocks miR-155 binding show increased AID levels, compared with wilde type (WT) cells and disrupted affinity maturation. miR-155 thus closely regulates AID expression in cells to prevent hypermutational activity. These in vivo experiments confirm that miR-155 is especially important for B cell development and identify AID as a key target (Dorsett et al., 2008; Teng et al., 2008).

Taken together, these studies strongly support a functional role of miR-155 in both innate and adaptive immune responses.

**miRNA expression in TAMs**

Several studies investigated the function of miRNAs that are either up regulated or down regulated in macrophages upon inflammatory stimulation (e.g., by LPS, IFN, inflammatory cytokines, etc.). Conversely, miRNAs that are constitutively expressed by tissue macrophages (and thus are not upregulated by inflammatory stimuli) are still poorly characterized. Further studies are necessary to identify and address the biological relevance of the miRNAs that are constitutively expressed in distinct tissue macrophage subtypes.

Macrophages constitute an important fraction of the tumor-associated stromal cells. In tumors, macrophages express a high amount of proangiogenic and protumoral genes, which contribute to tumor growth and progression. In spite of the well-recognized role of macrophages in promoting tumor growth, the molecular intrinsic

signals that control the expression of protumoral genes in macrophages are poorly known. It is conceivable that miRNAs expressed by TAMs-could finely tune the expression of hundreds of protumoral genes and thus control TAM behavior and function in tumors.

# Scope of the thesis

Macrophages are scavenger cells that clear tissues from invading pathogens and other foreign agents, and also regulate tissue homeostasis by scavenging necrotic cell debris and ECM molecules during tissue growth and remodeling. Macrophages are also regulators of tumor growth; tumor-associated macrophages (TAMs) support tumor growth by diverse mechanisms, including the promotion of angiogenesis and tissue remodeling (Coffelt et al., 2010a; Qian and Pollard, 2010). Evidence for their role in tumor progression has been established by several different experimental approaches, including the inhibition of tumor-derived TAM chemoattractants (Lin et al., 2001) or cell depletion studies (De Palma et al., 2005) in mouse models of cancer. It is increasingly appreciated that TAMs comprise molecularly and functionally distinct subsets (Pucci et al., 2009; Qian and Pollard, 2010; Squadrito and De Palma, 2011). In this regard, one particular TAM subset, the Tie2-expressing monocytes (TEMs), has been shown to play an important role in the promotion of tumor angiogenesis (De Palma et al., 2005; De Palma et al., 2003b).

The fact that, number and/or distribution of TAMs correlates to prognosis in different types of human malignancy promoted the development of novel therapies targeting TAMs to modulate host immune responses to solid tumors.

Chapter 2

Among the angiogenic molecules, the Tie2 ligands angiopoietins (ANGs) represent an important class. We and others, previously demonstrated that TEMs, but not $TIE2^-$ monocytes, respond to ANG2 stimulation in vitro (Coffelt et al., 2010b; Murdoch et al., 2007b; Venneri et al., 2007), suggesting that the ANG2-TIE2 axis may also regulate TEM functions in vivo. As first main goal of this thesis we asked whether targeting the ANG/TIE2 signaling pathway would inhibit tumor angiogenesis and growth also by interfering with TEM's proangiogenic activity. Towards this goal, we investigated the role of the ANG2/TIE2 axis in driving TEM-mediated tumor angiogenesis in various tumor models by employing both a monoclonal antibody to ANG2 and a conditional lentiviral vector platform for specifically knocking down TIE2 in TEMs (Mazzieri et al., 2011).

Chapter 3

Although it is known that many miRNAs are highly expressed by human macrophages cultured *in vitro* (Tserel et al., 2011), the biological significance of miRNA expression by TAMs is still unclear. Therefore, the second main goal of this thesis was to investigate whether miRNAs, and in particular miR-155, could influence the *in vivo* function of TAMs. Recent studies have shown that miR-155 increases substantially after exposure of monocytes/macrophages and myeloid dendritic cells to a variety of inflammatory stimuli (Brown et al., 2007; O'Connell et al., 2007). By

combining a myeloid specific miR-155 knockdown LV platform with bone marrow transplantation into mouse tumor models, we studied the *in vivo* role of miR-155 in TAMs. These studies established an antitumoral role for the inflammation-associated miR-155 prompting further studies into its mechanism of action to provide a framework for selectively modulating macrophages activities in tumors.

# References


Adams, D.O., Johnson, W.J., and Marino, P.A. (1982). Mechanisms of target recognition and destruction in macrophage-mediated tumor cytotoxicity. Fed Proc *41*, 2212-2221.

Akira, S., Uematsu, S., and Takeuchi, O. (2006). Pathogen recognition and innate immunity. Cell *124*, 783-801.

An, H., Xu, H., Zhang, M., Zhou, J., Feng, T., Qian, C., Qi, R., and Cao, X. (2005). Src homology 2 domain-containing inositol-5-phosphatase 1 (SHIP1) negatively regulates TLR4-mediated LPS response primarily through a phosphatase activity- and PI-3K-independent mechanism. Blood *105*, 4685-4692.

Androulidaki, A., Iliopoulos, D., Arranz, A., Doxaki, C., Schworer, S., Zacharioudaki, V., Margioris, A.N., Tsichlis, P.N., and Tsatsanis, C. (2009). The kinase Akt1 controls macrophage response to lipopolysaccharide by regulating microRNAs. Immunity *31*, 220-231.

Arai, F., Hirao, A., Ohmura, M., Sato, H., Matsuoka, S., Takubo, K., Ito, K., Koh, G.Y., and Suda, T. (2004). Tie2/angiopoietin-1 signaling regulates hematopoietic stem cell quiescence in the bone marrow niche. Cell *118*, 149-161.

Augustin, H.G., Koh, G.Y., Thurston, G., and Alitalo, K. (2009). Control of vascular morphogenesis and homeostasis through the angiopoietin-Tie system. Nat Rev Mol Cell Biol *10*, 165-177.

Bala, S., Marcos, M., Kodys, K., Csak, T., Catalano, D., Mandrekar, P., and Szabo, G. (2011). Up-regulation of microRNA-155 in macrophages contributes to increased tumor necrosis factor {alpha} (TNF{alpha}) production via increased mRNA half-life in alcoholic liver disease. J Biol Chem *286*, 1436-1444.

Balkwill, F., and Mantovani, A. (2001). Inflammation and cancer: back to Virchow? Lancet *357*, 539-545.

Balkwill, F.R. (2012). The chemokine system and cancer. J Pathol *226*, 148-157.

Barrientos, S., Stojadinovic, O., Golinko, M.S., Brem, H., and Tomic-Canic, M. (2008). Growth factors and cytokines in wound healing. Wound Repair Regen *16*, 585-601.

Bartel, D.P. (2009). MicroRNAs: target recognition and regulatory functions. Cell *136*, 215-233.

Barton, W.A., Tzvetkova-Robev, D., Miranda, E.P., Kolev, M.V., Rajashankar, K.R., Himanen, J.P., and Nikolov, D.B. (2006). Crystal structures of the Tie2 receptor ectodomain and the angiopoietin-2-Tie2 complex. Nat Struct Mol Biol *13*, 524-532.

Bergers, G., and Benjamin, L.E. (2003). Tumorigenesis and the angiogenic switch. Nat Rev Cancer *3*, 401-410.

Bergers, G., Brekken, R., McMahon, G., Vu, T.H., Itoh, T., Tamaki, K., Tanzawa, K., Thorpe, P., Itohara, S., Werb, Z.*, et al.* (2000). Matrix metalloproteinase-9 triggers the angiogenic switch during carcinogenesis. Nat Cell Biol *2*, 737-744.

Biswas, S.K., Gangi, L., Paul, S., Schioppa, T., Saccani, A., Sironi, M., Bottazzi, B., Doni, A., Vincenzo, B., Pasqualini, F.*, et al.* (2006). A distinct and unique transcriptional program expressed by tumor-associated macrophages (defective NF-kappaB and enhanced IRF-3/STAT1 activation). Blood *107*, 2112-2122.

Brown, B.D., Gentner, B., Cantore, A., Colleoni, S., Amendola, M., Zingale, A., Baccarini, A., Lazzari, G., Galli, C., and Naldini, L. (2007). Endogenous microRNA can be broadly exploited to regulate transgene expression according to tissue, lineage and differentiation state. Nat Biotechnol *25*, 1457-1467.

Carmeliet, P., and Jain, R.K. (2011). Molecular mechanisms and clinical applications of angiogenesis. Nature *473*, 298-307.

Chambers, A.F., Groom, A.C., and MacDonald, I.C. (2002). Dissemination and growth of cancer cells in metastatic sites. Nat Rev Cancer *2*, 563-572.

Chinetti-Gbaguidi, G., and Staels, B. (2011). Macrophage polarization in metabolic disorders: functions and regulation. Curr Opin Lipidol *22*, 365-372.

Coffelt, S.B., Lewis, C.E., Naldini, L., Brown, J.M., Ferrara, N., and De Palma, M. (2010a). Elusive identities and overlapping phenotypes of proangiogenic myeloid cells in tumors. Am J Pathol *176*, 1564-1576.

Coffelt, S.B., Tal, A.O., Scholz, A., De Palma, M., Patel, S., Urbich, C., Biswas, S.K., Murdoch, C., Plate, K.H., Reiss, Y.*, et al.* (2010b). Angiopoietin-2 regulates gene expression in TIE2-expressing monocytes and augments their inherent proangiogenic functions. Cancer Res *70*, 5270-5280.

Colotta, F., Allavena, P., Sica, A., Garlanda, C., and Mantovani, A. (2009). Cancer-related inflammation, the seventh hallmark of cancer: links to genetic instability. Carcinogenesis *30*, 1073-1081.

Condeelis, J., and Pollard, J.W. (2006). Macrophages: obligate partners for tumor cell migration, invasion, and metastasis. Cell *124*, 263-266.

Coussens, L.M., and Werb, Z. (2002). Inflammation and cancer. Nature *420*, 860-867.

Cremer, T.J., Ravneberg, D.H., Clay, C.D., Piper-Hunter, M.G., Marsh, C.B., Elton, T.S., Gunn, J.S., Amer, A., Kanneganti, T.D., Schlesinger, L.S.*, et al.* (2009). MiR-155 induction by F. novicida but not the virulent F. tularensis results in SHIP down-regulation and enhanced pro-inflammatory cytokine response. PLoS One *4*, e8508.

Curiel, T.J., Coukos, G., Zou, L., Alvarez, X., Cheng, P., Mottram, P., Evdemon-Hogan, M., Conejo-Garcia, J.R., Zhang, L., Burow, M.*, et al.* (2004). Specific recruitment of regulatory T cells in ovarian carcinoma fosters immune privilege and predicts reduced survival. Nat Med *10*, 942-949.

Czech, B., and Hannon, G.J. (2011). Small RNA sorting: matchmaking for Argonautes. Nat Rev Genet *12*, 19-31.

Davis, S., Papadopoulos, N., Aldrich, T.H., Maisonpierre, P.C., Huang, T., Kovac, L., Xu, A., Leidich, R., Radziejewska, E., Rafique, A.*, et al.* (2003). Angiopoietins have distinct modular domains essential for receptor binding, dimerization and superclustering. Nat Struct Biol *10*, 38-44.

De Palma, M., Mazzieri, R., Politi, L.S., Pucci, F., Zonari, E., Sitia, G., Mazzoleni, S., Moi, D., Venneri, M.A., Indraccolo, S.*, et al.* (2008). Tumor-targeted interferon-alpha delivery by Tie2-expressing monocytes inhibits tumor growth and metastasis. Cancer Cell *14*, 299-311.

De Palma, M., Venneri, M.A., Galli, R., Sergi Sergi, L., Politi, L.S., Sampaolesi, M., and Naldini, L. (2005). Tie2 identifies a hematopoietic lineage of proangiogenic monocytes required for tumor vessel formation and a mesenchymal population of pericyte progenitors. Cancer Cell *8*, 211-226.

De Palma, M., Venneri, M.A., Roca, C., and Naldini, L. (2003). Targeting exogenous genes to tumor angiogenesis by transplantation of genetically modified hematopoietic stem cells. Nat Med *9*, 789-795.

de Visser, K.E., and Coussens, L.M. (2006). The inflammatory tumor microenvironment and its impact on cancer development. Contrib Microbiol *13*, 118-137.

DeNardo, D.G., Andreu, P., and Coussens, L.M. (2010). Interactions between lymphocytes and myeloid cells regulate pro- versus anti-tumor immunity. Cancer Metastasis Rev *29*, 309-316.

DeNardo, D.G., Barreto, J.B., Andreu, P., Vasquez, L., Tawfik, D., Kolhatkar, N., and Coussens, L.M. (2009). CD4(+) T cells regulate pulmonary metastasis of mammary carcinomas by enhancing protumor properties of macrophages. Cancer Cell *16*, 91-102.

Desai, K.V., Xiao, N., Wang, W., Gangi, L., Greene, J., Powell, J.I., Dickson, R., Furth, P., Hunter, K., Kucherlapati, R.*, et al.* (2002). Initiating oncogenic event determines gene-expression patterns of human breast cancer models. Proc Natl Acad Sci U S A *99*, 6967-6972.

Dorsett, Y., McBride, K.M., Jankovic, M., Gazumyan, A., Thai, T.H., Robbiani, D.F., Di Virgilio, M., Reina San-Martin, B., Heidkamp, G., Schwickert, T.A.*, et al.* (2008). MicroRNA-155 suppresses activation-induced cytidine deaminase-mediated Myc-Igh translocation. Immunity *28*, 630-638.

Dumont, D.J., Gradwohl, G., Fong, G.H., Puri, M.C., Gertsenstein, M., Auerbach, A., and Breitman, M.L. (1994). Dominant-negative and targeted null mutations in the endothelial receptor tyrosine kinase, tek, reveal a critical role in vasculogenesis of the embryo. Genes Dev *8*, 1897-1909.

Dumont, D.J., Yamaguchi, T.P., Conlon, R.A., Rossant, J., and Breitman, M.L. (1992). tek, a novel tyrosine kinase gene located on mouse chromosome 4, is expressed in endothelial cells and their presumptive precursors. Oncogene *7*, 1471-1480.

Egeblad, M., Nakasone, E.S., and Werb, Z. (2010). Tumors as organs: complex tissues that interface with the entire organism. Dev Cell *18*, 884-901.

El Gazzar, M., and McCall, C.E. (2011). MicroRNAs regulatory networks in myeloid lineage development and differentiation: regulators of the regulators. Immunol Cell Biol.

Fantin, A., Vieira, J.M., Gestri, G., Denti, L., Schwarz, Q., Prykhozhij, S., Peri, F., Wilson, S.W., and Ruhrberg, C. (2010). Tissue macrophages act as cellular chaperones for vascular anastomosis downstream of VEGF-mediated endothelial tip cell induction. Blood *116*, 829-840.

Fazi, F., Rosa, A., Fatica, A., Gelmetti, V., De Marchis, M.L., Nervi, C., and Bozzoni, I. (2005). A minicircuitry comprised of microRNA-223 and transcription factors NFI-A and C/EBPalpha regulates human granulopoiesis. Cell *123*, 819-831.

Fidler, I.J., and Schroit, A.J. (1988). Recognition and destruction of neoplastic cells by activated macrophages: discrimination of altered self. Biochim Biophys Acta *948*, 151-173.

Fiedler, U., and Augustin, H.G. (2006). Angiopoietins: a link between angiogenesis and inflammation. Trends Immunol *27*, 552-558.

Fiedler, U., Scharpfenecker, M., Koidl, S., Hegen, A., Grunow, V., Schmidt, J.M., Kriz, W., Thurston, G., and Augustin, H.G. (2004). The Tie-2 ligand angiopoietin-2 is stored in and rapidly released upon stimulation from endothelial cell Weibel-Palade bodies. Blood *103*, 4150-4156.

Finch, C.E., and Crimmins, E.M. (2004). Inflammatory exposure and historical changes in human life-spans. Science *305*, 1736-1739.

Fischer, C., Mazzone, M., Jonckx, B., and Carmeliet, P. (2008). FLT1 and its ligands VEGFB and PlGF: drug targets for anti-angiogenic therapy? Nat Rev Cancer *8*, 942-956.

Fontana, L., Pelosi, E., Greco, P., Racanicchi, S., Testa, U., Liuzzi, F., Croce, C.M., Brunetti, E., Grignani, F., and Peschle, C. (2007). MicroRNAs 17-5p-20a-106a control monocytopoiesis through AML1 targeting and M-CSF receptor upregulation. Nat Cell Biol *9*, 775-787.

Fukao, T., Fukuda, Y., Kiga, K., Sharif, J., Hino, K., Enomoto, Y., Kawamura, A., Nakamura, K., Takeuchi, T., and Tanabe, M. (2007). An

evolutionarily conserved mechanism for microRNA-223 expression revealed by microRNA gene profiling. Cell *129*, 617-631.

Gabhann, J.N., Higgs, R., Brennan, K., Thomas, W., Damen, J.E., Ben Larbi, N., Krystal, G., and Jefferies, C.A. (2010). Absence of SHIP-1 results in constitutive phosphorylation of tank-binding kinase 1 and enhanced TLR3-dependent IFN-beta production. J Immunol *184*, 2314-2320.

Gentner, B., Schira, G., Giustacchini, A., Amendola, M., Brown, B.D., Ponzoni, M., and Naldini, L. (2009). Stable knockdown of microRNA in vivo by lentiviral vectors. Nat Methods *6*, 63-66.

Gocheva, V., Wang, H.W., Gadea, B.B., Shree, T., Hunter, K.E., Garfall, A.L., Berman, T., and Joyce, J.A. (2010). IL-4 induces cathepsin protease activity in tumor-associated macrophages to promote cancer growth and invasion. Genes Dev *24*, 241-255.

Gordon, S., and Martinez, F.O. (2010). Alternative activation of macrophages: mechanism and functions. Immunity *32*, 593-604.

Gouon-Evans, V., Rothenberg, M.E., and Pollard, J.W. (2000). Postnatal mammary gland development requires macrophages and eosinophils. Development *127*, 2269-2282.

Grivennikov, S.I., Greten, F.R., and Karin, M. (2010). Immunity, inflammation, and cancer. Cell *140*, 883-899.

Guy, C.T., Cardiff, R.D., and Muller, W.J. (1992). Induction of mammary tumors by expression of polyomavirus middle T oncogene: a transgenic mouse model for metastatic disease. Mol Cell Biol *12*, 954-961.

Hagemann, T., Wilson, J., Burke, F., Kulbe, H., Li, N.F., Pluddemann, A., Charles, K., Gordon, S., and Balkwill, F.R. (2006). Ovarian cancer cells polarize macrophages toward a tumor-associated phenotype. J Immunol *176*, 5023-5032.

Halin, S., Rudolfsson, S.H., Van Rooijen, N., and Bergh, A. (2009). Extratumoral macrophages promote tumor and vascular growth in an orthotopic rat prostate tumor model. Neoplasia *11*, 177-186.

Han, J., Lee, Y., Yeom, K.H., Nam, J.W., Heo, I., Rhee, J.K., Sohn, S.Y., Cho, Y., Zhang, B.T., and Kim, V.N. (2006). Molecular basis for the recognition of primary microRNAs by the Drosha-DGCR8 complex. Cell *125*, 887-901.

Hanahan, D., and Weinberg, R.A. (2000). The hallmarks of cancer. Cell *100*, 57-70.

Hurst, J., Maniar, N., Tombarkiewicz, J., Lucas, F., Roberson, C., Steplewski, Z., James, W., and Perras, J. (1993). A novel model of a metastatic human breast tumour xenograft line. Br J Cancer *68*, 274-276.

Hussain, S.P., Hofseth, L.J., and Harris, C.C. (2003). Radical causes of cancer. Nat Rev Cancer *3*, 276-285.

Johnnidis, J.B., Harris, M.H., Wheeler, R.T., Stehling-Sun, S., Lam, M.H., Kirak, O., Brummelkamp, T.R., Fleming, M.D., and Camargo, F.D. (2008). Regulation of progenitor cell proliferation and granulocyte function by microRNA-223. Nature *451*, 1125-1129.

Khanna, C., and Hunter, K. (2005). Modeling metastasis in vivo. Carcinogenesis *26*, 513-523.

Kim, J.B., O'Hare, M.J., and Stein, R. (2004). Models of breast cancer: is merging human and animal models the future? Breast Cancer Res *6*, 22-30.

Kim, V.N., Han, J., and Siomi, M.C. (2009). Biogenesis of small RNAs in animals. Nat Rev Mol Cell Biol *10*, 126-139.

Kuang, D.M., Zhao, Q., Peng, C., Xu, J., Zhang, J.P., Wu, C., and Zheng, L. (2009). Activated monocytes in peritumoral stroma of hepatocellular carcinoma foster immune privilege and disease progression through PD-L1. J Exp Med *206*, 1327-1337.

Lee, S.J., Evers, S., Roeder, D., Parlow, A.F., Risteli, J., Risteli, L., Lee, Y.C., Feizi, T., Langen, H., and Nussenzweig, M.C. (2002). Mannose receptor-mediated regulation of serum glycoprotein homeostasis. Science *295*, 1898-1901.

Leek, R.D., Lewis, C.E., Whitehouse, R., Greenall, M., Clarke, J., and Harris, A.L. (1996). Association of macrophage infiltration with angiogenesis and prognosis in invasive breast carcinoma. Cancer Res *56*, 4625-4629.

Lemmon, M.A., and Schlessinger, J. (2010). Cell signaling by receptor tyrosine kinases. Cell *141*, 1117-1134.

Li, M.O., Wan, Y.Y., Sanjabi, S., Robertson, A.K., and Flavell, R.A. (2006). Transforming growth factor-beta regulation of immune responses. Annu Rev Immunol *24*, 99-146.

Lin, E.Y., Jones, J.G., Li, P., Zhu, L., Whitney, K.D., Muller, W.J., and Pollard, J.W. (2003). Progression to malignancy in the polyoma middle T oncoprotein mouse breast cancer model provides a reliable model for human diseases. Am J Pathol *163*, 2113-2126.

Lin, E.Y., Li, J.F., Gnatovskiy, L., Deng, Y., Zhu, L., Grzesik, D.A., Qian, H., Xue, X.N., and Pollard, J.W. (2006). Macrophages regulate the angiogenic switch in a mouse model of breast cancer. Cancer Res *66*, 11238-11246.

Lin, E.Y., Nguyen, A.V., Russell, R.G., and Pollard, J.W. (2001). Colony-stimulating factor 1 promotes progression of mammary tumors to malignancy. J Exp Med *193*, 727-740.

Lin, E.Y., and Pollard, J.W. (2007). Tumor-associated macrophages press the angiogenic switch in breast cancer. Cancer Res *67*, 5064-5066.

Lindsay, M.A. (2008). microRNAs and the immune response. Trends Immunol *29*, 343-351.

Liu, G., Friggeri, A., Yang, Y., Park, Y.J., Tsuruta, Y., and Abraham, E. (2009). miR-147, a microRNA that is induced upon Toll-like receptor stimulation, regulates murine macrophage inflammatory responses. Proc Natl Acad Sci U S A *106*, 15819-15824.

Luo, J., Solimini, N.L., and Elledge, S.J. (2009). Principles of cancer therapy: oncogene and non-oncogene addiction. Cell *136*, 823-837.

Ma, F., Liu, X., Li, D., Wang, P., Li, N., Lu, L., and Cao, X. (2010). MicroRNA-466l upregulates IL-10 expression in TLR-triggered macrophages by antagonizing RNA-binding protein tristetraprolin-mediated IL-10 mRNA degradation. J Immunol *184*, 6053-6059.

MacDonald, K.P., Palmer, J.S., Cronau, S., Seppanen, E., Olver, S., Raffelt, N.C., Kuns, R., Pettit, A.R., Clouston, A., Wainwright, B.*, et al.* (2010). An antibody against the colony-stimulating factor 1 receptor depletes the resident subset of monocytes and tissue- and tumor-associated macrophages but does not inhibit inflammation. Blood *116*, 3955-3963.

Maeda, H., and Akaike, T. (1998). Nitric oxide and oxygen radicals in infection, inflammation, and cancer. Biochemistry (Mosc) *63*, 854-865.

Maglione, J.E., Moghanaki, D., Young, L.J., Manner, C.K., Ellies, L.G., Joseph, S.O., Nicholson, B., Cardiff, R.D., and MacLeod, C.L. (2001). Transgenic Polyoma middle-T mice model premalignant mammary disease. Cancer Res *61*, 8298-8305.

Mantovani, A., Allavena, P., Sica, A., and Balkwill, F. (2008). Cancer-related inflammation. Nature *454*, 436-444.

Mantovani, A., Sozzani, S., Locati, M., Allavena, P., and Sica, A. (2002). Macrophage polarization: tumor-associated macrophages as a paradigm for polarized M2 mononuclear phagocytes. Trends Immunol *23*, 549-555.

Mazzieri, R., Pucci, F., Moi, D., Zonari, E., Ranghetti, A., Berti, A., Politi, L.S., Gentner, B., Brown, J.L., Naldini, L.*, et al.* (2011). Targeting the ANG2/TIE2 axis inhibits tumor growth and metastasis by impairing angiogenesis and disabling rebounds of proangiogenic myeloid cells. Cancer Cell *19*, 512-526.

McCoy, C.E., Sheedy, F.J., Qualls, J.E., Doyle, S.L., Quinn, S.R., Murray, P.J., and O'Neill, L.A. (2010). IL-10 inhibits miR-155 induction by toll-like receptors. J Biol Chem *285*, 20492-20498.

Mills, C.D., Kincaid, K., Alt, J.M., Heilman, M.J., and Hill, A.M. (2000). M-1/M-2 macrophages and the Th1/Th2 paradigm. J Immunol *164*, 6166-6173.

Mills, C.D., Shearer, J., Evans, R., and Caldwell, M.D. (1992). Macrophage arginine metabolism and the inhibition or stimulation of cancer. J Immunol *149*, 2709-2714.

Movahedi, K., Laoui, D., Gysemans, C., Baeten, M., Stange, G., Van den Bossche, J., Mack, M., Pipeleers, D., In't Veld, P., De Baetselier, P.*, et al.* (2010). Different tumor microenvironments contain functionally distinct subsets of macrophages derived from Ly6C(high) monocytes. Cancer Res *70*, 5728-5739.

Murdoch, C., Muthana, M., Coffelt, S.B., and Lewis, C.E. (2008). The role of myeloid cells in the promotion of tumour angiogenesis. Nat Rev Cancer *8*, 618-631.

Murdoch, C., Tazzyman, S., Webster, S., and Lewis, C.E. (2007). Expression of Tie-2 by human monocytes and their responses to angiopoietin-2. J Immunol *178*, 7405-7411.

Nakasa, T., Miyaki, S., Okubo, A., Hashimoto, M., Nishida, K., Ochi, M., and Asahara, H. (2008). Expression of microRNA-146 in rheumatoid arthritis synovial tissue. Arthritis Rheum *58*, 1284-1292.

Nasarre, P., Thomas, M., Kruse, K., Helfrich, I., Wolter, V., Deppermann, C., Schadendorf, D., Thurston, G., Fiedler, U., and Augustin, H.G. (2009). Host-derived angiopoietin-2 affects early stages of tumor development and vessel maturation but is dispensable for later stages of tumor growth. Cancer Res *69*, 1324-1333.

Negrini, S., Gorgoulis, V.G., and Halazonetis, T.D. (2010). Genomic instability--an evolving hallmark of cancer. Nat Rev Mol Cell Biol *11*, 220-228.

Nucera, S., Biziato, D., and De Palma, M. (2011). The interplay between macrophages and angiogenesis in development, tissue injury and regeneration. Int J Dev Biol *55*, 495-503.

O'Connell, R.M., Chaudhuri, A.A., Rao, D.S., and Baltimore, D. (2009). Inositol phosphatase SHIP1 is a primary target of miR-155. Proc Natl Acad Sci U S A *106*, 7113-7118.

O'Connell, R.M., Rao, D.S., Chaudhuri, A.A., Boldin, M.P., Taganov, K.D., Nicoll, J., Paquette, R.L., and Baltimore, D. (2008). Sustained expression of microRNA-155 in hematopoietic stem cells causes a myeloproliferative disorder. J Exp Med *205*, 585-594.

O'Connell, R.M., Taganov, K.D., Boldin, M.P., Cheng, G., and Baltimore, D. (2007). MicroRNA-155 is induced during the macrophage inflammatory response. Proc Natl Acad Sci U S A *104*, 1604-1609.

O'Connell, R.M., Zhao, J.L., and Rao, D.S. (2011). MicroRNA function in myeloid biology. Blood *118*, 2960-2969.

O'Neill, L.A., Sheedy, F.J., and McCoy, C.E. (2011). MicroRNAs: the fine-tuners of Toll-like receptor signalling. Nat Rev Immunol *11*, 163-175.

Orlikowsky, T., Dannecker, G.E., Wang, Z., Horowitz, H., Niethammer, D., and Hoffmann, M.K. (1999). Activation or destruction of T cells via macrophages. Pathobiology *67*, 298-301.

Plytycz, B., and Seljelid, R. (2003). From inflammation to sickness: historical perspective. Arch Immunol Ther Exp (Warsz) *51*, 105-109.

Pollard, J.W. (2004). Tumour-educated macrophages promote tumour progression and metastasis. Nat Rev Cancer *4*, 71-78.

Pucci, F., Venneri, M.A., Biziato, D., Nonis, A., Moi, D., Sica, A., Di Serio, C., Naldini, L., and De Palma, M. (2009). A distinguishing gene signature shared by tumor-infiltrating Tie2-expressing monocytes, blood "resident" monocytes, and embryonic macrophages suggests common functions and developmental relationships. Blood *114*, 901-914.

Qian, B., Deng, Y., Im, J.H., Muschel, R.J., Zou, Y., Li, J., Lang, R.A., and Pollard, J.W. (2009). A distinct macrophage population mediates metastatic breast cancer cell extravasation, establishment and growth. PLoS One *4*, e6562.

Qian, B.Z., Li, J., Zhang, H., Kitamura, T., Zhang, J., Campion, L.R., Kaiser, E.A., Snyder, L.A., and Pollard, J.W. (2011). CCL2 recruits inflammatory monocytes to facilitate breast-tumour metastasis. Nature *475*, 222-225.

Qian, B.Z., and Pollard, J.W. (2010). Macrophage diversity enhances tumor progression and metastasis. Cell *141*, 39-51.

Rodriguez, A., Vigorito, E., Clare, S., Warren, M.V., Couttet, P., Soond, D.R., van Dongen, S., Grocock, R.J., Das, P.P., Miska, E.A.*, et al.* (2007). Requirement of bic/microRNA-155 for normal immune function. Science *316*, 608-611.

Rosa, A., Ballarino, M., Sorrentino, A., Sthandier, O., De Angelis, F.G., Marchioni, M., Masella, B., Guarini, A., Fatica, A., Peschle, C.*, et al.* (2007). The interplay between the master transcription factor PU.1 and miR-424 regulates human monocyte/macrophage differentiation. Proc Natl Acad Sci U S A *104*, 19849-19854.

Roviezzo, F., Tsigkos, S., Kotanidou, A., Bucci, M., Brancaleone, V., Cirino, G., and Papapetropoulos, A. (2005). Angiopoietin-2 causes inflammation in vivo by promoting vascular leakage. J Pharmacol Exp Ther *314*, 738-744.

Ruggiero, T., Trabucchi, M., De Santa, F., Zupo, S., Harfe, B.D., McManus, M.T., Rosenfeld, M.G., Briata, P., and Gherzi, R. (2009). LPS induces KH-type splicing regulatory protein-dependent processing of microRNA-155

precursors in macrophages. FASEB journal : official publication of the Federation of American Societies for Experimental Biology *23*, 2898-2908.

Saharinen, P., Bry, M., and Alitalo, K. (2010). How do angiopoietins Tie in with vascular endothelial growth factors? Curr Opin Hematol *17*, 198-205.

Sato, T.N., Tozawa, Y., Deutsch, U., Wolburg-Buchholz, K., Fujiwara, Y., Gendron-Maguire, M., Gridley, T., Wolburg, H., Risau, W., and Qin, Y. (1995). Distinct roles of the receptor tyrosine kinases Tie-1 and Tie-2 in blood vessel formation. Nature *376*, 70-74.

Scharpfenecker, M., Fiedler, U., Reiss, Y., and Augustin, H.G. (2005). The Tie-2 ligand angiopoietin-2 destabilizes quiescent endothelium through an internal autocrine loop mechanism. J Cell Sci *118*, 771-780.

Seegar, T.C., Eller, B., Tzvetkova-Robev, D., Kolev, M.V., Henderson, S.C., Nikolov, D.B., and Barton, W.A. (2010). Tie1-Tie2 interactions mediate functional differences between angiopoietin ligands. Mol Cell *37*, 643-655.

Sharda, D.R., Yu, S., Ray, M., Squadrito, M.L., De Palma, M., Wynn, T.A., Morris, S.M., Jr., and Hankey, P.A. (2011). Regulation of macrophage arginase expression and tumor growth by the Ron receptor tyrosine kinase. J Immunol *187*, 2181-2192.

Sheedy, F.J., Palsson-McDermott, E., Hennessy, E.J., Martin, C., O'Leary, J.J., Ruan, Q., Johnson, D.S., Chen, Y., and O'Neill, L.A. (2010). Negative regulation of TLR4 via targeting of the proinflammatory tumor suppressor PDCD4 by the microRNA miR-21. Nat Immunol *11*, 141-147.

Sica, A., Allavena, P., and Mantovani, A. (2008a). Cancer related inflammation: the macrophage connection. Cancer Lett *267*, 204-215.

Sica, A., and Bronte, V. (2007). Altered macrophage differentiation and immune dysfunction in tumor development. J Clin Invest *117*, 1155-1166.

Sica, A., Larghi, P., Mancino, A., Rubino, L., Porta, C., Totaro, M.G., Rimoldi, M., Biswas, S.K., Allavena, P., and Mantovani, A. (2008b). Macrophage polarization in tumour progression. Semin Cancer Biol *18*, 349-355.

Sonkoly, E., Wei, T., Janson, P.C., Saaf, A., Lundeberg, L., Tengvall-Linder, M., Norstedt, G., Alenius, H., Homey, B., Scheynius, A.*, et al.* (2007). MicroRNAs: novel regulators involved in the pathogenesis of psoriasis? PLoS One *2*, e610.

Squadrito, M.L., and De Palma, M. (2011). Macrophage regulation of tumor angiogenesis: implications for cancer therapy. Mol Aspects Med *32*, 123-145.

Starnes, L.M., Sorrentino, A., Pelosi, E., Ballarino, M., Morsilli, O., Biffoni, M., Santoro, S., Felli, N., Castelli, G., De Marchis, M.L.*, et al.* (2009). NFI-A directs the fate of hematopoietic progenitors to the erythroid or granulocytic lineage and controls beta-globin and G-CSF receptor expression. Blood *114*, 1753-1763.

Stein, M., Keshav, S., Harris, N., and Gordon, S. (1992). Interleukin 4 potently enhances murine macrophage mannose receptor activity: a marker of alternative immunologic macrophage activation. J Exp Med *176*, 287-292.

Stratmann, A., Risau, W., and Plate, K.H. (1998). Cell type-specific expression of angiopoietin-1 and angiopoietin-2 suggests a role in glioblastoma angiogenesis. Am J Pathol *153*, 1459-1466.

Sundberg, C., Kowanetz, M., Brown, L.F., Detmar, M., and Dvorak, H.F. (2002). Stable expression of angiopoietin-1 and other markers by cultured pericytes: phenotypic similarities to a subpopulation of cells in maturing vessels during later stages of angiogenesis in vivo. Lab Invest *82*, 387-401.

Swann, J.B., Vesely, M.D., Silva, A., Sharkey, J., Akira, S., Schreiber, R.D., and Smyth, M.J. (2008). Demonstration of inflammation-induced cancer and cancer immunoediting during primary tumorigenesis. Proc Natl Acad Sci U S A *105*, 652-656.

Taganov, K.D., Boldin, M.P., Chang, K.J., and Baltimore, D. (2006). NF-kappaB-dependent induction of microRNA miR-146, an inhibitor targeted to signaling proteins of innate immune responses. Proc Natl Acad Sci U S A *103*, 12481-12486.

Tam, W. (2001). Identification and characterization of human BIC, a gene on chromosome 21 that encodes a noncoding RNA. Gene *274*, 157-167.

Teng, G., Hakimpour, P., Landgraf, P., Rice, A., Tuschl, T., Casellas, R., and Papavasiliou, F.N. (2008). MicroRNA-155 is a negative regulator of activation-induced cytidine deaminase. Immunity *28*, 621-629.

Thai, T.H., Calado, D.P., Casola, S., Ansel, K.M., Xiao, C., Xue, Y., Murphy, A., Frendewey, D., Valenzuela, D., Kutok, J.L.*, et al.* (2007). Regulation of the germinal center response by microRNA-155. Science *316*, 604-608.

Tili, E., Croce, C.M., and Michaille, J.J. (2009). miR-155: on the crosstalk between inflammation and cancer. Int Rev Immunol *28*, 264-284.

Tili, E., Michaille, J.J., Cimino, A., Costinean, S., Dumitru, C.D., Adair, B., Fabbri, M., Alder, H., Liu, C.G., Calin, G.A.*, et al.* (2007). Modulation of miR-155 and miR-125b levels following lipopolysaccharide/TNF-alpha stimulation and their possible roles in regulating the response to endotoxin shock. J Immunol *179*, 5082-5089.

Tili, E., Michaille, J.J., Costinean, S., and Croce, C.M. (2008). MicroRNAs, the immune system and rheumatic disease. Nat Clin Pract Rheumatol *4*, 534-541.

Torroella-Kouri, M., Silvera, R., Rodriguez, D., Caso, R., Shatry, A., Opiela, S., Ilkovitch, D., Schwendener, R.A., Iragavarapu-Charyulu, V., Cardentey, Y.*, et al.* (2009). Identification of a subpopulation of macrophages in mammary tumor-bearing mice that are neither M1 nor M2 and are less differentiated. Cancer Res *69*, 4800-4809.

Tserel, L., Runnel, T., Kisand, K., Pihlap, M., Bakhoff, L., Kolde, R., Peterson, H., Vilo, J., Peterson, P., and Rebane, A. (2011). MicroRNA expression profiles of human blood monocyte-derived dendritic cells and macrophages reveal miR-511 as putative positive regulator of Toll-like receptor 4. J Biol Chem *286*, 26487-26495.

Vakkila, J., and Lotze, M.T. (2004). Inflammation and necrosis promote tumour growth. Nat Rev Immunol *4*, 641-648.

Valenzuela, D.M., Griffiths, J.A., Rojas, J., Aldrich, T.H., Jones, P.F., Zhou, H., McClain, J., Copeland, N.G., Gilbert, D.J., Jenkins, N.A.*, et al.* (1999). Angiopoietins 3 and 4: diverging gene counterparts in mice and humans. Proc Natl Acad Sci U S A *96*, 1904-1909.

Velu, C.S., Baktula, A.M., and Grimes, H.L. (2009). Gfi1 regulates miR-21 and miR-196b to control myelopoiesis. Blood *113*, 4720-4728.

Venneri, M.A., De Palma, M., Ponzoni, M., Pucci, F., Scielzo, C., Zonari, E., Mazzieri, R., Doglioni, C., and Naldini, L. (2007). Identification of proangiogenic TIE2-expressing monocytes (TEMs) in human peripheral blood and cancer. Blood *109*, 5276-5285.

Vigorito, E., Perks, K.L., Abreu-Goodger, C., Bunting, S., Xiang, Z., Kohlhaas, S., Das, P.P., Miska, E.A., Rodriguez, A., Bradley, A.*, et al.*

(2007). microRNA-155 regulates the generation of immunoglobulin class-switched plasma cells. Immunity *27*, 847-859.

Wagsater, D., Bjork, H., Zhu, C., Bjorkegren, J., Valen, G., Hamsten, A., and Eriksson, P. (2008). ADAMTS-4 and -8 are inflammatory regulated enzymes expressed in macrophage-rich areas of human atherosclerotic plaques. Atherosclerosis *196*, 514-522.

Ward, N.L., and Dumont, D.J. (2002). The angiopoietins and Tie2/Tek: adding to the complexity of cardiovascular development. Semin Cell Dev Biol *13*, 19-27.

Weigelt, B., Peterse, J.L., and van 't Veer, L.J. (2005). Breast cancer metastasis: markers and models. Nat Rev Cancer *5*, 591-602.

Wyckoff, J., Wang, W., Lin, E.Y., Wang, Y., Pixley, F., Stanley, E.R., Graf, T., Pollard, J.W., Segall, J., and Condeelis, J. (2004). A paracrine loop between tumor cells and macrophages is required for tumor cell migration in mammary tumors. Cancer Res *64*, 7022-7029.

Wyckoff, J.B., Wang, Y., Lin, E.Y., Li, J.F., Goswami, S., Stanley, E.R., Segall, J.E., Pollard, J.W., and Condeelis, J. (2007). Direct visualization of macrophage-assisted tumor cell intravasation in mammary tumors. Cancer Res *67*, 2649-2656.

Wynn, T.A., and Barron, L. (2010). Macrophages: master regulators of inflammation and fibrosis. Semin Liver Dis *30*, 245-257.

Xiao, C., and Rajewsky, K. (2009). MicroRNA control in the immune system: basic principles. Cell *136*, 26-36.

Yang, J.S., and Lai, E.C. (2011). Alternative miRNA biogenesis pathways and the interpretation of core miRNA pathway mutants. Mol Cell *43*, 892-903.

Yuan, H.T., Venkatesha, S., Chan, B., Deutsch, U., Mammoto, T., Sukhatme, V.P., Woolf, A.S., and Karumanchi, S.A. (2007). Activation of the orphan endothelial receptor Tie1 modifies Tie2-mediated intracellular signaling and cell survival. Faseb J *21*, 3171-3183.

# CHAPTER 2.

# Targeting the ANG2/TIE2 axis Inhibits Tumor Growth and Metastasis by Impairing Angiogenesis and Disabling Rebounds of Pro-angiogenic Myeloid Cells

Roberta Mazzieri[1,2,*], Ferdinando Pucci[1,2,3,*], Davide Moi[1,2], **Erika Zonari**[1,2,6], Anna Ranghetti[1,2], Alvise Berti[3], Letterio S. Politi[4], Bernhard Gentner[2,3], Jeffrey L. Brown[5], Luigi Naldini[1,2,3,†], and Michele De Palma[1,2,†]

[1]Angiogenesis and Tumor Targeting Research Unit;
[2] San Raffaele-Telethon Institute for Gene Therapy (HSR-TIGET), Division of Regenerative Medicine, Stem Cells and Gene Therapy, San Raffaele Scientific Institute, Milan, Italy.
[3]Vita-Salute San Raffaele University Medical School, Milan, Italy
[4]Neuroradiology Department, San Raffaele Hospital, Milan, Italy.
[5]AstraZeneca Pharmaceuticals, Waltham, MA.
[6]Univeristà degli Studi di Milano - Bicocca

*: These Authors contributed equally to this work
†: These Authors share senior authorship
Correspondence: depalma.michele@hsr.it (MDP) or naldini.luigi@hsr.it (LN).

**Cancer cell 2011 Apr 12;19(4):512-26**

*In this work, the candidate contributed to the development and execution of the in vivo studies with the anti-Ang2 antibody.*

## Summary

Tumor-infiltrating myeloid cells convey pro-angiogenic programs that counteract the efficacy of anti-angiogenic therapy. Here, we show that blocking angiopoietin-2 (ANG2), a TIE2 ligand and angiogenic factor expressed by activated endothelial cells (ECs), regresses the tumor vasculature and inhibits progression of late-stage, metastatic MMTV-PyMT mammary carcinomas and RIP1-Tag2 pancreatic insulinomas. ANG2 blockade did not inhibit recruitment of $MRC1^{+}$ TIE2-expressing macrophages (TEMs), but impeded their upregulation of *Tie2*, association with blood vessels, and ability to restore angiogenesis in tumors. Conditional *Tie2* gene knock-down in TEMs was sufficient to decrease tumor angiogenesis. Our findings support a model wherein the ANG2-TIE2 axis mediates cell-to-cell interactions between TEMs and ECs that are important for tumor angiogenesis and can be targeted to induce effective antitumor responses.

## Introduction

Among the signaling molecules that regulate the tumor vasculature are members of the vascular-endothelial growth factor (VEGF) pathway, some of which represent validated targets of anti-angiogenic therapies (Chung et al., 2010; Kerbel, 2008). However, anti-angiogenic treatments targeting the VEGF pathway rarely induce durable tumor responses, both in mice and cancer patients (Bergers and Hanahan, 2008), and may also favor metastasis in selected tumor models (Ebos et al., 2009; Paez-Ribes et al., 2009). Recently, tumor resistance or recurrence after anti-angiogenic therapy have been causally linked to the recruitment of bone marrow (BM)-derived myeloid cells (Shojaei et al., 2007). Damaging the tumor vasculature indeed enhances tumor hypoxia, which in turn upregulates the expression of several myeloid cell chemoattractants (e.g., stromal-cell derived factor-1, SDF1) that rouse the influx of myeloid cells to treated tumors (Bergers and Hanahan, 2008; Chan et al., 2009; Du et al., 2008). Once recruited to the tumors, myeloid cells promote angiogenesis by releasing angiogenic and tissue-remodeling factors (Coffelt et al., 2010a; De Palma et al., 2005), and also stimulate tumor cell intravasation, dissemination and metastasis (DeNardo et al., 2009; Qian and Pollard, 2010).

Angiopoietins (ANG) constitute another important class of angiogenic molecules (Augustin et al., 2009; Huang et al., 2010; Saharinen et al., 2010). ANG2 is upregulated by hypoxia and may trigger angiogenesis via an autocrine loop in endothelial cells (ECs), which express the

ANG2 receptor, TIE2. Experimental evidence supports the notion that the ANG2-TIE2 axis promotes angiogenesis in tumors by destabilizing the blood vessels (e.g., by decreasing pericyte coverage) and sensitizing ECs to proliferation signals mediated by other pro-angiogenic factors, namely VEGF (Augustin et al., 2009; Saharinen et al., 2010). However, in the absence of VEGF, ANG2 promotes EC apoptosis and consequent blood vessel regression (Augustin et al., 2009; Chae et al., 2010; Holash et al., 1999; Saharinen et al., 2010). ANG1, another TIE2 ligand, is known to promote vascular maturation by increasing EC-pericyte interactions (Augustin et al., 2009; Saharinen et al., 2010; Suri et al., 1996). Because the phenotypes of *Angpt1*-deficient and *Angpt2*-overexpressing mice are similar, ANG2 has long been regarded as an antagonist for ANG1, although more recent studies have indicated that ANG2 may function as a context-dependent TIE2 agonist (Augustin et al., 2009; Saharinen et al., 2010). Genetic or pharmacological targeting of ANG2 reduced tumor angiogenesis and delayed the growth of subcutaneous tumors to variable extent in different studies (Brown et al., 2010; Hashizume et al., 2010; Nasarre et al., 2009b; Oliner et al., 2004); the role of ANG2 in tumor angiogenesis and growth – and its therapeutic significance as a molecular target – remain controversial and poorly defined (Augustin et al., 2009; Saharinen et al., 2010). Furthermore, the benefits of targeting ANG2 need to be assessed in clinically relevant tumor models, such as spontaneous and metastatic tumors.

Expression of the ANG receptor, TIE2, is not restricted to ECs. TIE2 is weakly expressed by some circulating monocytes and is

significantly up-regulated upon their homing to tumors and differentiation into a subset of perivascular macrophages (De Palma et al., 2003, 2005, 2008) These TIE2-expressing macrophages (TEMs) have features of M2-polarized tumor-associated macrophages (TAMs) (Mantovani and Sica, 2010), promote both developmental and tumor angiogenesis (Fantin et al., 2010; Pucci et al., 2009) and are required for the formation of tumor blood vessels (De Palma et al., 2003, 2005). Because tumor-infiltrating TEMs promote vascular re-growth following therapy-induced vascular damage (Kioi et al., 2010; Kozin et al., 2010), targeting these cells might increase the efficacy of anti-angiogenic treatments by counteracting myeloid-cell mediated angiogenesis and resistance to therapy (Bergers and Hanahan, 2008).

TEMs, but not $TIE2^{-}$ monocytes, respond to ANG2 stimulation *in vitro* (Coffelt et al., 2010b; Murdoch et al., 2007; Venneri et al., 2007), suggesting that the ANG2-TIE2 axis may also regulate TEM functions *in vivo*. We then asked whether targeting the ANG/TIE2 signaling pathway would inhibit tumor angiogenesis and growth also by interfering with TEM's pro-angiogenic activity.

## Results

### ANG2 blockade inhibits tumor growth in mammary tumor models

To specifically neutralize ANG2, we used a fully humanized monoclonal antibody (clone 3.19.3) that efficiently blocks ANG2, but not ANG1 binding to TIE2 (Brown et al., 2010). Bi-weekly injections of 3.19.3, but not control immunoglobulins (IgGs) or saline (vehicle) alone, inhibited tumor growth by ~50% in MMTV-PyMT transgenic mice, which spontaneously develop aggressive and metastatic mammary carcinomas (Figure 1A and supp S1A, Mazzieri et al. 2011). We observed tumor inhibition after both early (starting at 7 weeks of age) and late (starting at 12 weeks of age) treatment schedules, indicating that ANG2 has a functional role also during late-stage tumorigenesis. Of note, the 8-week–long early treatment schedule did not select for resistance to therapy.

In order to obtain synchronized, late-stage tumors, we injected tumor cells derived from 16-week-old MMTV-PyMT mice orthotopically in the third mammary fat pad of syngenic mice. We then treated established tumors (15 days post-tumor cell injection) by either short (2 weeks) or extended (9 weeks) treatment schedules. Both treatment schedules inhibited tumor growth (Figure 1B). Following a short treatment schedule, the tumors remained inhibited for another 2 weeks, but then resumed their growth without showing accelerated growth kinetics. Upon an extended treatment schedule, the tumors remained unceasingly inhibited and appeared largely necrotic and

fibrotic at the end of the experiments (Figure 1C). Overall, ANG2 blockade inhibited the growth of orthotopic MMTV-PyMT tumors by 70-80% and extended mouse survival significantly in several independent experiments.

We observed antitumor activity of 3.19.3 also in subcutaneous A431 human carcinomas grown in athymic mice (Supp S1B, Mazzieri et al. 2011). Taken together, these results indicate that ANG2 blockade inhibits primary tumor growth without eliciting detectable resistance to the treatment, even in late-stage tumors or upon prolonged treatment schedules.

**ANG2 blockade regresses the vasculature and inhibits angiogenesis in mammary tumor models**

We then analyzed angiogenesis in spontaneous and orthotopic MMTV-PyMT carcinomas (Figure 2A-B), as well as subcutaneously growing A431 human carcinomas (Supp S2A, Mazzieri et al. 2011). We measured vascular parameters by immunofluorescence staining (IFS) and confocal microscopy of tumor sections (orthotopic MMTV-PyMT model) and flow cytometry of tumor cell suspensions obtained from multiple tumor biopsies (spontaneous MMTV-PyMT model). In orthotopic MMTV-PyMT (Figure 2A) and subcutaneous A431 (Supp S2A, Mazzieri et al. 2011) carcinomas treated according to a short schedule, 3.19.3 greatly reduced the relative tumor vascular area (measured by IFS of $CD31^+$ blood vessels). In spontaneous MMTV-PyMT tumors treated according to a late schedule, 3.19.3 significantly reduced the proportion of viable ECs among tumor-derived cells

(measured by flow cytometry; Figure 2B and Supp S2AB Mazzieri et al. 2011). Together, these data indicate profound anti-angiogenic activity of 3.19.3 in the tumor models tested.

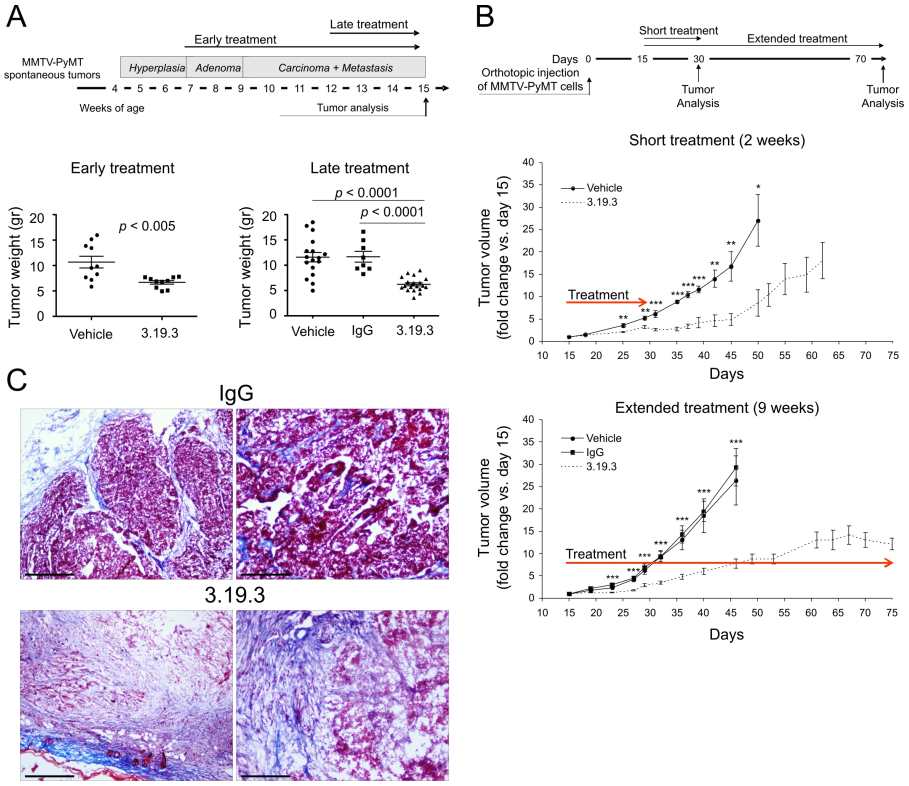


**Figure 1**. **ANG2 blockade inhibits tumor growth in MMTV-PyMT mammary tumor models**

***A****: Tumor growth in transgenic MMTV-PyMT mice. Top panel: Schematics of the early and late treatment trials. Bottom panels: Tumor weight (mean tumor weight ± SEM) of 15 week-old mice treated according to early (1 experiment; n = 10/group) or late (3*

*experiments combined; n = 8-19/group) schedules. Each dot in the plots corresponds to 1 mouse bearing multiple mammary tumors. Statistical analyses by unpaired Student's t-test.*

***B**: Tumor growth in mice carrying orthotopic, late-stage MMTV-PyMT mammary tumors. Top panel: Schematics of the experimental design. Middle and bottom panels: Tumor growth (mean tumor volume ± SEM, shown as fold-change vs. first day [day 15] of treatment) in short (middle; n = 8 mice/group) and extended (bottom; n = 10-12 mice/group) treatment trials. Statistical analyses were performed on actual tumor volume data by unpaired Student's t-test. *: $p < 0.01$; **: $p < 0.005$; ***: $p < 0.001$.*

***C**: Masson's trichrome staining of orthotopic, late-stage MMTV-PyMT mammary tumors treated according to an extended (9 weeks) treatment schedule. Collagen's blue staining demonstrates abundant fibrotic tissue and scant tumor cells in 3.19.3-treated tumors (day 78). Left panels show tumor periphery. Scale bars: 600 μm (left panels) and 300 μm (right panels). Images are representative of 5 3.19.3-treated (day 78) and 3 control IgG-treated (day 48) tumors.*

Although 3.19.3-treated tumors contained vascular-like structures heavily coated by $NG2^+$ pericytes, the inner EC lining was often discontinuous or even absent (Figure 2A; Supp Movie S1 and S2, Mazzieri et al. 2011). This feature, together with the lower ratio of $CD31^+/NG2^+$ area (Figure 2B), strongly suggested regression of established blood vessels in 3.19.3-treated tumors. Consistent with

impaired angiogenesis and vascular regression, 3.19.3 reduced tumor perfusion and dramatically increased tumor hypoxia (Figure 2C) and necrosis (Figure 2A and 2C). Of note, large hypoxic or necrotic tumor areas were frequently observed in proximity to $CD31^+$ blood vessels (Figure 2C) or $NG2^+$ sheaths lacking EC lining (Figure 2A) in the tumors of 3.19.3-treated but not untreated mice.

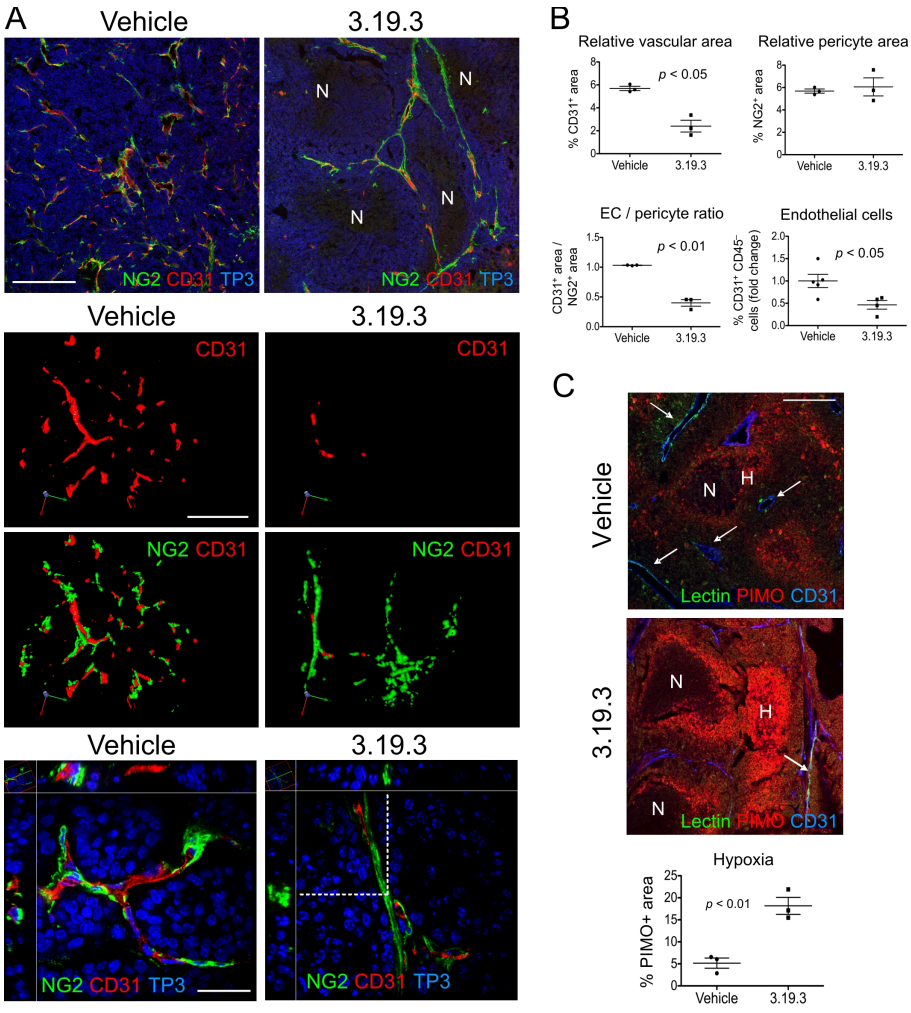

**Figure 2**. **ANG2 blockade regresses the vasculature and inhibits angiogenesis in MMTV-PyMT mammary tumor models**

***A**: NG2 (green) and CD31 (red) immunostaining, and TO-PRO-3 (TP3) nuclear staining (blue) of orthotopic, late-stage MMTV-PyMT mammary tumors treated according to a short (2 weeks) schedule and analyzed immediately after discontinuation of therapy. Top panels show confocal images of representative tumor sections; N indicates necrotic tumor areas. Scale bar: 300 μm. Middle panels show images of 3-dimensional models obtained by surface rendering of the confocal z-stacks, after superimposition of multiple confocal planes (section thickness: 16 μm). Scale bar: 150 μm. Bottom panels show superimposition of multiple confocal z-stacks imaging individual blood vessels. Scale bar: 50 μm. Results are representative of two independent experiments and 10 tumors/group analyzed.*

***B**: Morphometric (Relative vascular area; Relative pericyte area; Endothelial / pericyte ratio) and flow cytometry (Endothelial cells) analyses of angiogenesis in orthotopic (morphometric analyses) and spontaneous (flow cytometry) MMTV-PyMT mammary tumors. Each dot in the plots corresponds to 1 tumor; scatter plots show mean values ± SEM. Statistical analyses by unpaired Student's t-test.*

***C**: Top panels: Lectin (green), hypoxia (PIMO; red) and CD31 (blue) immunostaining of orthotopic, late-stage MMTV-PyMT mammary tumors treated according to a short (2 weeks) schedule. N indicates necrotic tumor areas; H indicates hypoxic areas; arrows indicate lectin$^+$/CD31$^+$ perfused blood vessels. Scale bar: 150 μm. Results are representative of two independent experiments and 8 tumors/group*

*analyzed. Bottom panel: Quantification of hypoxia in 3 representative tumors (mean % of PIMO$^+$ area ± SEM). Statistical analyses by unpaired Student's t-test.*

**ANG2 blockade inhibits progression and angiogenesis of late-stage pancreatic islet tumors**

It has been reported that late-stage RIP1-Tag2 pancreatic islet tumors are insensitive to VEGF/VEGFR2 blockade (Casanovas et al., 2005; Shojaei et al., 2008). We then investigated whether late-stage islet tumors are sensitive to ANG2 blockade following a treatment schedule similar to that used by Hanahan and co-workers (Casanovas et al., 2005). To this aim, we treated 12-week old, RIP1-Tag2 mice with biweekly injections of either vehicle or 3.19.3 for 3.5 weeks (Figure 3A). The mice were euthanized at 15.5 weeks of age, when most of the vehicle- but not 3.19.3-treated mice showed signs of distress (data not shown). We also euthanized a group of untreated mice at 12 weeks of age (t0), in order to obtain pancreatic tissue at a time-point coinciding with the initiation of therapy (Figure 3A).

3.19.3 significantly reduced the mean tumor area (vs. vehicle; Figure 3A) calculated by measuring each of the islet tumors scored in the largest pancreatic section (28-72 tumors *per* section; supp S3, Mazzieri et al. 2011). Of note, large tumors exceeding 0.5 mm$^2$ of area were significantly fewer in 3.19.3-treated than control mice (Figure 3A and supp S3, Mazzieri et al. 2011), indicating that ANG2 blockade effectively inhibited the progression of advanced tumors in

RIP1-Tag2 mice. Furthermore, 3.19.3 did not increase local invasion by islet tumors, as shown by the similar proportions of non-invasive, partially invasive (IC1) or entirely invasive (IC2) tumors (Ebos et al., 2009; Paez-Ribes et al., 2009) in 3.19.3-treated and control mice (Figure 3B).

We then studied tumor angiogenesis. 3.19.3 greatly reduced the relative tumor vascular area, measured by IFS of $CD31^+$ blood vessels (Figure 3C-D). Of note, the relative tumor vascular area was similar in t0 (12 weeks of age) and vehicle-treated (15.5 weeks of age) mice, but was reduced by more than 50% in 3.19.3-treated mice (15.5 weeks of age). As seen in MMTV-PyMT carcinomas, 3.19.3 enhanced pericyte coverage of tumor blood vessels (Figure 3C-D). These data indicate profound anti-angiogenic activity of ANG2 blockade in late-stage, pancreatic islet tumors.

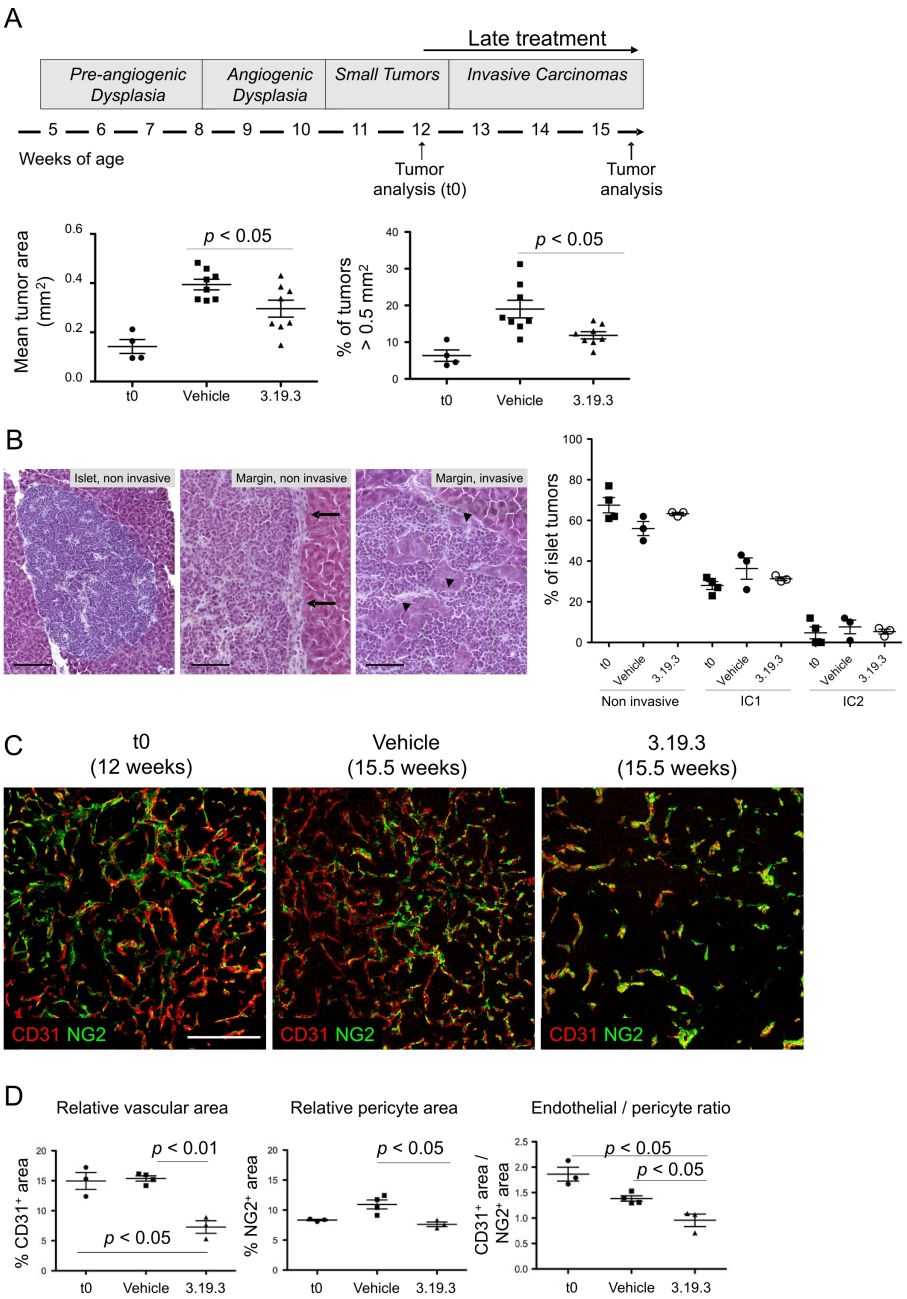
A
Late treatment
Pre-angiogenic Dysplasia
Angiogenic Dysplasia
Small Tumors
Invasive Carcinomas
5 6 7 8 9 10 11 12 13 14 15
Weeks of age
Tumor analysis (t0)
Tumor analysis
Mean tumor area (mm²)
p < 0.05
t0
Vehicle
3.19.3
% of tumors > 0.5 mm²
p < 0.05
B
Islet, non invasive
Margin, non invasive
Margin, invasive
% of islet tumors
Non invasive
IC1
IC2
C
t0 (12 weeks)
Vehicle (15.5 weeks)
3.19.3 (15.5 weeks)
CD31 NG2
D
Relative vascular area
Relative pericyte area
Endothelial / pericyte ratio
% CD31⁺ area
p < 0.01
p < 0.05
% NG2⁺ area
CD31⁺ area / NG2⁺ area

**Figure 3**. **ANG2 blockade inhibits progression and angiogenesis of late-stage, RIP1-Tag2 pancreatic islet tumors**

***A****: Top panel: schematics of the late treatment trial. Bottom left panel: mean tumor area (± SEM; two independent experiments combined; n = 4-8/group). Bottom right panel: proportion (%) of tumors exceeding 0.5 mm$^2$ of area (mean value ± SEM; two independent experiments combined; n = 4-8/group). Each dot in the plots corresponds to 1 mouse, of which multiple islet tumors contained in the largest pancreatic section were analyzed. Statistical analyses by unpaired Student's t-test.*

***B****: Left panels: Haematoxylin-Eosin (H&E) staining of pancreatic sections showing examples of non-invasive (left and middle panels) and invasive (right panel) islet tumors. Scale bars: 300 μm (left panel) and 150 μm (middle and right panel). Right panel: Proportion (%; mean value ± SEM) of tumors with non-invasive, partially invasive (IC1) or entirely invasive (IC2) margins. Each dot in the plots corresponds to 1 mouse, of which multiple islet tumors contained in the largest pancreatic section were analyzed.*

***C****: NG2 (green) and CD31 (red) immunostaining of islet tumors. Scale bar: 150 μm. Results are representative of two independent experiments and 3-4 tumors/group analyzed.*

***D****: Morphometric analyses of angiogenesis (Relative vascular area; Relative pericyte area; Endothelial / pericyte ratio; mean values ± SEM) in islet tumors analyzed at the indicated time-points. Each dot in the plots corresponds to 1 mouse, of which multiple tumors were*

*analyzed. Statistical analyses by unpaired Student's t-test.*

**ANG2 blockade upregulates the expression of pro-angiogenic genes in mammary tumors**

We then analyzed the expression of a panel of angiogenesis-associated and myeloid-cell growth factor/chemoattractant genes by qPCR (Supp S4, Mazzieri et al. 2011) in tumor lysates obtained from spontaneous MMTV-PyMT carcinomas treated according to a late schedule (Figure 1A). Although none of the investigated genes showed major changes, the pro-angiogenic genes *Angpt2*, *Fgf2*, *Hgf, Pdgfb*, *Vegfa*, *Vegfb*, *Mmp9* and *Sdf1* were all upregulated in 3.19.3-treated vs. untreated tumors (Figure 4). Of note, enhanced expression of *Fgf2*, *Sdf1* and *Hgf* has been previously associated with tumor resistance to various anti-angiogenic or radiation treatments (Casanovas et al., 2005; Kozin et al., 2010; Shojaei et al., 2010).

Whereas *Sdf1*, *Vegfa* and *Angpt2* were slightly upregulated, other myeloid-cell growth factor/chemoattractant genes (e.g., *Bv8*/prokinecitin-1, *Csf1*/M-CSF, *Csf2*/GM-CSF and *Csf3*/G-CSF) did not show significant changes in 3.19.3-treated vs. untreated tumors (Figure 4). Interestingly, *Tie2* was significantly downregulated, whereas the expression of other EC receptors (e.g., *Vegfr1*, *Vegfr2*, and *Cxcr4*) was similar in 3.19.3-treated vs. untreated tumors (Figure 4). *Igf1*, which is an EC antiapoptotic/survival factor highly expressed by TEMs (Pucci et al., 2009), was strongly upregulated in 3.19.3-treated vs. untreated tumors. In summary, these data suggest that

mammary tumors upregulate, albeit marginally, the expression of several pro-angiogenic genes following ANG2 blockade; nevertheless, the treated tumors did not show evidence for rebound angiogenesis (Figure 2A-C) or growth resistance (Figure 1A-C).

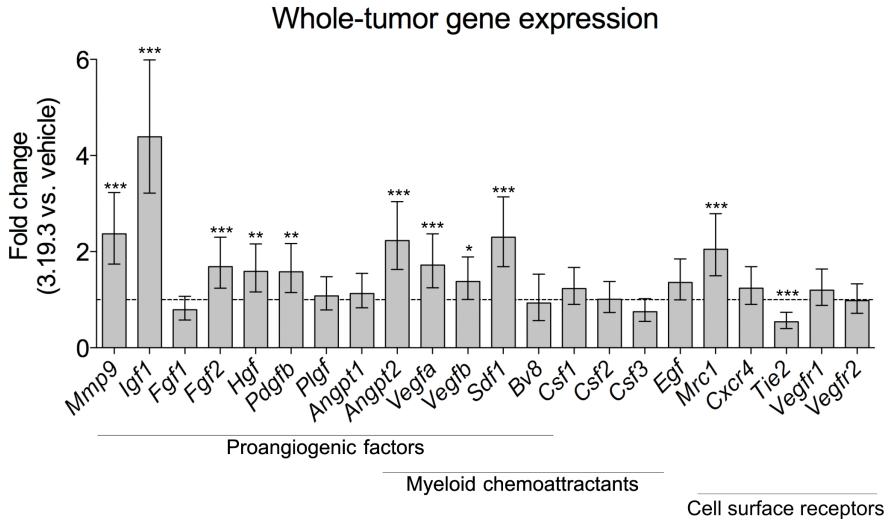


**Figure 4. ANG2 blockade upregulates the expression of pro-angiogenic genes in mammary tumors.**

*Gene expression by qPCR in whole-tumor lysates obtained from spontaneous MMTV-PyMT tumors treated with 3.19.3 (mean fold-change over reference value [vehicle]). For each mouse (n = 3-4 mice/group), 2-3 small tumor biopsies were obtained and pooled together. Error bars represent 95% confidence interval (1.96*SEM). Gapdh and Hprt were used as reference genes. Genes differentially expressed between 3.19.3- and vehicle-treated tumors are indicated by the asterisks (*: $p < 0.05$; ***: $p < 0.001$).*

**ANG2 blockade does not inhibit tumor infiltration by TEMs but impedes their association with blood vessels**

We previously showed that TEMs can be distinguished from TIE2$^-$ TAMs by their cell surface marker profile (TEMs: CD11b$^+$/F4/80$^+$/MRC1$^{high}$/CD11c$^-$; TIE2$^-$ TAMs: CD11b$^+$/F4/80$^+$/MRC1$^{low/-}$/CD11c$^+$) (Pucci et al., 2009) and perivascular location (De Palma et al., 2005). Because TIE2$^-$ TAMs express higher amounts of classic proinflammatory genes than TEMs (Pucci et al., 2009), we here refer the former to as 'inflammatory TAMs'.

ANG2 was previously shown to be a TEM chemoattractant (Coffelt et al., 2010b; Murdoch et al., 2007; Venneri et al., 2007). We then asked whether ANG2 blockade inhibited TEM recruitment to the tumors. We found that MMTV-PyMT carcinomas contained substantial numbers of MRC1$^+$ TEMs (Figure 5A-B). Unexpectedly, ANG2 blockade enhanced tumor infiltration by MRC1$^+$ TEMs, but not inflammatory TAMs or total CD11b$^+$ myeloid cells, both in spontaneous (Figure 5A and Supp S5A, Mazzieri et al. 2011) and orthotopic (Figure 5B) MMTV-PyMT tumors. The enhanced recruitment of MRC1$^+$ TEMs in 3.19.3-treated tumors may be fostered by increased tumor hypoxia and/or expression of SDF1 (Figures 2C and 4), which are known TEM recruiting signals (Kioi et al., 2010; Kozin et al., 2010). Interestingly, whereas in control tumors the MRC1$^+$ cells were mostly associated with CD31$^+$ blood vessels (a typical TEM feature), in 3.19.3-treated tumors these cells were more

homogeneously spread in the tumor mass and frequently disengaged from the blood vessels (Figure 5A-B).

ANG2 blockade did not increase $MRC1^+$ TEM infiltration in RIP1-Tag2 islet tumors but, similar to findings in MMTV-PyMT carcinomas, displaced them from the blood vessels (Figure 5C). This was true also in the scant tumor regions characterized by a relatively high vascular area (Supp S5B, Mazzieri et al. 2011). Together, these data suggest that ANG2 is not required for TEM recruitment to the tumors but regulates their interaction with angiogenic blood vessels.

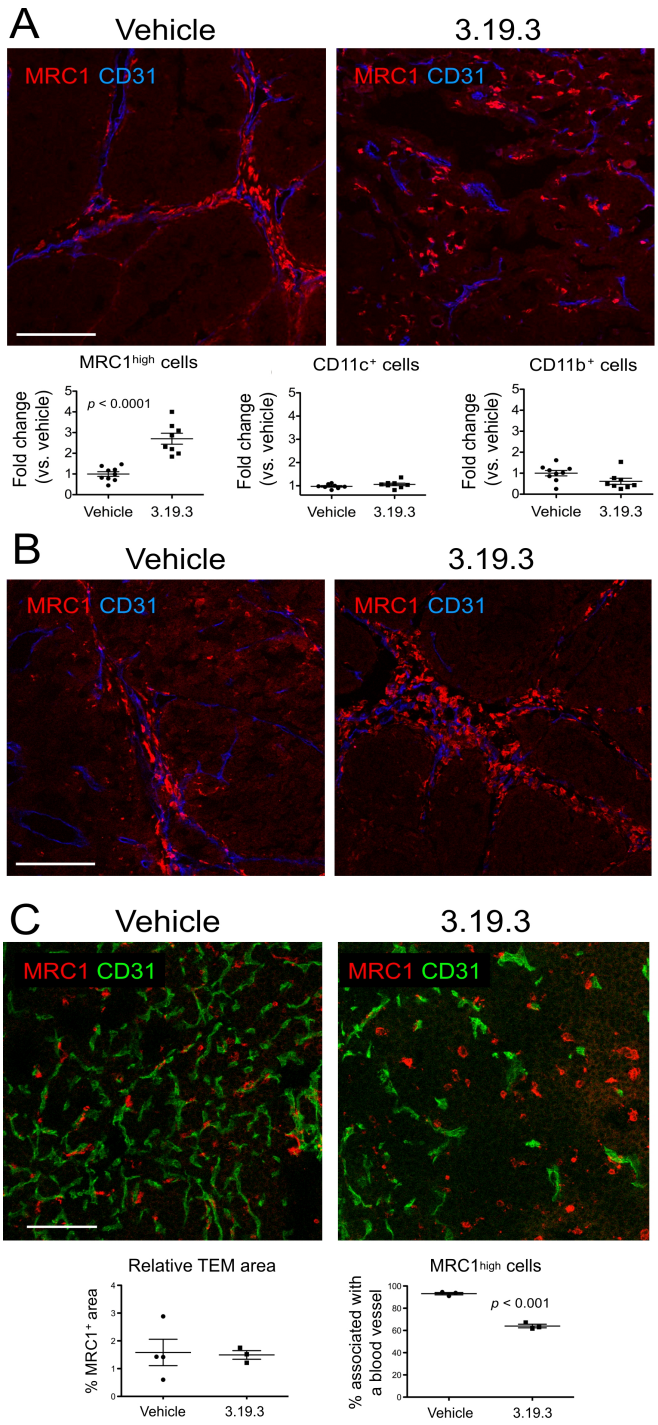
A
Vehicle
3.19.3
MRC1 CD31
MRC1 CD31
MRC1high cells
CD11c+ cells
CD11b+ cells
Fold change (vs. vehicle)
p < 0.0001
Vehicle
3.19.3
B
Vehicle
3.19.3
MRC1 CD31
MRC1 CD31
C
Vehicle
3.19.3
MRC1 CD31
MRC1 CD31
Relative TEM area
% MRC1+ area
MRC1high cells
% associated with a blood vessel
p < 0.001
Vehicle
3.19.3

**Figure 5. ANG2 blockade does not inhibit tumor infiltration by TEMs but impedes their association with blood vessels**

***A**: Top panels: MRC1 (red) and CD31 (blue) immunostaining of spontaneous, late-stage MMTV-PyMT mammary tumors treated according to a late schedule and analyzed at 15 weeks of age (see Figure 1A). Scale bar: 150 μm. Results are representative of three independent experiments and 3-5 tumors/group analyzed. Bottom panels: Flow cytometry analyses of myeloid cell infiltrates in tumors treated as above (mean frequency of tumor-derived cells ± SEM, shown as fold-change vs. reference [vehicle]). Each dot in the plots corresponds to 1 mouse; tumor samples were obtained from three independent experiments. Statistical analyses by unpaired Student's t-test.*

***B**: MRC1 (red) and CD31 (blue) immunostaining of orthotopic, late-stage MMTV-PyMT mammary tumors treated according to a short schedule (see Figure 1B) and analyzed 2 weeks after the first treatment. Scale bar: 150 μm. Results are representative of two independent experiments and 10 tumors/group analyzed.*

***C:** Top panels: MRC1 (red) and CD31 (blue) immunostaining of late-stage RIP1-Tag2 islet tumors treated according to a late schedule and analyzed at 15.5 weeks of age (see Figure 3A). Scale bar: 100 μm. Results are representative of two independent experiments, 3-4 mice/group and several tumors analyzed. Bottom panels: Morphometric analyses (mean values ± SEM) of $MRC1^+$ cell infiltration (left) and association with blood vessels (right) in islet*

*tumors treated as above. Each dot in the plots corresponds to 1 mouse, of which multiple tumors were analyzed.*

**ANG2 blockade impedes tumor TEM upregulation of *Tie2***

Because 3.19.3 strongly inhibited tumor angiogenesis, the finding of increased numbers of $MRC1^+$ TEMs in 3.19.3-treated MMTV-PyMT carcinomas appeared paradoxical in view of the pro-angiogenic activity of these cells. In order to investigate whether ANG2 blockade altered gene expression in TEMs, we isolated TEMs ($7AAD^-$ /$CD11b^+$/$CD31^{low}$/$MRC1^{high}$/$CD11c^-$), inflammatory TAMs ($7AAD^-$ /$CD11b^+$/$CD31^{low}$/$MRC1^{low/-}$/$CD11c^+$) and ECs ($7AAD^-$ /$CD31^{high}$/$CD11b^-$) from both 3.19.3-treated and untreated, orthotopic MMTV-PyMT carcinomas, and analyzed the expression of a panel of genes of interest (Supp S4, Mazzieri et al. 2011) in the sorted cells. In agreement with our previous gene expression studies performed in the N202 mammary tumor model (Pucci et al., 2009), *Tie2*, *Igf1*, *Sdf1* and *Mrc1* were all highly upregulated in TEMs vs. inflammatory TAMs isolated from untreated MMTV-PyMT tumors (Figure 6A and Supp S4, Mazzieri et al. 2011). The higher expression level of *Igf1*, *Mrc1* and *Sdf1* in whole mammary tumor lysates of 3.19.3-treated (vs. untreated) mice (Figure 4) is therefore consistent with their enhanced infiltration by TEMs (Figure 5A-B and Supp S5A, Mazzieri et al. 2011).

Interestingly, the expression level of *Tie2* – but not other TEM distinguishing genes – was significantly lower (8-10–fold in 4

independent experiments) in TEMs isolated from 3.19.3-treated than control tumors (Figure 6B, supp S4, Mazzieri et al. 2011, and data not shown). Because *Tie2* is strongly upregulated in TEMs locally in the tumor microenvironment (De Palma et al., 2008), these data strongly suggested that neutralization of ANG2 had impeded the upregulation of TIE2 in tumor-infiltrating TEMs. On the other hand, ANG2 blockade did not change the expression level of any of the investigated genes in inflammatory TAMs (Figure 6C and Supp S4, Mazzieri et al. 2011). Except for *Sdf1*, which was upregulated, none of the genes analyzed in ECs (including *Tie2*) displayed significant changes following ANG2 blockade (Figure 6D and Supp S4, Mazzieri et al. 2011).

To verify that, regardless of their differential expression level of *Tie2*, the $MRC1^+$ cells represented *bona fide* TEMs in both 3.19.3-treated and untreated tumors, we transplanted lethally irradiated, 6-week–old MMTV-PyMT mice with *Tie2*-GFP BM cells (De Palma et al., 2005) and analyzed the tumors at 15 weeks of age after a late treatment schedule (Supp S6, Mazzieri et al. 2011). Anti-GFP IFS of tumor sections specifically marked the $MRC1^+$ cells and labeled similar proportions of these cells in 3.19.3- and vehicle-treated mice (Supp S6, Mazzieri et al. 2011). Together with the gene expression data in Figure 6B above, these results indicate that the $MRC1^+$ cells of 3.19.3-treated tumors maintain a distinguishing TEM phenotype but fail to upregulate *Tie2*, a molecular switch that could be required to promote TEM association with angiogenic blood vessels and execution of their pro-angiogenic activity.

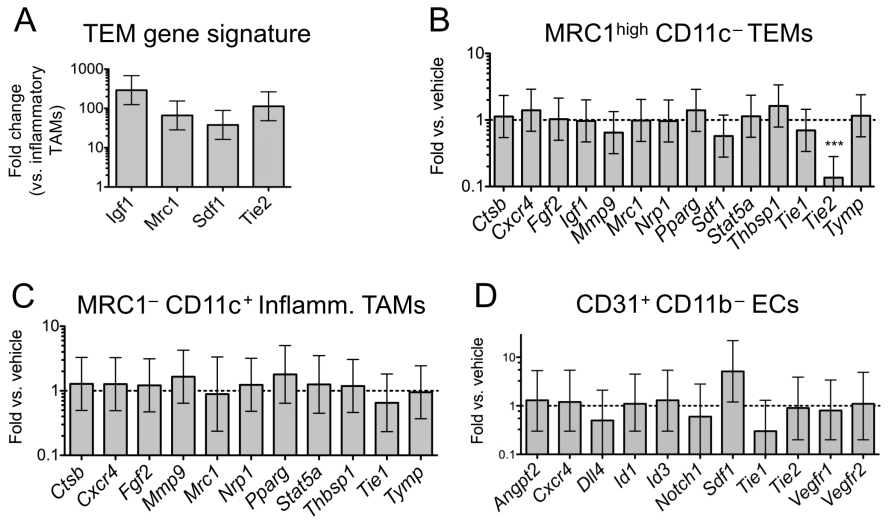


**Figure 6. ANG2 blockade impedes tumor TEM upregulation of *Tie2.***

***A**: Gene expression by qPCR in TEMs and inflammatory TAMs isolated from untreated, orthotopic MMTV-PyMT tumors (mean fold-change over reference value [inflammatory TAMs]; n = 2) analyzed 4 weeks post-tumor injection. Error bars represent 95% confidence interval (1.96*SEM); β2m was used as reference gene. **B-D**: Gene expression by qPCR in TEMs (B; n = 2), inflammatory TAMs (C; n = 2) and ECs (D; n = 3) isolated from orthotopic, late-stage MMTV-PyMT tumors treated with 3.19.3 according to a short schedule (mean fold-change over reference value [vehicle]). Error bars represent 95% confidence interval (1.96*SEM); β2m was used as reference gene. ***: $p < 0.001$. The expression of Tie2 in TEMs was further analyzed in two additional experiments and confirmed to be significantly lower ($p < 0.001$) in 3.19.3- vs. vehicle- treated tumors.*

**Conditional *Tie2* gene knock-down in TEMs reduces tumor angiogenesis and perfusion in mammary tumors**

We then asked whether the impeded upregulation of *Tie2* in TEMs contributed to the anti-angiogenic activity of ANG2 blockade in MMTV-PyMT carcinomas. To address this question, we silenced TIE2 specifically in the mature hematopoietic cells of tumor-bearing mice. We previously described the delivery of short interfering RNA (siRNA) using microRNA (miRNA)-based lentiviral vectors (LVs) (Amendola et al., 2009). To silence TIE2, we replaced the stem sequence of miR-233 with validated siRNA sequences targeting *Tie2* and obtained the artificial miRNA, amiR(*Tie2*); we also generated a control amiR targeting *Luciferase*, amiR(*Luc*) (Amendola et al., 2009). To enable inducible gene silencing, we here combined two separate LVs (Figure 7A). In the first vector (LV1), the amiR is placed downstream to a tetracycline-responsive element (TRE)-containing promoter, which also controls the expression of a marker gene (orange fluorescent protein, OFP). In the second vector (LV2), a reverse tetracycline transactivator (rtTA-m2) is placed under the control of the ubiquitously active phosphoglycerate kinase (*PGK*) promoter (*PGK*-rtTA). In order to suppress rtTA expression and, consequently, *Tie2* gene knock-down in hematopoietic stem cells (HSCs), which require TIE2 for their maintenance in the stem cell niche (Arai et al., 2004), we modified the rtTA expression cassette by incorporating target sequences for miR-126 (miR-126T) in the UTR. By this strategy, rtTA expression is suppressed specifically in HSCs via endogenous miRNA-mediated mRNA degradation, as only HSCs

express high-level miR-126 among hematopoietic-lineage cells (Gentner et al., 2010). We then generated FVB/*PGK*-rtTA-miR-126T (LV2) transgenic mice by LV-mediated transgenesis, as previously described (De Palma et al., 2005), and used them as hematopoietic stem/progenitor cell (HS/PC) donors for *ex vivo* LV1-transduction and transplantation. We validated the inducible gene knock-down platform both *in vitro* and *in vivo*, showing: (i) absence of amiR-induced cell toxicity and counter-selection (Supp S7A-B, Mazzieri et al. 2011) and lack of saturation of the endogenous miRNA pathway (Supp S7C, Mazzieri et al. 2011) *in vitro*; (ii) efficient and doxycycline-dependent amiR expression in HS/PCs *ex vivo* (Supp S7D-E, Mazzieri et al. 2011), circulating monocytes (Supp S7F, Mazzieri et al. 2011) and tumor-infiltrating TEMs (Supp S7G, Mazzieri et al. 2011) *in vivo*; and (iii) virtually complete de-targeting of amiR expression from primitive HSCs *in vivo* (Supp S7H-I, Mazzieri et al. 2011). Furthermore, expression of the amiR(*Tie2*) did not perturb whole blood cell counts (Supp S7J, Mazzieri et al. 2011), leukocyte (Supp S7K, Mazzieri et al. 2011) and monocyte (Supp S7L, Mazzieri et al. 2011) subsets, nor did it induce counter-selection of LV1-transduced cells (Supp S7M, Mazzieri et al. 2011) in the transplanted mice (compared with amiR(*Luc*) mice).

To study the effects of *Tie2* gene knock-down in a model of spontaneous tumorigenesis, we generated MMTV-PyMT/amiR(*Tie2*) and MMTV-PyMT/amiR(*Luc*) mice (2 independent experiments; n = 12-14 mice/group) by HS/PC transduction and transplantation, as described above. We treated the mice with doxycycline starting at 4

weeks post-transplant (9.5 weeks of age), when the angiogenic switch and malignant conversion occur in this tumor model (De Palma et al., 2008; Lin et al., 2006). We euthanized the mice at 15 weeks of age and analyzed their tumors by flow cytometry and IFS of frozen sections.

The frequency of TEMs and inflammatory TAMs among the tumor-infiltrating $CD11b^{+}/Gr1^{-}$ myelomonocytic cells was similar in MMTV-PyMT/amiR(*Tie2*) and MMTV-PyMT/amiR(*Luc*) mice (Figure 7B), indicating that *Tie2* gene knock-down did not detectably affect TEM recruitment to the tumors. However, when we analyzed tumor angiogenesis, we observed significant differences between MMTV-PyMT/amiR(*Tie2*) and MMTV-PyMT/amiR(*Luc*) mice (Figure 7C-D). The $CD31^{+}$ blood vessels of amiR(*Tie2*) tumors appeared smaller, fewer and less perfused ($lectin^{+}$) than in the controls (Figure 7C). Both the $CD31^{+}$ and $lectin^{+}$ relative vascular area, measured by IFS of tumor sections, were significantly lower in amiR(*Tie2*) than amiR(*Luc*) mice (Figure 7D), indicating decreased angiogenesis and, possibly, increased vessel immaturity or collapse. Flow cytometric analyses of tumor cell suspensions confirmed the lower proportion of $lectin^{+}/CD31^{+}/CD45^{-}$ ECs in the tumors of amiR(*Tie2*) mice (Figure 7E). We observed decreased angiogenesis/perfusion also in FVB/amiR(*Tie2*) mice either challenged with orthotopic MMTV-PyMT (Supp S7N, Mazzieri et al. 2011) or subcutaneous N202 (Supp S7O, Mazzieri et al. 2011) mammary carcinomas. These data indicate that *Tie2* knock-down by RNAi and, consequently, its impeded upregulation in tumor-

infiltrating TEMs, reduces tumor angiogenesis and blood vessel functionality in mammary tumor models.

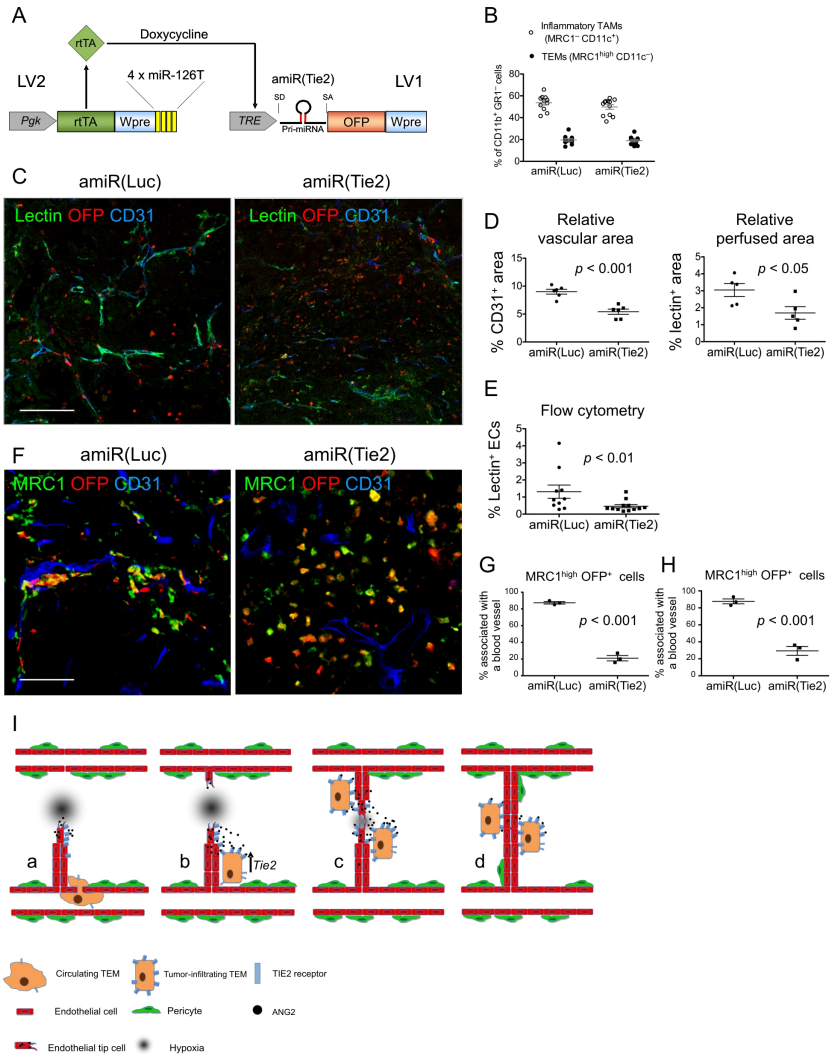

**Figure 7. Conditional *Tie2* gene knock-down in TEMs reduces tumor angiogenesis and impedes TEM association with blood vessels**

***A**: Schematics of the LV constructs used for Tie2 gene knock-down in BM-derived cells.*

***B**: Flow cytometry analyses of mononuclear phagocyte infiltrates (MRC1$^{high}$/CD11c$^{-}$ TEMs and MRC1$^{low}$/CD11c$^{+}$ inflammatory TAMs) in tumors of MMTV-PyMT/amiR(Tie2) and MMTV-PyMT/amiR(Luc) mice. Each dot in the plot corresponds to 1 mouse (n = 11-12 mice/group); results are shown as mean values ± SEM. Two independent experiments are shown after combining the data.*

***C**: Lectin (green), OFP (red) and CD31 (blue) immunostaining of tumor sections of MMTV-PyMT/amiR(Tie2) and MMTV-PyMT/amiR(Luc) mice. Scale bar: 150 μm. Results are representative of two independent experiments and 11-12 tumors/group analyzed. For each tumor, 3-5 sections were analyzed.*

***D**: The plots show mean values ± SEM of morphometric analyses of angiogenesis in tumors of MMTV-PyMT/amiR(Tie2) and MMTV-PyMT/amiR(Luc) mice. Each dot indicates 1 individual tumor; for each tumor, 3-5 sections were analyzed. Statistical analyses by unpaired Student's t-test.*

***E**: The plot shows mean values ± SEM of lectin$^{+}$CD31$^{+}$CD45$^{-}$ ECs in tumors of MMTV-PyMT/amiR(Tie2) and MMTV-PyMT/amiR(Luc) mice. Each dot indicates 1 individual mouse; for each mouse, 2-3 tumor biopsies were obtained and pooled together before analysis. Statistical analyses by unpaired Student's t-test.*

***F**: MRC1 (green), OFP (red) and CD31 (blue) immunostaining of tumors sections of MMTV-PyMT/amiR(Tie2) and MMTV-PyMT/amiR(Luc) mice. Scale bar: 75 µm. Results are representative of two independent experiments and 10 tumors/group analyzed. For each tumor, 3-5 sections were analyzed. $OFP^{+}MRC1^{high}$ TEMs appear yellow; untransduced $MRC1^{high}$ TEMs appear green; $OFP^{+}MRC1^{-}$ cells represent BM-derived cells distinct from TEMs.*

***G-H**: Analysis of $OFP^{+}MRC1^{high}$ TEM / $CD31^{+}$ blood-vessel association in tumors of amiR(Tie2) and amiR(Luc) mice (G: spontaneous MMTV-PyMT tumors; H: orthotopic MMTV-PyMT tumors grown in FVB mice). Individual $OFP^{+}MRC1^{high}$ TEMs were scored as either associated or not with $CD31^{+}$ blood vessels. Histograms show mean values (± SEM) of the percentage of $OFP^{+}MRC1^{high}$ TEMs associated with $CD31^{+}$ blood vessels. In G, data were obtained from 3 mice/group and 2 tumors/mouse; in H, data were obtained from 3 tumors/group. Statistical analyses by unpaired Student's t-test.*

***I**: TEM-EC interactions mediated by ANG2-TIE2 promote vascular morphogenesis in tumors. Circulating TEMs express low-level TIE2 (**a**), but the receptor is upregulated upon their extravasation and exposure to ANG2 in the perivascular microenvironment (**b**). TEMs adhere to ANG2-expressing sprouting blood vessels (**b**) and promote vascular growth (**c, d**).*

**Conditional *Tie2* gene knock-down in TEMs impedes their association with tumor blood vessels**

We noted that the distribution of $OFP^+MRC1^+$ cells differed in the tumors of amiR(*Tie2*) and amiR(*Luc*) mice, both in spontaneous (Figure 7F-G) and orthotopic (Figure 7H) MMTV-PyMT tumor models. Indeed, there were fewer $OFP^+MRC1^+$ TEMs associated with $CD31^+$ tumor blood vessels in amiR(*Tie2*) than amiR(*Luc*) mice (Figure 7G-H), suggesting that *Tie2* knock-down in TEMs had hampered their ability to associate with angiogenic blood vessels. Together with the ANG2 blockade data shown above, these findings indicate that TIE2 expression by TEMs is required for their association with angiogenic blood vessels, and that disrupting such association (either by interfering with *Tie2* expression in TEMs, or by neutralizing the TIE2 ligand, ANG2) limits the formation of intra-tumoral vascular networks (Figure 7I).

Whereas *Tie2* knock-down in TEMs was sufficient to significantly decrease angiogenesis in multiple tumor models (Figures 7C-E and Supp S7N-O, Mazzieri et al. 2011), it failed to reproducibly inhibit tumor growth (data not shown). It should be noted, however, that the frequency of $OFP^+$ TEMs ranged from 50% to 90% (average: 70%) in the tumors of both amiR(*Tie2*) and amiR(*Luc*) mice (Supp S7P, Mazzieri et al. 2011), indicating that *Tie2* gene knock-down had occurred in the majority but not all tumor-infiltrating TEMs.

**ANG2 blockade inhibits spontaneous and pre-established mammary tumor metastasis**

We then asked whether angiogenesis inhibition following ANG2 blockade affected tumor cell dissemination and outgrowth of pulmonary metastases in MMTV-PyMT transgenic mice. We analyzed the lungs of 3.19.3-treated and control mice from either early (one experiment; 8 weeks of treatment; n = 10 mice/group) or late (two independent experiments; 3 weeks of treatment; n = 10 mice/group) treatment trials. Both in early and late treatment trials, 3.19.3 effectively inhibited spontaneous metastasis in MMTV-PyMT mice (Figure 8A-B and Supp S8, Mazzieri et al. 2011). In order to discriminate direct vs. indirect effects of 3.19.3 on metastasis formation, we used a model in which metastatic growth is independent on the primary tumor. To this aim, we intravenously injected tumor cells obtained from late-stage MMTV-PyMT carcinomas into wild-type mice; by this approach, pulmonary metastases form in the absence of a primary tumor. Starting at 1 day after tumor cell inoculation, mice were treated with 3.19.3 for 25 days or left untreated, and the lungs analyzed thereafter. Whereas 3.19.3 did not significantly decrease the number of metastases in the lung parenchyma, it dramatically inhibited the progression from a micro- to a macro-metastatic stage, as shown by volumetric analysis of the pulmonary tumor burden (Figure 8C). These data provide direct evidence that ANG2 blockade not only inhibits primary tumor growth and its metastatic dissemination, but also directly suppresses the growth of established metastases.

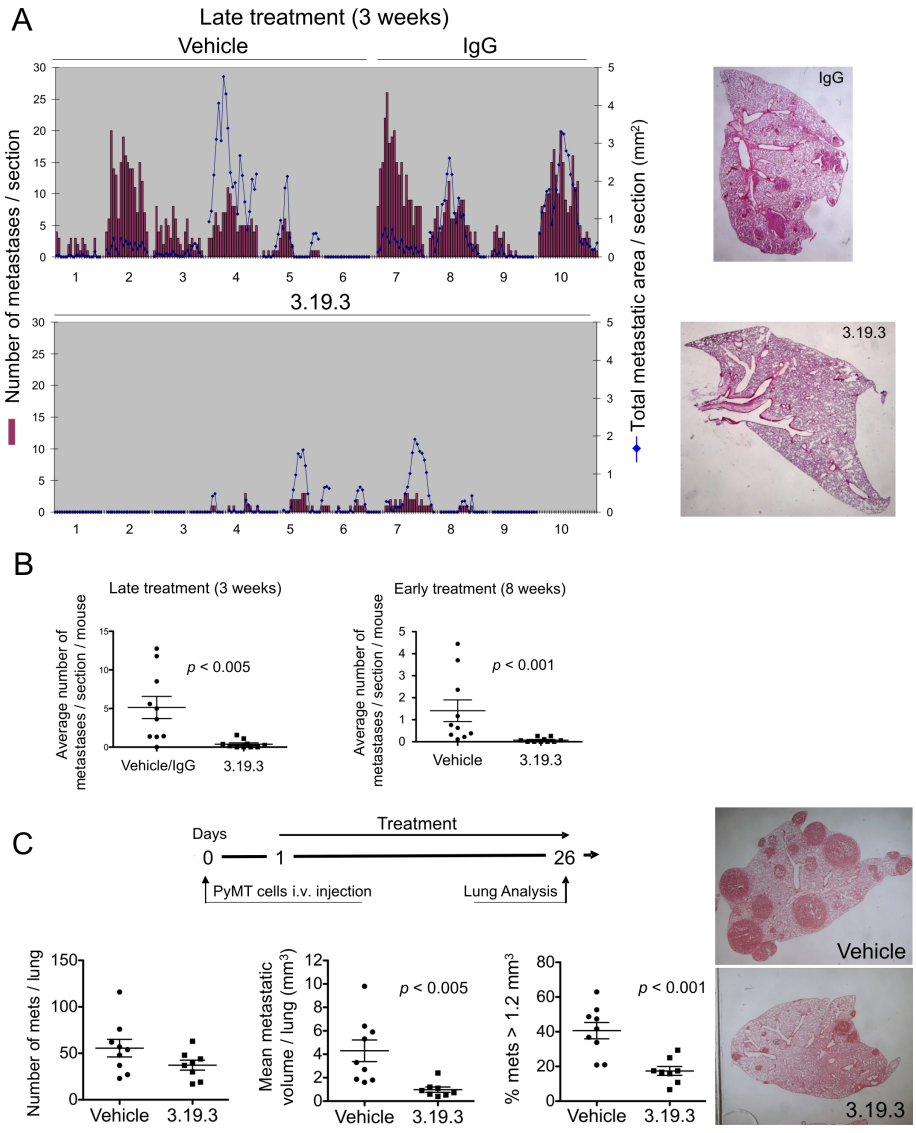


**Figure 8. ANG2 blockade inhibits spontaneous and pre-established mammary tumor metastasis.**

***A****: Spontaneous metastasis model. Left panels: Number of metastatic foci (bars) and total metastatic area (broken line) in individual serial sections (each bar) obtained from the entire left lung of MMTV-PyMT*

*mice treated with 3.19.3, control IgGs or vehicle after a late schedule (see Figure 1A), and analyzed at 15 weeks of age. Right panels: H/E staining of representative whole lung sections.*

***B**: Spontaneous metastasis model. Number of metastatic foci (mean values ± SEM) per section per mouse in mice treated according to either late (3 weeks; left) or early (8 weeks; right. Supp S8, Mazzieri et al. 2011) schedules; each dot represents 1 mouse. Statistical analyses by Mann-Whitney test.*

***C**: Pre-established metastasis model. Top left panel: Schematics of experimental design. Bottom left panels: Morphometric analyses of metastasis (mean values ± SEM) in the lungs of mice either treated with 3.19.3 (n = 8) or vehicle alone (n = 9). Each dot in the plots represents 1 mouse. Results combine two independent experiments. Statistical analyses by Mann-Whitney test (left and middle panel) or unpaired Student's t-test (right panel). Right panels: H/E staining of representative whole lung sections.*

## Discussion

Here, we demonstrate that ANG2 blockade: (i) inhibits angiogenesis and induces vascular regression in multiple tumor models, including tumors that are prone to develop resistance to anti-VEGF/VEGFR therapy; (ii) inhibits tumor growth in multiple tumor models, including late-stage spontaneous tumors; (iii) limits the metastatic dissemination of primary tumors and the outgrowth of established metastasis; (iv) impedes, in tumor-infiltrating TEMs, the transcriptional upregulation of *Tie2*, which is required for their association with tumor blood vessels and pro-angiogenic activity.

### Sustained anti-angiogenic and antitumor activity of ANG2 blockade

We neutralized ANG2 using an ANG2-specific monoclonal antibody (3.19.3) that potently binds ANG2 with at least 500-fold greater affinity compared with ANG1 (Brown et al., 2010). 3.19.3 markedly reduced the relative tumor vascular area in each tumor model tested, including spontaneous MMTV-PyMT mammary and RIP1-Tag2 pancreatic islet tumors. In these tumor models, ANG2 neutralization increased pericyte coverage of the remnant blood vessels, similar to previous findings in subcutaneous tumors (Hashizume et al., 2010; Nasarre et al., 2009). Because ANG1 promotes pericyte-EC interactions, it is possible that ANG2 blockade by 3.19.3 increased ANG1 bioavailability for interaction with TIE2, thus enhancing pericyte coverage of the blood vessels and suppressing angiogenesis.

In agreement with previous findings (Fiedler et al., 2004), our gene expression data indicate that ANG2 is highly expressed in tumor ECs (see Figure S4). The role of ANG2 in tumor angiogenesis is, however, still controversial. L1-7N, a previously described ANG2-specific peptibody (Oliner et al., 2004), did not reduce vascular density detectably in the tumor models tested (Hashizume et al., 2010). Furthermore, genetic models of *Angpt2* deficiency or over-expression failed to unequivocally establish the importance of ANG2 in tumor angiogenesis (Chae et al., 2010; Nasarre et al., 2009).

Contrary to some of the earlier data, our findings indicate that 3.19.3 regresses the tumor vasculature and inhibits the growth of both early and late-stage tumors, pointing to a critical role of ANG2 during tumor progression. It is possible that some of the previously reported strategies of ANG2 inhibition might have overlooked the importance of ANG2 for tumor angiogenesis, particularly when both ANG2 and ANG1 – which have opposite functions in tumor angiogenesis – were concomitantly targeted, e.g., by soluble TIE2 delivery or ANG1/ANG2-bispecific antibodies (Huang et al., 2010).

In MMTV-PyMT tumor models, 3.19.3 induced tumor blood vessel regression, increased tumor hypoxia, fibrosis and necrosis, and enhanced the recruitment of $MRC1^+$ TAMs (i.e., TEMs) to the tumors. Such tumor responses were previously found – in the context of other anti-angiogenic treatments (e.g., anti-VEGF/VEGFR) and/or tumor models – to associate with the activation of alternate pro-angiogenic pathways and drug resistance (Bergers and Hanahan, 2008; Casanovas et al., 2005; Shojaei et al., 2007). Accordingly, we observed increased

expression of several pro-angiogenic genes (e.g., *Vegfa*, *Fgf2* and *Sdf1*) in 3.19.3-treated mammary tumors. We currently ignore whether such upregulation of pro-angiogenic factors in 3.19.3-treated tumors is truly indicative of tumor adaptation to circumvent ANG2 blockade, rather than representing an epiphenomenon associated with enhanced tumor hypoxia or fibrosis. In either case, we did not find evidence for drug resistance or rebound angiogenesis in tumors treated according to various ANG2 blockade schedules, pointing to a requisite role of ANG2 for tumor angiogenesis. Importantly, ANG2 blockade also inhibited angiogenesis and progression of late-stage, pancreatic insulinomas in RIP1-Tag2 mice, a mouse tumor model previously shown to develop resistance to anti-VEGF/VEGFR2 therapy (Casanovas et al., 2005; Shojaei et al., 2008). Although we did not directly compare ANG2 blockade with VEGF/VEGFR2 blockade, our data suggest that effective ANG2 inhibition may have the potential to achieve anti-angiogenic and antitumor activity also in tumors that are resistant to anti-VEGF therapy.

**Antimetastatic activity of ANG2 blockade**

An important finding of this study is that ANG2 blockade markedly inhibited metastasis in two metastasis models. 3.19.3 strongly inhibited spontaneous pulmonary metastases in MMTV-PyMT mice, both following short and extended (8 weeks) treatment schedules. These data argue that ANG2 blockade, at variance with certain models of anti-VEGF therapy (Ebos et al., 2009; Paez-Ribes et al., 2009), has potent antimetastatic activity and does not select for

proinvasive/prometastatic tumor phenotypes. Because 3.19.3 reduced angiogenesis and increased pericyte coverage of the remaining blood vessels in the primary tumors, it is likely that tumor cell intravasation and dissemination were directly inhibited at the primary tumor site. Of note, the genetic disruption of pericyte coverage elicited increased metastasis in the *Rip1*-Tag2 pancreatic islet tumor model (Xian et al., 2006).

Our data further indicate that 3.19.3 impairs the growth of micrometastases at the post-seeding step. Indeed, pre-established micro-metastases failed to develop into large macrometastases following ANG2 blockade, a phenomenon possibly due to inhibition of the angiogenic switch that occurs at the metastatic site concomitant to micro- to macrometastasis transition.

**The ANG2-TIE2 pathway regulates TEMs' pro-angiogenic activity**

TIE2 is expressed at very low level in circulating monocytes, but is strongly upregulated (up to 100-fold) in tumor-associated TEMs (De Palma et al., 2008). ANG2 may thus signal both autocrinally on ECs (Augustin et al., 2009) and iuxtacrinally on perivascular, $TIE2^+$ macrophages. The latter circumstance is supported by experimental evidence that ANG2 agonistically enhances the pro-angiogenic activity of human blood-derived $TIE2^+$, but not $TIE2^-$ monocytes *in vitro* (Coffelt et al., 2010b). Because the $MRC1^+$ TEMs recruited to 3-19-3-treated mammary tumors expressed much lower *Tie2* than those of untreated tumors, it can be envisioned that EC-derived ANG2

stimulates TIE2 expression on perivascular TEMs and that such feedback may be essential for the execution of productive angiogenesis. Although it cannot be excluded that TIE2 upregulation in TEMs is mediated indirectly by ANG2, ANG2 blockade specifically modulated the *Tie2* mRNA among several angiogenic genes analyzed, suggesting that this response is intimately linked to TIE2 signaling. Of note, several growth factors – including ANGs – can regulate the expression of their receptor tyrosine kinases at the transcriptional level via autoregulatory feedback loops (Hashimoto et al., 2004). Intriguingly, we did not observe transcriptional modulation of *Tie2* in ECs following ANG2 blockade; this may suggest that ANG2-mediated modulation of *Tie2* expression involves different TIE2 heterodimers (Seegar et al., 2010) and/or signaling adaptors (e.g., integrins) in ECs and TAMs.

To investigate the role of TIE2 in TEMs, we developed a gene knock-down platform that effectively protects the hematopoietic compartment from potential toxicity consequent to RNA interference in HSCs. Indeed, our previous attempts to knock-down *Tie2* using constitutive LVs caused obvious hematopoietic toxicity (data not shown). By using inducible LVs coupled to de-targeting from HSCs (Gentner et al., 2010), we showed that *Tie2* knock-down in BM-derived cells significantly inhibits angiogenesis and microvascular perfusion in MMTV-PyMT mice, without affecting hematopoiesis detectably. Remarkably, by targeting the TIE2 receptor in TEMs, we recapitulated some of the features of TEM elimination (De Palma et

al., 2005), indicating that TIE2 is a pivotal biological effector and therapeutic target in these cells.

TAMs comprise molecularly and functionally distinct subpopulations (Qian and Pollard, 2010). TEMs express lower amounts of VEGF than classic TAMs (Pucci et al., 2009) and do not reside in hypoxic, avascular tumor areas (De Palma et al., 2005). Thus, it is likely that TEMs exert a requisite pro-angiogenic function by supporting tumor angiogenesis downstream to VEGF-induced vascular activation. Because the lower expression of *Tie2* in the TEMs of 3.19.3-treated mammary tumors was not associated with deregulated expression of a panel of classic pro- and anti-angiogenic genes, one can envision that TIE2 expression by TEMs regulates blood vessel formation in tumors by non-canonical (e.g., VEGF-independent) angiogenic mechanisms. Indeed, our findings of impeded association between TEMs and tumor blood vessels both after specific *Tie2* knock-down in TEMs and extracellular blockade of ANG2 support the concept that the ANG2/TIE2 axis is crucial to establish cell-to-cell interactions between TEMs and ECs. Such scenario is in agreement with a recent study showing that $TIE2^+$ perivascular macrophages physically interact with the $TIE2^+$ endothelial tip cells of nascent blood vessels, and are essential to promote vascular anastomosis during embryonic development (Fantin et al., 2010). Furthermore, $TIE2^+$ hematopoietic cells adhere to $TIE2^+$ ECs and stimulate angiogenesis in para-aortic splanchnopleural mesoderm explant cultures (Takakura et al., 1998). Both ANG1 and ANG2 induce homomeric TIE2 complex formation in cell-to-cell endothelial junctions (Saharinen et al., 2008). ANG2-

mediated TEM-EC interactions may thus facilitate the navigation of endothelial sprouts through the dense extracellular matrix, eventually enabling the fusion of nascent blood vessels in angiogenic tissues (see Figure 7I).

*Tie2* silencing in TEMs, although consistently inhibited angiogenesis and tumor blood vessel perfusion by almost 50%, did not reproducibly inhibit tumor growth in the investigated mouse tumor models. Similarly, previous reports showed that the genetic deletion of certain pro-angiogenic factors in ECs or myeloid cells may reduce tumor angiogenesis without decreasing tumor growth rates (Nasarre et al., 2009; Stockmann et al., 2008). It should be noted that in our *Tie2* silencing studies, from 10 to 50% of the tumor-associated TEMs were TIE2-competent ($OFP^{-}$) in the different mice. This is expected from the chimeric composition of hematopoiesis following transplantation of *ex vivo*-transduced HS/PCs and the non-exhaustive doxycycline-mediated gene induction. Thus, it cannot be excluded that fully exhaustive *Tie2* targeting in tumor-infiltrating macrophages would impair angiogenesis and tumor vessel function to an extent becoming critical for tumor growth.

In conclusion, our data indicate that the TIE2 receptor expressed by perivascular TEMs is a crucial regulator of ANG2-mediated pro-angiogenic programs in tumors. Because tumor-infiltrating myeloid cells are known to convey protumoral and pro-angiogenic programs that can counteract the efficacy of anti-angiogenic treatments (Bergers and Hanahan, 2008), the combined targeting of angiogenic ECs and

pro-angiogenic TEMs by selective ANG2/TIE2-pathway inhibitors may extend the reach of anti-angiogenic therapy in cancer patients.

## Experimental Procedures

### Mice

FVB and CD1 athymic mice were purchased by Charles River Laboratory (Calco, Milan, Italy). FVB/MMTV-PyMT and C57Bl/6/RIP1-Tag2 mice were obtained from the NCI-Frederick Mouse Repository (MD) and established as colonies at the San Raffaele animal facility. FVB/*Pgk*-rtTA-miR-126T transgenic mice were generated by LV-mediated transgenesis. FVB/*Tie2*-GFP transgenic mice were generated previously (De Palma et al., 2005). All procedures were performed according to protocols approved by the Animal Care and Use Committee of the Fondazione San Raffaele del Monte Tabor (IACUC 324 and 335) and communicated to the Ministry of Health and local Authorities according to the Italian Law.

### ANG2 blockade by 3.19.3

Tumor-bearing mice were randomized into vehicle (phosphate buffered saline), IgG (Endobulin, Baxter, Italy) and treatment (3.19.3; AstraZeneca Pharmaceuticals, Waltham, MA) groups. 3.19.3 and IgGs were administered by i.p. injections after a twice weekly schedule at doses of 10 mg/kg for the indicated periods of time, as described previously (Brown et al.).

### Hematopoietic stem/progenitor cell (HS/PC) isolation, transduction and transplantation for Tie2 knockdown in TEMs

BM was obtained from 6-12 week–old FVB/*PGK*-rtTA-miR-126T

(LV2) transgenic mice. Lineage-negative cells enriched in HS/PCs were isolated using a cell purification kit (StemCell Technologies) and transduced by concentrated LVs. Briefly, $10^6$ cells/ml were pre-stimulated for 4-6 hours in serum-free StemSpan medium (StemCell Technologies) containing a cocktail of cytokines (IL-3, SCF, TPO and FLT-3L, all from Peprotech) and transduced with amiR-expressing LVs (LV1) with a dose equivalent to $10^8$ LV Transducing Units/ml, for 12 hours in medium containing cytokines. After transduction, $10^6$ cells were infused into the tail vein of lethally irradiated, 5.5-week–old, female FVB or FVB/MMTV-PyMT mice (radiation dose: 1150 cGy split in 2 doses).

**Induction of *Tie2* gene knock-down by doxycycline administration**

Starting at 4 weeks after HS/PC transplantation (i.e., 9.5 weeks of age), FVB or MMTV-PyMT mice were moved to doxycycline-containing food (Charles River) and received intra-peritoneal injections of doxycycline (0.5 mg/mouse) every third day, until the end of the experiments (12.5-13.5 weeks of age for FVB and 15 weeks of age for MMTV-PyMT mice).

**Statistical analysis**

In all studies, values are expressed as mean ± standard error (SEM) or 95% confidence intervals (1.96*SEM), as indicated. Statistical analyses were performed by unpaired Student's *t*-test, or Mann-Whitney test, as indicated. Differences were considered statistically

significant at $p < 0.05$. Statistical methods are described in full in the Supplemental Experimental Procedures.

**Supplemental Data**

The Supplemental Data include Supplemental Experimental Procedures, Supplemental References, figures and movies can be found with this article online at doi:10.1016/j.ccr.2011.02.005.

# References

Amendola, M., Passerini, L., Pucci, F., Gentner, B., Bacchetta, R., and Naldini, L. (2009). Regulated and multiple miRNA and siRNA delivery into primary cells by a lentiviral platform. Mol Ther *17*, 1039-1052.

Arai, F., Hirao, A., Ohmura, M., Sato, H., Matsuoka, S., Takubo, K., Ito, K., Koh, G. Y., and Suda, T. (2004). Tie2/angiopoietin-1 signaling regulates hematopoietic stem cell quiescence in the bone marrow niche. Cell *118*, 149-161.

Augustin, H. G., Young Koh, G., Thurston, G., and Alitalo, K. (2009). Control of vascular morphogenesis and homeostasis through the angiopoietin-Tie system. Nat Rev Mol Cell Biol *10*, 165-177.

Bergers, G., and Hanahan, D. (2008). Modes of resistance to anti-angiogenic therapy. Nature Reviews Cancer *8*, 592-603.

Brown, J. L., Cao, Z. A., Pinzon-Ortiz, M., Kendrew, J., Reimer, C., Wen, S., Zhou, J. Q., Tabrizi, M., Emery, S., McDermott, B.*, et al.* (2010) A human monoclonal anti-ANG2 antibody leads to broad antitumor activity in combination with VEGF inhibitors and chemotherapy agents in preclinical models. Mol Cancer Ther *9*, 145-156.

Casanovas, O., Hicklin, D. J., Bergers, G., and Hanahan, D. (2005). Drug resistance by evasion of anti-angiogenic targeting of VEGF signaling in late-stage pancreatic islet tumors. Cancer cell *8*, 299-309.

Chae, S. S., Kamoun, W. S., Farrar, C. T., Kirkpatrick, N. D., Niemeyer, E., de Graaf, A. M., Sorensen, A. G., Munn, L. L., Jain, R. K., and Fukumura, D. (2010). Angiopoietin-2 Interferes with Anti-VEGFR-2- Induced Vessel Normalization and Survival Benefit in Mice Bearing Gliomas. Clin Cancer Res. *16*, 3618-27.

Chan, D. A., Kawahara, T. L., Sutphin, P. D., Chang, H. Y., Chi, J. T., and Giaccia, A. J. (2009). Tumor vasculature is regulated by PHD2-mediated

angiogenesis and bone marrow-derived cell recruitment. Cancer cell *15*, 527-538.

Chung, A. S., Lee, J., and Ferrara, N. (2010). Targeting the tumour vasculature: insights from physiological angiogenesis. Nature Reviews Cancer *10*, 505-514.

Coffelt, S. B., Lewis, C. E., Naldini, L., Brown, J. M., Ferrara, N., and De Palma, M. (2010a). Elusive identities and overlapping phenotypes of pro-angiogenic myeloid cells in tumors. The American journal of pathology *176*, 1564-1576.

Coffelt, S. B., Tal, A. O., Scholz, A., De Palma, M., Patel, S., Urbich, C., Biswas, S. K., Murdoch, C., Plate, K. H., Reiss, Y., and Lewis, C. E. (2010b). Angiopoietin-2 Regulates Gene Expression in TIE2-Expressing Monocytes and Augments Their Inherent Pro-angiogenic Functions. Cancer research. *70*, 5270-80.

De Palma, M., Venneri, M. A., Roca, C., and Naldini, L. (2003). Targeting exogenous genes to tumor angiogenesis by transplantation of genetically modified hematopoietic stem cells. Nature medicine *9*, 789-795.

De Palma, M., Venneri, M. A., Galli, R., Sergi Sergi, L., Politi, L. S., Sampaolesi, M., and Naldini, L. (2005). Tie2 identifies a hematopoietic lineage of pro-angiogenic monocytes required for tumor vessel formation and a mesenchymal population of pericyte progenitors. Cancer cell *8*, 211-226.

De Palma, M., Mazzieri, R., Politi, L. S., Pucci, F., Zonari, E., Sitia, G., Mazzoleni, S., Moi, D., Venneri, M. A., Indraccolo, S.*, et al.* (2008). Tumor-targeted interferon-alpha delivery by Tie2-expressing monocytes inhibits tumor growth and metastasis. Cancer cell *14*, 299-311.

DeNardo, D. G., Barreto, J. B., Andreu, P., Vasquez, L., Tawfik, D., Kolhatkar, N., and Coussens, L. M. (2009). CD4(+) T cells regulate pulmonary metastasis of mammary carcinomas by enhancing protumor properties of macrophages. Cancer cell *16*, 91-102.

Du, R., Lu, K. V., Petritsch, C., Liu, P., Ganss, R., Passegue, E., Song, H., Vandenberg, S., Johnson, R. S., Werb, Z., and Bergers, G. (2008). HIF1alpha induces the recruitment of bone marrow-derived vascular modulatory cells to regulate tumor angiogenesis and invasion. Cancer cell *13*, 206-220.

Ebos, J. M., Lee, C. R., Cruz-Munoz, W., Bjarnason, G. A., Christensen, J. G., and Kerbel, R. S. (2009). Accelerated metastasis after short-term treatment with a potent inhibitor of tumor angiogenesis. Cancer cell *15*, 232-239.

Fantin, A., Vieira, J. M., Gestri, G., Denti, L., Schwarz, Q., Prykhozhij, S., Peri, F., Wilson, S. W., and Ruhrberg, C. Tissue macrophages act as cellular chaperones for vascular anastomosis downstream of VEGF-mediated endothelial tip cell induction. Blood *116*, 829-840.

Fiedler, U., Scharpfenecker, M., Koidl, S., Hegen, A., Grunow, V., Schmidt, J. M., Kriz, W., Thurston, G., and Augustin, H. G. (2004). The Tie-2 ligand angiopoietin-2 is stored in and rapidly released upon stimulation from endothelial cell Weibel-Palade bodies. Blood *103*, 4150-4156.

Gentner, B., Visigalli, I., Hiramatsu, H., Lechman, E., Ungari, S., Giustacchini, A., Schira, G., Amendola, M., Quattrini, A., Martino, S.*, et al.* (2010). Identification of Hematopoietic Stem Cell-Specific miRNAs Enables Gene Therapy of Globoid Cell Leukodystrophy. Sci Transl Med *2*, 58ra84.

Hashimoto, T., Wu, Y., Boudreau, N., Li, J., Matsumoto, M., and Young, W. (2004). Regulation of tie2 expression by angiopoietin--potential feedback system. Endothelium *11*, 207-210.

Hashizume, H., Falcon, B. L., Kuroda, T., Baluk, P., Coxon, A., Yu, D., Bready, J. V., Oliner, J. D., and McDonald, D. M. Complementary actions of inhibitors of angiopoietin-2 and VEGF on tumor angiogenesis and growth. Cancer research *70*, 2213-2223.

Holash, J., Maisonpierre, P. C., Compton, D., Boland, P., Alexander, C. R., Zagzag, D., Yancopoulos, G. D., and Wiegand, S. J. (1999). Vessel

cooption, regression, and growth in tumors mediated by angiopoietins and VEGF. Science (New York, NY *284*, 1994-1998.

Huang, H., Bhat, A., Woodnutt, G., and Lappe, R. (2010). Targeting the ANGPT-TIE2 pathway in malignancy. Nature Reviews Cancer *10*, 575-585.

Kerbel, R. S. (2008). Tumor angiogenesis. N Engl J Med *358*, 2039-2049.

Kioi, M., Vogel, H., Schultz, G., Hoffman, R. M., Harsh, G. R., and Brown, J. M. (2010). Inhibition of vasculogenesis, but not angiogenesis, prevents the recurrence of glioblastoma after irradiation in mice. The Journal of clinical investigation *120*, 694-705.

Kozin, S. V., Kamoun, W. S., Huang, Y., Dawson, M. R., Jain, R. K., and Duda, D. G. (2010) Recruitment of Myeloid but not Endothelial Precursor Cells Facilitates Tumor Regrowth after Local Irradiation. Cancer research. *70*, 5679-85.

Lin, E. Y., Li, J. F., Gnatovskiy, L., Deng, Y., Zhu, L., Grzesik, D. A., Qian, H., Xue, X. N., and Pollard, J. W. (2006). Macrophages regulate the angiogenic switch in a mouse model of breast cancer. Cancer research *66*, 11238-11246.

Mantovani, A., and Sica, A. Macrophages, innate immunity and cancer: balance, tolerance, and diversity. Curr Opin Immunol *22*, 231-237.

Murdoch, C., Tazzyman, S., Webster, S., and Lewis, C. E. (2007). Expression of Tie-2 by human monocytes and their responses to angiopoietin-2. J Immunol *178*, 7405-7411.

Nasarre, P., Thomas, M., Kruse, K., Helfrich, I., Wolter, V., Deppermann, C., Schadendorf, D., Thurston, G., Fiedler, U., and Augustin, H. G. (2009). Host-derived angiopoietin-2 affects early stages of tumor development and vessel maturation but is dispensable for later stages of tumor growth. Cancer research *69*, 1324-1333.

Oliner, J., Min, H., Leal, J., Yu, D., Rao, S., You, E., Tang, X., Kim, H., Meyer, S., Han, S. J*., et al.* (2004). Suppression of angiogenesis and tumor growth by selective inhibition of angiopoietin-2. Cancer cell *6*, 507-516.

Paez-Ribes, M., Allen, E., Hudock, J., Takeda, T., Okuyama, H., Vinals, F., Inoue, M., Bergers, G., Hanahan, D., and Casanovas, O. (2009). Anti-angiogenic therapy elicits malignant progression of tumors to increased local invasion and distant metastasis. Cancer cell *15*, 220-231.

Pucci, F., Venneri, M. A., Biziato, D., Nonis, A., Moi, D., Sica, A., Di Serio, C., Naldini, L., and De Palma, M. (2009). A distinguishing gene signature shared by tumor-infiltrating Tie2-expressing monocytes, blood "resident" monocytes, and embryonic macrophages suggests common functions and developmental relationships. Blood *114*, 901-914.

Qian, B. Z., and Pollard, J. W. (2010). Macrophage diversity enhances tumor progression and metastasis. Cell *141*, 39-51.

Saharinen, P., Bry, M., and Alitalo, K. (2010). How do angiopoietins Tie in with vascular endothelial growth factors? Curr Opin Hematol *17*, 198-205.

Saharinen, P., Eklund, L., Miettinen, J., Wirkkala, R., Anisimov, A., Winderlich, M., Nottebaum, A., Vestweber, D., Deutsch, U., Koh, G. Y*., et al.* (2008). Angiopoietins assemble distinct Tie2 signalling complexes in endothelial cell-cell and cell-matrix contacts. Nature cell biology *10*, 527-537.

Seegar, T. C., Eller, B., Tzvetkova-Robev, D., Kolev, M. V., Henderson, S. C., Nikolov, D. B., and Barton, W. A. (2010). Tie1-Tie2 interactions mediate functional differences between angiopoietin ligands. Mol Cell *37*, 643-655.

Shojaei, F., Wu, X., Malik, A. K., Zhong, C., Baldwin, M. E., Schanz, S., Fuh, G., Gerber, H. P., and Ferrara, N. (2007). Tumor refractoriness to anti-VEGF treatment is mediated by CD11b+Gr1+ myeloid cells. Nat Biotechnol *25*, 911-920.

Shojaei, F., Singh, M., Thompson, J. D., and Ferrara, N. (2008). Role of Bv8 in neutrophil-dependent angiogenesis in a transgenic model of cancer progression. Proceedings of the National Academy of Sciences of the United States of America *105*, 2640-2645.

Shojaei, F., Lee, J. H., Simmons, B. H., Wong, A., Esparza, C. O., Plumlee, P. A., Feng, J., Stewart, A. E., Hu-Lowe, D. D., and Christensen, J. G. (2010). HGF/c-Met Acts as an Alternative Angiogenic Pathway in Sunitinib-Resistant Tumors. Cancer research. *70*, 10090-100.

Stockmann, C., Doedens, A., Weidemann, A., Zhang, N., Takeda, N., Greenberg, J. I., Cheresh, D. A., and Johnson, R. S. (2008). Deletion of vascular endothelial growth factor in myeloid cells accelerates tumorigenesis. Nature *456*, 814-818.

Suri, C., Jones, P. F., Patan, S., Bartunkova, S., Maisonpierre, P. C., Davis, S., Sato, T. N., and Yancopoulos, G. D. (1996). Requisite role of angiopoietin-1, a ligand for the TIE2 receptor, during embryonic angiogenesis. Cell *87*, 1171-1180.

Takakura, N., Huang, X. L., Naruse, T., Hamaguchi, I., Dumont, D. J., Yancopoulos, G. D., and Suda, T. (1998). Critical role of the TIE2 endothelial cell receptor in the development of definitive hematopoiesis. Immunity *9*, 677-686.

Venneri, M. A., De Palma, M., Ponzoni, M., Pucci, F., Scielzo, C., Zonari, E., Mazzieri, R., Doglioni, C., and Naldini, L. (2007). Identification of pro-angiogenic TIE2-expressing monocytes (TEMs) in human peripheral blood and cancer. Blood *109*, 5276-5285.

Xian, X., Hakansson, J., Stahlberg, A., Lindblom, P., Betsholtz, C., Gerhardt, H., and Semb, H. (2006). Pericytes limit tumor cell metastasis. The Journal of clinical investigation *116*, 642-651.

# CHAPTER 3

# A role of miR-155 in enabling tumor-infiltrating innate immune cells to mount effective anti-tumor responses

**Erika Zonari,**[1,3] Ferdinando Pucci,[1,2] Massimo Saini,[1,2] Roberta Mazzieri,[1,2] Letterio S. Politi,[3] Bernhard Gentner,[1,2,5] and Luigi Naldini[1,2,5,*]

[1]Telethon Institute for Gene Therapy, San Raffaele Institute, Milano, Italy
[2]'Vita-Salute San Raffaele' University Medical School, Milano, Italy
[3]Università degli Studi di Milano-Bicocca
[4]Neuroradiology Division, Head and Neck Department, and CERMAC, San Raffaele Hospital, Milano, Italy
[5]These Authors share senior authorship
*: Correspondence: naldini.luigi@hsr.it (LN)

*Manuscript in preparation*

## Summary

Activation of a productive immune response requires transient upregulation of miR155 in the hematopoietic compartment. In order to investigate miR-155 in the context of tumor-associated immune responses, we stably knocked down (KD) miR-155 in the myeloid compartment of MMTV-PyMT mice (PyMT), a mouse model of spontaneous breast carcinogenesis that closely mimics tumor-host interactions seen in humans. Notably, myeloid cell specific miR-155 KD significantly accelerated tumor growth, as reflected by increased tumor mass and more pronounced secondary hematopoietic changes, i.e. leukocytosis and anemia. Mechanistically, miR155 KD reduces classical activation of tumor macrophages creating an imbalance towards a protumoral microenvironment as evidenced by up-regulation of the Th2 gene "IL13" in $CD4^+$ T cells.

Our studies are one of the first to implicate a miRNA in modulating myeloid responses in the tumor microenvironment. This study further highlights the importance of tumor infiltrating hematopoietic cells in fighting cancer development and establishes an antitumoral function of a prototypical oncomir, underscoring the context-specificity of miRNA regulation.

## Introduction

An inflammatory microenvironment has recently been proposed as a seventh hallmark of cancer. Innate and adaptive immune responses, modulated and potentially subverted by the tumor cells, create an environment of "smoldering" inflammation transforming an anti-tumor defense mechanism into a potent promoter of tumor growth.

Tumor associated macrophages (TAMs) are heterogeneous, with some subsets acting as bona fide antigen presenting cells (APCs) eliciting antitumor responses, and others fulfilling tissue remodeling functions thus favoring tumor progression by supporting angiogenesis, invasion and metastasis (Lin et al., 2001; De Palma et al., 2003; De Palma et al., 2005; Qian and Pollard, 2010). It has been speculated that dynamic changes of the tumor microenvironment may occur during the transition from early neoplastic events toward advanced tumor stages (Sica and Bronte, 2007). These events comprise a switch in TAM function from an anti-tumoral inflammatory response towards a pro-tumoral phenotype (Sica and Bronte, 2007).

The macrophage inflammatory response to infection involves the upregulation of several miRNAs, such as miR-155, miR-146, miR-147, miR-21 and miR-9 (O'Connell et. al, 2007; Taganov et al., 2006). Among these, miR-155 is expressed by a variety of immune cell types, including B and T lymphocytes, macrophages, dendritic cells, and by hematopoietic progenitor/stem cell populations (Eis et al., 2005; Kluiver et al., 2005; O'Connell et al., 2008; Rodriguez et al., 2007; Thai et al., 2007). In basal conditions, miR-155 is expressed to

low levels in most of these cell types. After activation by immune stimuli such as antigen, Toll-like Receptor ligands and inflammatory cytokines, miR-155 expression is rapidly increased (O'Connell et al., 2007; Rodriguez et al., 2007; Thai et al., 2007).

miR-155-deficient mice have global immune defects characterized by decreased dendritic cells (DC) function and defective B and T cell responses (Rodriguez et al., 2007; Thai et al., 2007). Specifically, the failure of miR-155-deficient mice to acquire protective immunity after *Salmonella typhimurium* infection was found to be owing to a failure of DCs to efficiently activate T cells, probably due to the failure of DCs to functionally activate costimulatory signals and to a defective antigen presentation; miR-155 may also be responsible for the impaired cytokine production observed in these mice (Rodriguez et al., 2007). The adaptive immune response in these mice was also found to be skewed towards a T helper 2 (TH2)-type immune response associated with the production of Th2 cytokines including IL-4, IL-5 and IL-10. These data strongly suggest that miR-155 is normally required for a TH1-type response and for the polarization of T cells towards a pro-inflammatory phenotype (Rodriguez et al., 2007).

Taken together, miR-155 can be regarded as a multi-functional miRNA with context-specific modes of action. To comprehensively understand its role in cancer, studies must account for the cellular heterogeneity of tumors. To our knowledge, studies on the function of miR-155 in pro-inflammatory TAMs tumor microenvironment are still missing. In this work, we wanted to address the role of miR-155 in

TAMs. Using a myeloid cell specific loss of function approach, we establish that miR-155 is actively contributing to antitumor immunity, especially during the early stages of breast carcinogenesis.

## Results

### miR-155 expression in tumor-infiltrating inflammatory macrophages

In order to investigate the expression of miRNA-155 in tumor infiltrating cells, we purified hematopoietic subpopulations from the CD45-positive fraction of spontaneous mammary tumors taken from 13 week old MMTV-PyMT transgenic mice (Husemann et al. 2008; Lin et al. 2003; Lin et al. 2001). We sorted $CD4^+$ T lymphocytes ($CD11b^-CD4^+$) and tumor-associated macrophages (TAMs) further divided into the $CD11b^+CD11c^+MRC1^-$ proinflammatory subset and the $CD11b^+CD11c^-MRC1^+$ protumoral subset (Mazzieri et al., 2011; Pucci et al., 2009), and measured the expression level of miR-155 by quantitative PCR (qPCR) (Figure 1A). miR-155 was most highly expressed in the tumor-infiltrating $CD4^+$ T lymphocytes. In agreement with previously published data (Kohlhaas et al., 2009; Lu et al., 2009; Rodriguez et al., 2007; Thai et al., 2007), high miR-155 activity found in $CD4^+$ cells segregated with the $CD4^+CD25^+$ subset, which is mainly composed of regulatory T (Treg) cells (data not shown show data). miR-155 was also detectable in $CD4^+$ T-cells and $CD11c^+$ inflammatory TAMs, but not $MRC1^+$ protumoral TAMs (Figure 1A). miR-155 expression in $CD11c^+$ cells may be consistent with activated inflammatory macrophages/dendritic cells, as it has been reported that miR-155 is strongly induced in dendritic cells upon activation (Brown et al., 2007; O'Connell et al., 2007; Tili et al., 2007). Indeed, treatment of primary bone marrow (BM)-derived $CD11c^+$ myeloid cells with

lipopolysaccharide (LPS, an inflammatory stimulus) induced miR-155 expression by twenty-fold (to levels > 1 log above let-7a, Suppl. Figure S1).

In order to investigate whether miR-155 has a functional role in inflammatory myeloid cells of tumor-bearing mice, we developed a lentiviral vector (LV) platform which allows stable knock-down of miR-155 specifically in myeloid but not T-cells. To this aim, we exploited the spleen focus forming virus (SFFV) promoter to drive the expression of multiple miR-155 knock down (miR-155 KD) target sequences coupled to a destabilized green fluorescent protein (dGFP) reporter (Figure 1B) (Gentner et al., 2009). This promoter drives transgene expression to high level in monocytes and dendritic cells, intermediate level in granulocytes and B lymphocytes, and very low level in T lymphocytes (Figure 1C). Since stable miRNA knockdown requires high expression levels of the KD cassette (Gentner et al., 2009), this vector should enable fairly allows us to perform specific miR-155 knockdown in the myeloid lineage.

The miR-155 KD vector was tested for its ability to knock down miR-155 in Raw 264.7 cells, which show a basal expression of miR-155 similar to inflammatory TAMs (Suppl. Figure S2). We then measured the protein expression levels of PU.1, a previously reported miR-155 target, in Raw 264.7 cells after transduction with the miR-155 KD vector or a control vector (Ctrl) carrying a scrambled target sequence not complementary to any known microRNA (Figure 1D). Both in steady state conditions and upon LPS treatment, PU.1 was upregulated up to 2-fold in miR-155 KD cells as measured by Western blot

(Figure 1D). Similarly, RT-qPCR of PU.1 and SHIP1, another known miR-155 target, showed a 1.3- to 1.7-fold upregulation upon miR-155 KD, while overexpression of miR-155 (miR-155 OE) by overexpressing LV (Amendola et al., 2009b) resulted in a 40-50% downregulation (Figure 1E).

In summary, these data indicate efficient inhibition of miR-155 regulation in myeloid cells by our KD vector throughout a broad range of miR-155 expression levels (i.e., basal and after LPS stimulation), while T lymphocytes are spared due to the minimal activity of the SFFV promoter in this cell type.

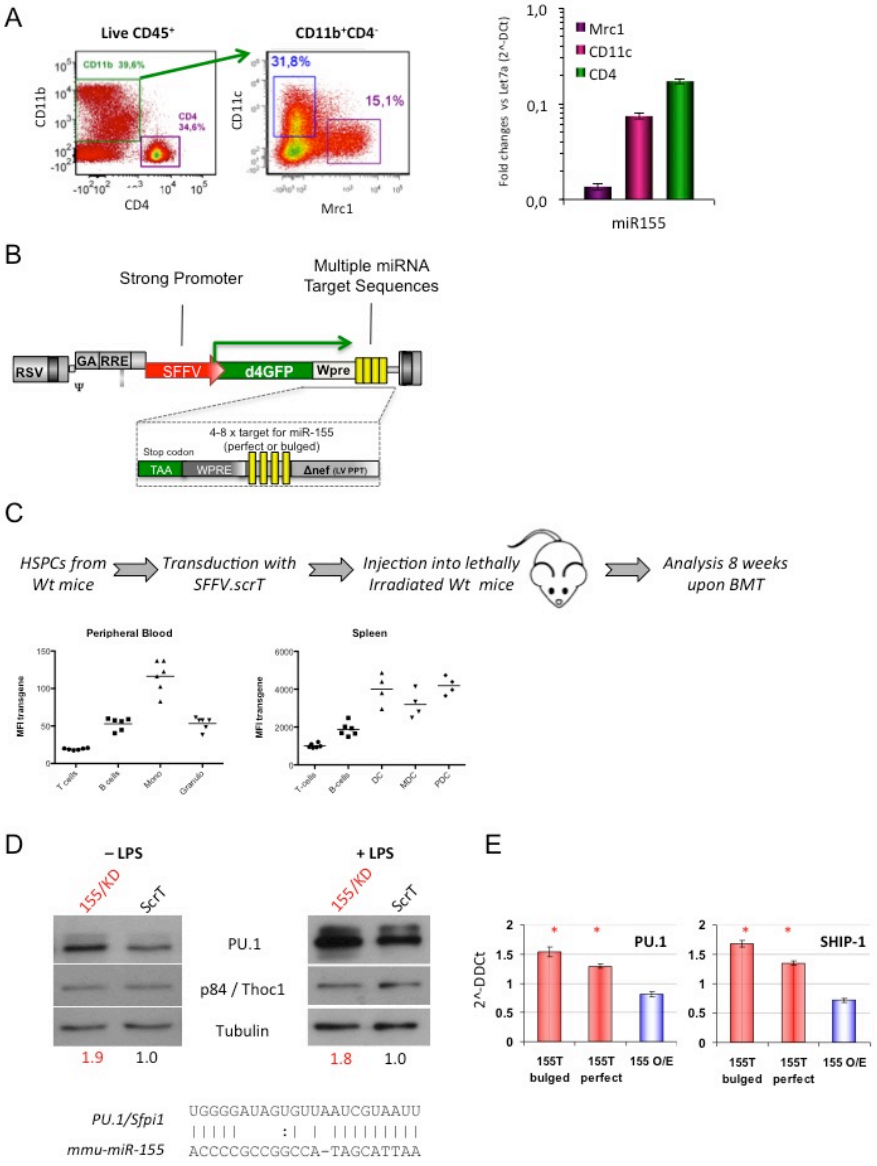
A
Live CD45+
CD11b+CD4-
CD11b 39,6%
CD4 34,6%
31,8%
15,1%
CD11b
CD4
CD11c
Mrc1
Fold changes vs Let7a (2^-DCt)
1,0
0,1
0,0
Mrc1
CD11c
CD4
miR155
B
Strong Promoter
Multiple miRNA Target Sequences
RSV
GA
RRE
SFFV
d4GFP
Wpre
Ψ
4-8 x target for miR-155 (perfect or bulged)
Stop codon
TAA
WPRE
Δnef (LV PPT)
C
HSPCs from Wt mice
Transduction with SFFV.scrT
Injection into lethally Irradiated Wt mice
Analysis 8 weeks upon BMT
Peripheral Blood
Spleen
MFI transgene
T cells
B cells
Mono
Granulo
DC
MDC
PDC
D
– LPS
+ LPS
155/KD
ScrT
PU.1
p84 / Thoc1
Tubulin
1.9
1.0
1.8
1.0
PU.1/Sfpi1
mmu-miR-155
UGGGGAUAGUGUUAAUCGUAAUU
ACCCCGCCGGCCA-TAGCATTAA
E
2^-DDCt
PU.1
SHIP-1
155T bulged
155T perfect
155 O/E

**Figure 1. Preferential expression of miR-155 in CD11c$^{+}$ TAMs and development of a vector platform for stable myeloid-specific miR-155 knock down.**

***A:*** *Left: Gating strategy for sorting and miR-155 TaqMan expression analysis of tumor-infiltrating hematopoietic cells. Right: Data show mean* $2^{-\Delta Ct}$ *values ± SEM vs. Let7a; n = 2-3 independent experiments.*

***B****: Lentiviral vector construct for specific myeloid miR-155 knock down (SFFV.dGFP.miR-155T).*

***C****: Top: Schematic of the bone marrow transplantation protocol. Bottom: MFI of transgene (GFP) in different hematopoietic subpopulations from the peripheral blood and the spleen of mice stably transplanted with hematopoietic stem/progenitor cells transduced with scrambled-target LV (scrT).*

***D****: Western blot analysis on PU.1, a natural target of miR-155. Raw 264.7 cells were transduced with the miR-155 KD or scrT control LVs and treated (right) or not (left) with LPS (1ng/ml) for 48h.*

***E****: Expression of the PU.1 and SHIP1 mRNA in Raw 264.7 cells transduced with miR-155 knock down vector with buldge or perfect target and miR-155 overexpressing vector. Data show mean* $2^{-\Delta\Delta Ct}$ *values ± SEM vs. β2m; n = 4 independent experiments. Statistical analysis of the data was performed on* $2^{-\Delta\Delta Ct}$ *values by unpaired Student's t-test. *:* $p < 0.05$.

**Myeloid-specific miR-155 knock down accelerates tumor growth in a spontaneous breast cancer model**

Having established a myeloid-specific miR-155 KD vector platform, we addressed the question whether miR-155 has a functional role in TAMs. To this aim, we transplanted MMTV-PyMT mice with HSPC transduced with the miR-155 KD vector or a control vector carrying scrambled target sequences (Figure 2A). At the time of transplant (5.5 weeks of age), MMTV-PyMT mice show hyperplasia of the breast epithelium with no detectable adenomas or carcinomas (De Palma et al., 2008). Spontaneous tumor development was monitored by magnetic resonance imaging (MRI) at 9 and 12 weeks of age (Figure 2B). Strikingly, miR-155 KD in BM-derived cells significantly increased tumor volume compared with the control group, and this effect was already evident at the late adenoma stage (9 week time-point). This finding further support a myeloid cell mediated phenotype, since T cell reconstitution has not yet occurred 3.5 weeks after HSPC transplantation (data not shown). Mice were euthanized between 12-13 weeks of age, and accelerated tumor growth in the miR-155 KD group was confirmed by the significantly increased weight of the surgically resected tumor masses (Figure 2C).

Next, we assessed the impact of miR-155 KD on hematopoiesis in the MMTV-PyMT mice. Blood cell counts by hemocytometric analysis showed no significant differences at the 9 week time-point, suggesting that miR-155 KD had no detectable impact on hematopoietic reconstitution (data not shown). However, at 12 weeks of age tumor-induced anemia and leukocytosis were significantly more severe in the

miR-155 KD group compared to the scrambled ctrl group (Figure 2D). Among the leukocytes, side scatter $(SSC)^{low}$ $CD11b^{+}$ monocytes showed the most significant increase in miR-155 KD (versus control) mice (Figure 2E). These cells have been reported to be protumoral and proangiogenic (Shojaei et al., 2008b; Sica and Bronte, 2007; Yang et al., 2004).

In summary, myeloid-specific miR-155 KD accelerates tumor development in a spontaneous mammary cancer model, suggesting that miR-155 acts on the early stages of carcinogenesis (Figure 2B and C) by a mechanism involving myeloid cells.

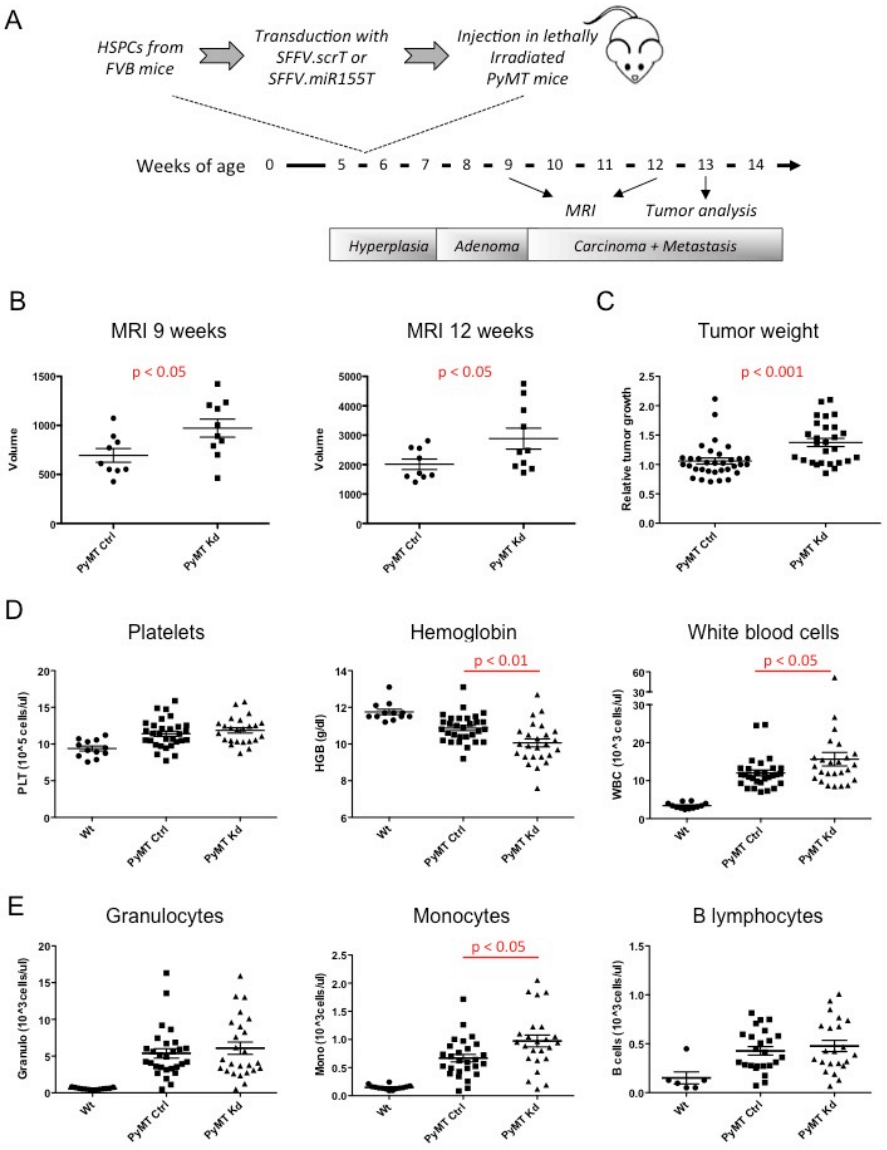


**Figure 2. Myeloid-specific miR-155 knock down accelerates tumor growth in a spontaneous breast cancer model**

***A:*** *Tumor growth in transgenic MMTV-PyMT mice. Schematic of the bone marrow transplantation protocol in MMTV-PyMT mice.*

***B:*** *Mammary tumor growth (mean volume ± SEM by MRI analysis of the three anterior mammary glands) at 9 and 12 weeks of age in control (PyMT Ctrl; n=9) and miR-155 knock down (PyMT Kd; n=10) MMTV-PyMT transplanted mice. Statistical analyses were performed by unpaired Student's t test.*

***C****: Relative tumor growth. Tumor weight normalized towards the median of control group for four different experiments (PyMT Ctrl n=33; PyMT Kd n=27). Each dot in the plot corresponds to one mouse bearing multiple mammary tumors. Statistical analysis was performed by Mann-Whitney U test.*

***D****: Blood cell counts and haematological parameters (mean ± SEM) in wilde type (Wt; n=12), HSPC-transplanted control (PyMT Ctrl; n=30) and miR-155 knock down (PyMT Kd; n=25) mice at 13 weeks of age. PLT, platelets (x10$^5$/ml); HGB, haemoglobin (g/dl); WBC, white blood cells (x10$^3$/ml). Results from four different experiments. Each dot in the plot corresponds to one mouse. Statistical analysis was performed by Mann-Whitney U test.*

***E****: FACS analysis on peripheral blood on transplanted mice at 13 weeks of age (mean ± SEM) in wilde type (Wt; n=12), HSPC-transplanted control (PyMT Ctrl; n=30) and miR-155 knock down (PyMT Kd; n=25) mice at 13 weeks of age. Absolute count of Granulo, granulocytes; Mono, monocytes; B cells, B lymphocytes (x10$^3$/ml). Each dot in the plot corresponds to one mouse. Statistical analysis was performed by Mann-Whitney U test.*

**miR-155 KD has no effect on the growth of established mammary carcinomas**

To investigate whether miR-155 KD in myeloid cells would also accelerate the growth of established carcinomas, we set up an orthotopic breast cancer model. Tumors from 16 week old PyMT mice (late carcinoma stage) were dissociated and orthotopically injected into the mammary fat pad of FVB mice stably reconstituted with HSPC expressing SFFV.miR-155 KD or SFFV.scrambled control vector. Even though hematopoietic reconstitution with miR-155 KD cells was as high as obtained in the PyMT mice, we observed no significant differences in tumor growth between the miR-155 KD and Ctrl group (Suppl. Figure S3). These data suggest that miR-155 in myeloid cells is dispensable for later stages of tumor progression.

**miR-155 knock down impairs the ability of myeloid cells to mount a proinflammatory response**

Tumor-infiltrating hematopoietic cells are important effectors of tumor rejection processes, especially during early-stage tumorigenesis, before tumor cells have acquired mechanisms of immune evasion (Schreiber et al., 2011; Willimsky and Blankenstein, 2007). We quantified by immunofluorescence staining of tumor sections the composition of the inflammatory cell infiltrate in 12 week-old MMTV-PyMT tumors from either miR-155 KD or Ctrl mice. Whereas the frequency of infiltrating $CD45^+$ hematopoietic cells (data not shown) and $CD68^+$ macrophages was similar in miR-155 KD and control tumors (Figure 3A and B), there was a significant

reduction in the expression of the activation marker (ionized binding adaptor molceule-1, Iba1) by innate immune cells specifically in miR-155 KD tumors (Figure 3A and B). Of note, flow cytometry analysis of dissociated tumors showed no differences in the relative proportion of $CD11b^+$ cells, $CD4^+$ or $CD8^+$ T lymphocytes, Treg, $CD19^+$ B lymphocytes and NK cells. These data suggest that myeloid-specific miR-155 KD does not impair the homing of hematopoietic cells to the tumor, nor does it impact on their survival within the tumor microenvironment. Rather, miR-155 KD may reduce activation of myeloid cells towards inflammatory macrophages/ dendritic cells.

We then investigated the impact of miR-155 KD on signaling pathways associated with miR-155 natural targets, first and foremost SHIP1. SHIP is a negative regulator of growth factor receptor-mediated PKB/AKT activation and myeloid cell survival. This protein can reduce activation of phosphodytil-inositol-3-kinase (PI3K) and thereby signal transduction by extracellular signals that depend on the PI3K/AKT axis. Western blot analysis of RAW 264.7 cells indicated reduced levels of AKT phosphorylation at Ser473, a major activatory phosphorylation site, upon miR-155 KD. This was accompanied by a consistent reduction in phosphorylation of GSK3b at Ser9, and S6 kinase at Ser235/236, two downstream substrates of AKT (Figure 3C). Thus, miR-155 KD impairs AKT activation in macrophages by increasing SHIP1 level.

GM-CSF is a pro-inflammatory cytokine involved in macrophage activation and maturation of antigen-presenting cells. Interestingly, GM-CSF was described to signal through the PI3K/AKT pathway that

we found regulated by miR-155. To elucidate whether miR-155 had an impact on the responsiveness of macrophages to GM-CSF, we assayed the activation of the PI3K/AKT pathway induced by GM-CSF in RAW264.7 cells with stable KD or OE of miR-155. Cells were starved in serum- and cytokine- free medium prior to stimulation with GM-CSF and then assayed for Phospho-Akt (Ser473) by flow cytometry. GM-CSF induced AKT phosphorylation was reduced in miR-155 KD cells and enhanced in miR-155 OE cells, and these effects were only evident in the transduced cells. Collectively, these data indicate that physiological expression of miR-155 in myeloid cells enhances GM-CSF dependent PI3K-AKT signaling in macrophages (Figure 3D) and provide a mechanistic explanation for the reduced occurrence of activated myeloid cells in miR-155 KD tumors.

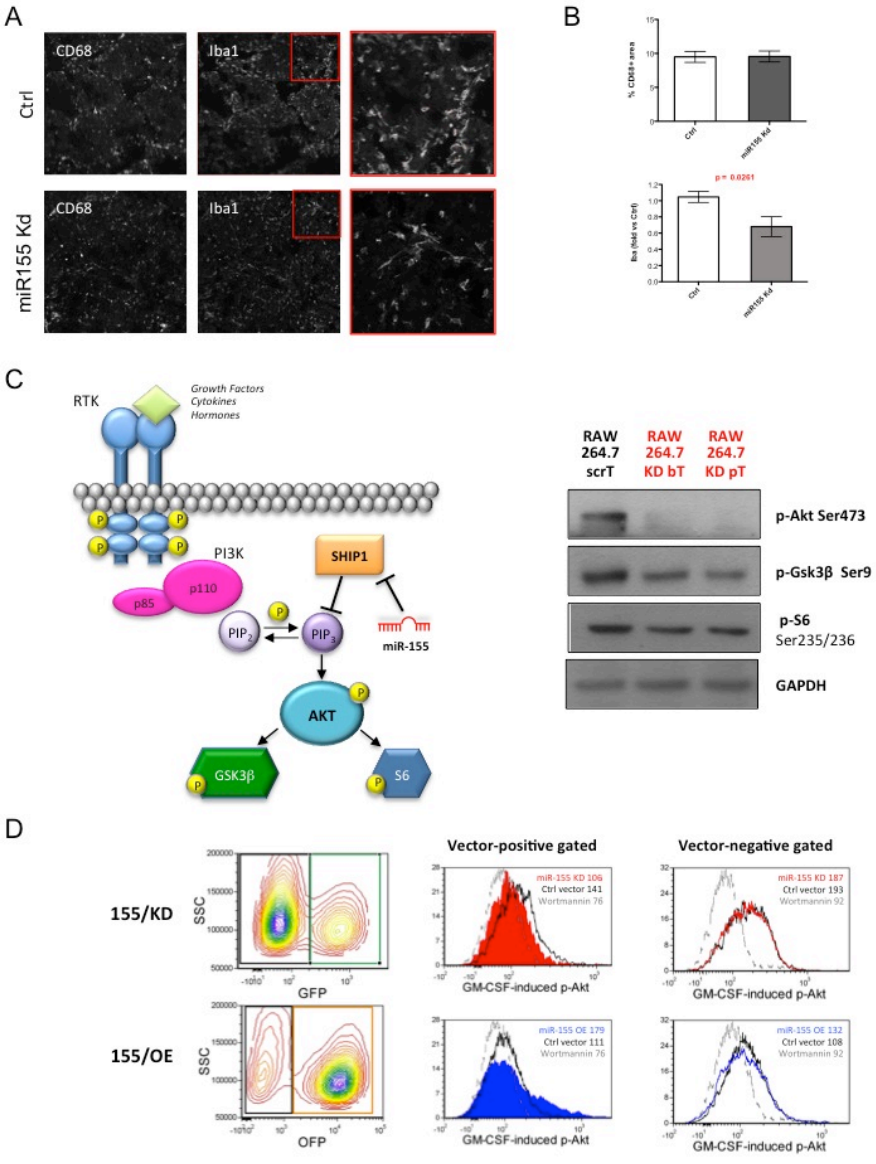
A
CD68
Iba1
Ctrl
miR155 Kd
B
C
RTK
Growth Factors
Cytokines
Hormones
PI3K
p110
p85
SHIP1
PIP2
PIP3
miR-155
AKT
GSK3β
S6
RAW 264.7 scrT
RAW 264.7 KD bT
RAW 264.7 KD pT
p-Akt Ser473
p-Gsk3β Ser9
p-S6 Ser235/236
GAPDH
D
155/KD
155/OE
SSC
GFP
OFP
Vector-positive gated
Vector-negative gated
GM-CSF-induced p-Akt

**Figure 3. miR-155 knockdown impairs Iba1 expression in tumor-infiltrating myeloid cells and Akt activation in myeloid Raw 264.7 cells.**

***A:*** *CD68 or Iba1 immunostaining of MMTV-PyMT tumors growth in control (Ctrl) or miR-155 knock down (miR-155 KD) transplanted mice. Tumor sections were analysed at 13 weeks of age. Photos are representative results obtained from six mice per group (20x magnification).*

***B:*** *Top panel shows quantification of myeloid cells infiltrates in tumors (mean percentage [%] of $CD68^+$ area ± SEM). Bottom panel shows quantification of $Iba1^+$ myeloid cell infiltrates in tumors (mean frequency of $Iba1^+$ cells ± SEM, shown as fold change versus reference [Ctrl]). Results are representative of two independent experiments and six tumors per group analysed. Statistical analysis was performed by Mann-Whitney U test.*

***C:*** *Left: simplified scheme illustrating the flow of signal through the SHIP1 - PI3K/AKT pathway.*

*Right: pAKT (Ser473), pGSK3b (Ser9), pS6 (Ser235/236) were measured in control (scrT) or miR-155 knock down (KD bT or pT) LV transduced Raw 264.7 cells by western blot. GAPDH was used as a loading control.*

***D:*** *Granulocytes-monocyte colony stimulating factor (GM-CSF) induced activation of AKT upon miR-155 knock down (miR-155 KD) or miR-155 overexpression (miR-155 OE) in Raw 264.7 cells. 3 hours starvation and re-stimulation with GM-CSF. Left FACS plots: GFP or Orange expression in Raw cells transduced with miR-155 KD or miR-*

*155 OE-LV and CTRL-LV (not shown) was gated into transduced and untransduced cells. Middle histograms: representative induction of pAKT (S473) in transduced GFP or mO2 expressing miR-155 KD cells (red), CTRL cells (black) or in miR-155 KD cells pretreated with the PI3K inhibitor Wortmannin (gray dashed line). Right: relative MFI of phospho-AKT S473 from untransduced cells.*

We then investigated the potential impact of failed activation of myeloid cells on other populations of adaptive immune cells recruited to the tumors. We performed gene expression analysis on FACS-sorted $CD4^+$ T cells isolated from MMTV-PyMT mammary tumors (Mazzieri et al., 2011) using a custom-made TaqMan Low Density Array carrying 95 genes including cytokines, chemokines, and genes involved in inflammation and immune response (Table 1). Interestingly, we observed several differentially expressed genes between miR-155 KD and Ctrl $CD4^+$ T cells; GM-CSF and IL-13 were both significantly upregulated in T-cells from miR-155 KD vs. control tumors, whereas other relevant genes such as IL-6 and CCR6 were significantly down-regulated. These data suggest a skewing of T cells towards a Th2 phenotype as a consequence of myeloid-specific miR-155 KD. Together, these data show a reduction in $Iba1^+$ activated inflammatory macrophages and skewing of $CD4^+$ T lymphocytes towards a Th2 phenotype in the tumors of mice with myeloid specific miR-155 KD.

**Table 1**

**Low-density array on $CD4^+$ tumor-infiltrating cells**

| Gene | p-value | Fold | dCt | SD |
|---|---|---|---|---|
| **Csf2** | * | **2,1** | **8,8** | **0,83** |
| **Il13** | * | **1,9** | **7,6** | **0,89** |
| **Il21** | | 1,7 | 13,0 | 1,29 |
| **Il5** | | 1,4 | 9,0 | 0,35 |
| **Bach1** | | 1,2 | 6,6 | 0,42 |
| **Myadm** | | 1,2 | 7,9 | 0,33 |
| **Ccr4** | | 1,2 | 6,8 | 0,48 |
| **Csf1** | | 1,2 | 8,6 | 0,37 |
| **18S** | | 1,1 | -11,0 | 0,08 |
| **Cdk6** | | 1,1 | 7,1 | 0,50 |
| **Jarid2** | | 1,1 | 6,8 | 0,23 |
| **Ctla4** | | 1,1 | 4,1 | 0,21 |
| **Cxcl11** | | 1,1 | 13,1 | 0,49 |
| **Irf1** | | 1,1 | 4,1 | 0,20 |
| **Actb** | | 1,0 | -1,5 | 0,21 |
| **Hprt** | | 1,0 | 6,2 | 0,19 |
| **Stat1** | | 1,0 | 4,4 | 0,12 |
| **Il17a** | | 1,0 | 10,2 | 2,03 |
| **Fas** | | 1,0 | 8,1 | 0,08 |
| **Ccr2** | | 1,0 | 6,1 | 0,23 |
| **Il15** | | 1,0 | 12,4 | 0,34 |
| **Il2** | | 1,0 | 8,4 | 0,66 |
| **Cd86** | | -1,0 | 10,4 | 0,15 |
| **Tnf** | | -1,0 | 6,8 | 0,43 |
| **Il2ra** | | -1,0 | 4,3 | 0,10 |
| **Irf8** | | -1,0 | 8,5 | 0,05 |
| **Fli1** | | -1,0 | 5,2 | 0,19 |
| **Cxcr3** | | -1,0 | 6,9 | 0,41 |
| **Tgfb1** | | -1,0 | 4,1 | 0,09 |
| **Nfkb1** | | -1,1 | 4,1 | 0,03 |
| **Ccr7** | | -1,1 | 2,2 | 0,40 |

| | | | |
|---|---|---|---|
| **Stat3** | -1,1 | 4,3 | 0,16 |
| **Socs1** | -1,1 | 5,7 | 0,36 |
| **Map3k5** | -1,1 | 6,6 | 0,18 |
| **Maf** | -1,1 | 9,8 | 0,51 |
| **Icos** | -1,1 | 4,1 | 0,26 |
| **Il6ra** | -1,1 | 4,3 | 0,35 |
| **H2-Ea** | -1,1 | 12,0 | 0,38 |
| **Tbx21** | -1,1 | 7,6 | 0,43 |
| **Inpp5d** | -1,1 | 6,6 | 0,22 |
| **Cebpb** | -1,1 | 7,3 | 0,13 |
| **Gata3** | -1,1 | 3,9 | 0,30 |
| **Cd28** | -1,1 | 4,0 | 0,33 |
| **Tnfsf10** | -1,1 | 7,5 | 0,33 |
| **Cd40** | -1,1 | 9,9 | 0,61 |
| **Itk** | -1,1 | 2,7 | 0,05 |
| **Cd80** | -1,1 | 8,1 | 0,44 |
| **Ccl2** | -1,1 | 9,9 | 0,65 |
| **Il10** | -1,1 | 11,2 | 0,76 |
| **Ikbke** | -1,2 | 4,3 | 0,06 |
| **Ly6a** | -1,2 | 5,9 | 0,27 |
| **Fes** | -1,2 | 11,0 | 0,32 |
| **Cd40lg** | -1,2 | 5,2 | 0,56 |
| **Fasl** | -1,2 | 6,1 | 0,12 |
| **Myc** | -1,2 | 6,6 | 0,38 |
| **Irf9** | -1,2 | 6,4 | 0,16 |
| **Ccl3** | -1,3 | 11,6 | 1,19 |
| **Hmox1** | -1,3 | 9,4 | 0,38 |
| **Ikbkb** | -1,3 | 5,6 | 0,12 |
| **Il18** | -1,3 | 12,6 | 0,81 |
| **Cxcl10** | -1,3 | 7,0 | 0,57 |
| **Ifng** | -1,3 | 7,9 | 0,70 |
| **Isg15** | -1,4 | 7,7 | 0,13 |
| **Oas1a** | -1,4 | 8,5 | 0,16 |
| **Il4** | -1,4 | 13,1 | 1,32 |
| **Eif2ak2** | -1,5 | 9,1 | 0,61 |
| **Gbp1** | -1,5 | 11,2 | 0,53 |

| | | | | |
|---|---|---|---|---|
| **Ptgs2** | | -1,5 | 11,6 | 1,65 |
| **Ccl5** | | -1,5 | 7,7 | 0,19 |
| **Il1a** | | -1,6 | 12,4 | 0,62 |
| **Il1b** | | -1,7 | 11,6 | 0,92 |
| **Ccr6** | . | -1,8 | 12,8 | 0,91 |
| **Il6** | * | -2,4 | 14,2 | 0,91 |
| **Csf1r** | * | -2,4 | 12,0 | 1,15 |
| **Sfpi1** | ** | -3,2 | 13,1 | 0,73 |

**Table 1. Genes expressed either differentially or not between control and miR-155 knock down $CD4^+$ tumor-infiltrate cells.**

*The expression level of each gene in tumor-derived $CD4^+$ from miR-155 knock down mice is indicated as fold-change vs. control mice (n=3). The ΔCT of each gene was calculated using β2m/Actinb as endogenous control.*

## Discussion

Here we describe for the first time the *in vivo* role of miR-155 in the context of tumor-associated immune responses. By specifically knocking down miR-155 in the myeloid compartment we observed: i) acceleration of tumor growth associated with more severe tumor-induced anemia and leukocytosis; ii) expansion of pro-tumoral $CD11b^+$ monocytes; iii) reduction in the expression of the macrophage activation marker Iba1; iv) skewing of $CD4^+$ T lymphocytes towards a Th2 phenotype, by up-regulation of IL-13.

Several lines of evidence suggest that knock down of miR-155 in myeloid cells and, particularly, in antigen-presenting cells (APC) such as macrophages is responsible for the acceleration of tumor growth that we observed. These include the myeloid-biased expression profile of the SFFV-driven knockdown vector, the timing of phenotype onset before lymphoreconstitution in the context of bone marrow transplantation and reduced expression of the activation marker Iba1 in tumor-associated macrophages. We further investigated the molecular consequences of miR-155 KD in a macrophage cell line. We found an upregulation of SHIP1 and, consequently, a reduction in the activation of the PI3K/AKT pathway at baseline and upon exposure to pro-inflammatory stimuli such as LPS and GM-CSF. SHIP1 is an inositol phosphatase and, together with PTEN, the main negative regulator of phosphoinositide 3-kinase (PI3K)/Akt signaling (Baran et al., 2003; Mondal et al., 2012). It represents one of the main direct targets of miR-155 (O'Connell et al.,

2009; Pedersen et al., 2009) and represses the production of pro-inflammatory cytokines (Parsa et al., 2006), phagosome maturation, and macrophage survival (Rajaram et al., 2009). Consistently, Akt promotes the production of pro-inflammatory cytokines such as TNFα, IL-6, and IL-12, while inhibiting the production of the anti-inflammatory cytokine IL-10 (Rajaram et al., 2006). We therefore hypothesize that miR155 KD shifted the macrophage phenotype towards a more anti-inflammatory and pro-tumoral phenotype, as supported by the reduced amount of Iba-1 staining in TAMs in the miR155 KD group of mice. Iba1, a significant component of phagocytic cups, participates in the early steps of phagocytosis and is specifically overexpressed in macrophages/microglia under inflammatory conditions. Its human homolog, allograft inflammatory factor-1 (AIF-1), is upregulated in macrophages upon allograft rejection and suppressed by the anti-inflammatory cytokine IL-10 (Zhou et al., 2011; Yang et al., 2007).

Using a custom made low density array containing cytokines and other inflammation associated genes, we could not detect significant gene expression differences in tumor macrophage subsets from miR-155 KD as compared to control mice. This might be due to the fact that the analysis had to be performed on late stage tumors since we were unable to collect sufficient material from earlier tumor stages or from draining lymph nodes which quickly become indistinguishable from the bulky tumor masses in this model. The antitumor activity of miR-155 KD hematopoietic cells was, however, most evident at the early stages of breast carcinogenesis but not in an

orthotopic breast cancer model upon injection of established carcinoma cells into the mammary fat pad, in line with the idea that antitumor immunity becomes less relevant once tumors have progressed and evolved mechanisms of immune evasion (Schreiber et al., 2011; Willimsky and Blankenstein, 2007). These technical limitations did not allow us to capture activated TAMs in the florid phase of antitumor immunity.

Interestingly, we observed alterations in the gene expression profile of $CD4^+$ tumor infiltrating lymphocytes in the miR-155 KD group. We found a significant upregulation of IL-13 and GM-CSF, and a downregulation of IL-6, Csf1r and Sfpi1. IL-13 is a classical Th2 cytokine suggesting a skewing of T cells towards a Th2 phenotype. In addition, downregulation of Sfpi1 might further reinforce Th2 functions since Sfpi1 knockout mice have been shown to have a lower T cell receptor activation threshold under Th2 culture conditions (Chang et al., 2009). On the other hand, IL-6 which we found significantly downregulated in the miR-155 KD group is a classical proinflammatory cytokine (Gabay et al., 2006). Macrophages and T cells interact closely, and it has been suggested that they mutually polarize each other to a pro-inflammatory M1/Th1 phenotype on one end, or to an alternative M2/Th2 activation state on the other end of the spectrum (Sica and Mantovani, 2012). Thus, the Th2 bias within the T cell compartment might indirectly reflect a proportional shift from classically (M1) activated TAMs to alternatively (M2) activated, pro-tumoral TAMs. Recent work has suggested that the receptor for IL-13, IL13Ra1, is directly targeted by

miR-155 in macrophages (Martinez-Nunez et al., 2011), further enhancing the effects of IL-13 upon miR-155 KD.

Even though unlikely, we cannot entirely exclude a direct effect of miR-155 KD on $CD4^+$ tumor infiltrating lymphocytes. A T cell specific miR-155 KD will be necessary to formally exclude this possibility. Likewise, we cannot fully exclude a biological effect of the myeloid-specific miR-155 KD vector on tumor infiltrating B lymphocytes. However, B lymphocytes do not seem to play a major role in our tumor model since breeding the PyMT oncogene onto a B cell deficient mouse background did not reveal differences in terms of tumor latency, tumor burden or tumor angiogenesis as compared to the classical PyMT model (DeNardo et al., 2009).

Another open question is the impact of miR-155 KD on myelopoiesis. It has been suggested that miR-155 positively regulated GM development by acting on myeloid bone marrow progenitors (O'Connell et al., 2008), a compartment in which the SFFV driven miR-155 KD vector is active (Gentner et al., 2009). However, in contrast to published data suggesting that miR-155 promotes macrophage differentiation (Mann et al., 2010) and myeloid colony formation (Hu et al., 2010), our *in vivo* results show an increase in the peripheral myeloid compartment ($CD11b^+$ monocytes) upon miR-155 KD. Thus, it is more likely that the expanded myeloid compartment is a consequence of the increased tumor burden upon myeloid specific miR-155 KD rather than a direct effect of the miR-155 KD vector on the BM compartment. This goes in line with the increased GM-CSF expression that we noted in tumor infiltrating $CD4^+$ T cells from the

miR-155 KD group as compared to control. GM-CSF is one of the principal myeloid growth factors stimulating myelopoiesis and recruiting myeloid cells to the tumor (Hamilton et al., 2008).

Extensive data indicate that miR-155 functions as an oncomiR in several solid tumors, such as thyroid carcinoma (Nikiforova et al., 2008), breast cancer (Iorio et al., 2005; Volinia et al., 2006), colon cancer (Volinia et al., 2006), cervical cancer (Wang et al., 2008), pancreatic ductal adenocarcinoma (Lee et al., 2007; Szafranska et al., 2007) and lung cancer where it is considered to be a marker of poor prognosis (Jay et al., 2007; Volinia et al., 2006; Yanaihara et al., 2006). miR-155 regulates multiple genes associated with cancer cell proliferation (Jiang et al., 2010; Xie et al., 2011; Chang and Sharan, 2011; Chang et al., 2011), apoptosis (Li et al., 2012; Meng et al., 2012; Zheng et al., 2012), metabolism (Jiang et al., 2012) and invasion (Dagan et al., 2012). Similarly, constitutive miR-155 expression in hematopoietic cells can result in the development of hematologic malignancies such as lymphoma and myeloproliferative disease (Costinean et al., 2009; Lee et al., 2012; Vargova et al., 2011; Yamanaka et al., 2009; Zanesi et al., 2010). These evidences have motivated the development of anti- miR-155 drugs as potential anticancer therapeutics (Gambari et al., 2011; Iorio et al., 2011; Iorio and Croce, 2012; Xia et al., 2010). Our data suggest a word of caution before unscrupulously applying anti miR-155 treatments to cancer patients. In this regard, it should be kept in mind that miR-155 has a physiological role in orchestrating a productive immune response. Previous work has highlighted the importance of miR-155 in acute

inflammatory insults (O'Connell et al., 2007; Rodriguez et al., 2007; Thai et al., 2007). Our data expand the role of miR-155 to myeloid cell mediated anti-tumoral responses, since blocking its physiological upregulation in these cells accelerated tumor development in a spontaneous breast cancer model. Very recently, using an opposite strategy, Cubillos-Ruiz and colleagues showed that reprogramming tumor-associated dendritic cells *in vivo* using microRNA mimetics triggers protective immunity against ovarian cancer. Replenishing miR-155 levels in tumor-associated DCs triggered potent anti-tumor responses that abrogated the progression of established ovarian cancers (Cubillos-Ruiz et al., 2012). Thus, a wave of miR-155 expression in hematopoietic cells is boosting immunity, and only failure to downregulate miR-155 may support oncogenesis, suggesting that miR-155 is, first of all, an "immunomiR" rather than an oncomiR. It remains to be determined whether the potential benefits of miR-155 inhibition (i.e., reduction in cell autonomous tumor cell growth in selected cancers with miR-155 overexpression) outweigh the state of immunosuppression induced by anti miR-155 therapies which can, paradoxically, favor tumor growth.

In summary, we here describe an anti-tumoral role of miR-155 as an integral effector of immunosurveillance thus limiting early steps of breast cancer development. This work highlights the context-specificity and complexity of microRNA regulation calling for a cell type specific approach which takes into consideration the heterogeneity of tumors composed of both cancer cells and a collection of nonmalignant host cells when studying miRNA function.

## Experimental Procedure

### Lentiviral vector (LV) construction and production

Mouse miR-155 target (miRT) sequences were designed based on miRNA sequences obtained from the miRNA Registry (http://microrna.sanger.ac.uk/). Oligonucleotides used for generating miRT sequences are shown below. For Bd.LV.mirT vectors, the corresponding Sense 1 (S1), Sense 2 (S2), Antisense 1 (AS1), and Antisense 2 (AS2) oligonucleotides were annealed, and ligated in the 3'UTR of the GFP expression cassette of the parent Bd.LV vector.

| | |
|---|---|
| S1 | CTAGAACCCCTATCACAATTAGCATTAACGATACCCCTATCACAATTAGCATTAAACGCGT |
| S2 | ACCCCTATCACAATTAGCATTAATCACACCCCTATCACAATTAGCATTAAC |
| AS1 | TTAATGCTAATTGTGATAGGGGTATCGTTAATGCTAATTGTGATAGGGGTT |
| AS2 | CCGGGTTAATGCTAATTGTGATAGGGGTGTGATTAATGCTAATTGTGATAGGGGTACGCGT |

Lentiviral vector platforms for miRNA stable knockdown were described previously (Gentner et al., 2009). For stable knockdown, from 4 to 8 tandem copies of a perfectly or imperfectly complementary miR-155 target sequence (perfectly 5' ACCCCTATCACAATTAGCATTAA 3', imperfectly 5' ACCCCTATCACAACATCTTAGCATTAA 3') were synthesized as described (Gentner et al., 2009) and cloned into the LV.SFFV.GFP backbones. Third generation lentiviral vector particles pseudotyped with VSV-G were generated as described (Follenzi et al., 2000; Guenechea et al., 2000).

**Cell lines**

Mouse RAW 264.7 cells were maintained in Iscove's modified Dulbecco's medium (IMDM; Sigma) supplemented with 10% fetal bovine serum (FBS; Gibco) and a combination of penicillin-streptomycin and glutamine.

**Mice**

FVB and C57BL/6N wilde-type mouse strains were purchased from Charles Rivers Laboratories (Milan, Italy) and maintained in specific-pathogen-free (SPF) conditions.

FVB/MMTV-PyMT mice were purchased from the NCIFrederick Mouse Repository and established as a colony at the San Raffaele animal facility. The strain was maintained by breeding hemizygous males with FVB wild-type females. All procedures were performed according to protocols approved by the Animal Care and Use Committee of the Fondazione San Raffaele del Monte Tabor (IACUC 324, 335) and communicated to the Ministry of Health and local authorities according to Italian law.

**Orthotopic MMTV-PyMT tumors**

To obtain primary tumor cells, late-stage tumors of 16-week-old MMTV-PyMT female mice were harvested and minced using a razor blade. The resulting cell suspension was passed through 40 μm nylon

filter (Fisher, PA) before transfer into culture dishes. Non-attached cells and debris were flushed away the day after plating and the remaining cells were carefully dissociated to give single cell suspensions. For mammary fat pad (MFP) tumor cell transplantation, mice were anesthetized with Avertin and $2x10^6$ tumor cells were injected in 50 µl of PBS in the right III MFP of 6-week–old FVB female mice with visual confirmation of MFP engorgement. Tumor size was determined by caliper measurements and tumor volume calculated by a rational ellipse formula (m1 x m1 x m2 x 0.5236, where m1 is the shorter axis and m2 is the longer axis).

**Murine bone marrow–derived DC differentiation**

BMDC were prepared by a modification of the procedure described by Min et al. *J. Immunol*. 2000.

Briefly, bone marrow cells were flushed from the femurs and tibiae of FVB or C57BL/6 mice. These cells were cultured in complete medium the presence of recombinant murine granulocyte-macrophage colony stimulating factor (GM-CSF, 25 ng/mL; R&D Systems, Minneapolis, MN) for 7 days. Cells were activated with LPS (1 ug/mL; Sigma Aldrich) at different time point.

**Hematopoietic Stem/Progenitor cells Transduction and Transplantation**

Donor mice (FVB or C57BL/6N female) between 6 and 8 weeks of age were euthanized by CO2, and bone marrow was retrieved by

femurs, tibias and humeri. Murine HSPCs were purified by lineage negative selection, using the "Biotin Mouse Lineage Panel" (BD Pharmingen) and the "StemSepTM Mouse Progenitor Enrichment Kit" (Stem Cell Technologies). LVs transduction was performed as previously described (Biffi et al., 2006; Brown et al., 2007; Gentner et al., 2008; 2010). Briefly, $10^6$ cells/ml were transduced with a LV dose equivalent to $10^8$ TU/ml for all the lentiviral vectors for 12 hours in serum-free StemSpan medium (StemCell Technologies) containing a cocktail of cytokines (20 ng/ml IL-3, 50 ng/ml TPO, 100 ng/ml SCF, and 100 ng/ml Flt-3l all from Serotec). After transduction, $10^6$ cells were infused into the tail vein of lethally irradiated 6-week-old female C57BL/6N or FVB or 5.5-week-old FVB/MMTV-PyMT mice (radiation doses were 1100 cGy for FVB mice; and 1300cGy for C57BL/6N). Transduced cells were also cultured in vitro for 10 days before FACS analysis.

Colony-forming cell assays were performed as described previously (De Palma and Naldini, 2002; De Palma et al., 2003).

**Magnetic Resonance Imaging (MRI)**

MRI examinations of MMTV-PyMT transgenic mice were performed on a 3.0 Tesla human scanner (Achieva 3T, Philips Medical Systems, the Netherlands), equipped with 80 mT/m gradients and a 40 mm volumetric coil (Micro-Mouse 40, Philips Medical Systems, the Netherlands). The mice were anaesthetized with Avertin. During acquisition, mice were positioned prone on a dedicated temperature

control apparatus to prevent hypothermia. For mammary gland imaging, a Turbo Spin Echo T2 (TR = 2500; TE = 80; turbo-factor = 9; FOV = 65x65mm; zero-filled voxel-size 100 x 100 x 800 micron) was acquired at 9 and/or 12 weeks of age. The larger field of view allowed evaluation of all five couples of mammary glands. Tumor volumes were calculated on a separate workstation (ViewForum 2.0) after manual segmentation of the lesion on the basis of signal intensity variation and enhancement characteristics, by summing individual volumes (calculated as lesion area x slice thickness) in each slice.

**Blood cell counts**

Blood samples were obtained at the end of the experiments, before euthanasia. Blood cell counts were determined using a Sysmex KX-21N (Kobe, JP) apparatus. For each mouse, 10 µL of PBS containing 45 mg/mL EDTA were added to 250 µl of peripheral blood.

**Flow cytometry**

For flow cytometry, we used a BD FACSCanto (BD Bioscience) apparatus. All cell suspensions were incubated on ice (unless otherwise specified) with rat anti-mouse FcγIII/II receptor (CD16/CD32) blocking antibodies (4 µg/ml; BD Inc.) together with the antibodies listed below (Table 1). After antibody staining, the cells were washed, stained with fluorochrome-labeled streptavidin (if required) and re-suspended in 7-amino-actinomycin D (7-AAD)-containing buffer, to exclude nonviable cells from further analyses.

*Tumors*

MMTV-PyMT mammary tumors were excised and made into single cell suspensions by collagenase IV (0.2 mg/ml, Worthington), dispase (2 mg/ml, Gibco) and DNaseI (0.1 mg/ml, Roche) treatment in IMDM medium supplemented with 5% fetal calf serum (FCS), glutamine and antibiotics. After 30' at 37°C in a shaking bath, the cell suspension was 40 μm-filtered and washed in cold phosphate buffered saline (PBS) containing 2mM EDTA and 0.5% bovine serum albumine (BSA). Cell suspensions were incubated with rat anti-mouse FcγIII/II receptor (Cd16/Cd32) blocking antibodies (4 μg/ml), labeled with 7-amino-actinomycin D (7-AAD) to stain nonviable cells and then stained using the antibodies listed in Table 1.

*Peripheral blood*

Peripheral blood was collected from the tail vein; BM cells were obtained by flushing the femurs. Staining of blood cells with monoclonal antibodies was performed at room temperature, for 10 min in 100 μl of whole blood. After addition of 100 μl of fetal calf serum to protect white blood cells, red blood cells were lysed using the TQ-Prep workstation (Beckman-Coulter). Leukocytes were incubated with rat anti-mouse FcγIII/II receptor (Cd16/Cd32) blocking antibodies (4 μg/ml) and then stained using the antibodies listed in Table 1.

We measured total monocytes as $CD3^-$ $CD19^-$ $CD11b^+$ $SSCH^{low}$ cells, granulocytes as $CD3^-$ $CD19^-$ $CD11b^+$ $SSCH^{high}$ cells, T lymphocytes as $CD3^+$ cells and B lymphocytes as $CD19^+$ cells.

**FACS-sorting of tumor infiltrating cells**

Tumor infiltrating cells were isolated from MMTV-PyMT mammary tumors. Briefly, tumors were excised and made into single-cell suspensions by collagenase IV (0.2 mg/ml, Worthington), dispase (2 mg/ml, Gibco) and DNaseI (0.1 mg/ml, Roche) treatment. Before sorting, all cell suspensions were incubated with rat anti-mouse FcγIII/II receptor (CD16/CD32) blocking antibodies (4 µg/ml, BD Inc.) together with monoclonal antibodies and 7-AAD to stain nonviable cells. We sorted the following cell subsets from MMTV-PyMT mammary tumors (n = 3 biological samples, i.e. independent tumors): $Mrc1^+$ TEMs as $7AAD^-/CD11b^+/MRC1^+/CD11c^-$ cells; Inflammatory TAMs as $7AAD^-/CD11b^+/MRC1^-/CD11c^+$ cells; CD4 T lymphocytes as $7AAD^-/CD11b^-/CD4^+$ cells.

To sort cells, we used a MoFlo apparatus (Dako). After sorting, purity of the cells was always >95%.

**Antibodies**

**Table 1**

| Protein name | Conjugation | Producer | Clone |
|---|---|---|---|
| CD16/32 FcBlock | - | BD Pharmigen | 2.4G2 |
| CD3 | PacificBlue (PB) | BioLegend | 17A2 |
| Gr1 | PB, APC | BioLegend | RB6-8C5 |
| CD11b | APCeFluor$^{tm}$780; PB | BioLegend | M1/70 |
| MRC1 | Biotin | BioLegend | MR5D3 |
| Streptavidin | PE; APC-Cy7; PB | BD Pharmigen | |
| CD11c | PC7 | eBioscience | N418 |
| CD19 | PC7; | BioLegend | 6D5 |
| NK1.1 | APC | BioLegend | PK136 |
| CD45 | PB | BioLegend | 30F11 |
| CD4 | APC, PB | BD Pharmigen | |
| CD8 | APC-eFluor$^{tm}$ 780 | eBioscience | 53-6.7 |

**Phosphoflow**

Phosphoflow cytometry was performed as published elsewhere (Krutzik et al., 2011). Briefly, RAW264.7 cells cultured in complete medium were washed with fresh medium and pelleted to eliminate conditioned medium. After 2 washes, cells were starved in serum free medium at 37°C for 3 hours. Then, cells were stimulated with GM-CSF (100ng/ul) for 10 minutes prior to fixation. As a negative control, cells were administered 100 nM Wortmannin (CST) 30 minutes

before stimulation. Cells were immediately fixed with paraformaldehyde (final concentration: 1.6%) for 10 minutes at room temperature. Cells were then centrifuged, washed once with PBS 1 % BSA to remove residual PFA and permeabilized with ice-cold Perm buffer III (BD Phosflow for 30 min at 4°C followed by 2 washes in order to remove traces of methanol). Phospho-AktSer473 was detected by a monoclonal antibody (clone D9E; Cell Signaling) conjugated to Alexafluor647 (#4075S). Staining was performed by incubating permeabilized cells with the phospho-specific antibody for 30 minutes on ice and at dark, diluted in PBS 1% BSA at a final concentration of 1:50. After incubation, cell were washed in PBS 1% BSA and then analyzed by flow cytometry.

The mean fluorescence intensity (arithmetic mean) of Phospho-Akt (Ser473) was determined for Ctrl vector transduced cells, miR-155 KD or miR-155 OE vector transduced cells and transduced cells pretreated with Wortmannin.

**Immunofluorescence staining (IFS) and confocal microscopy**

Tumors were made into 12–16 µm cryostatic sections, as described. Briefly, tumors were fixed for 2 hours in paraformaldehyde, equilibrated for 24 hours in PBS containing 10% sucrose 0,02% sodium azide, 24 hours in PBS/20% sucrose 0,02% sodium azide, and eventually 48 hours in PBS/30% sucrose 0,02% sodium azide. The samples were then embedded in O.C.T. compound for quick freezing in liquid nitrogen. Cryostatic sections were laid on slides and

immediately stained; when required, slides were frozen at −80°C. For immunofluorescence staining, sections were blocked with 5% goat serum (Vector Laboratories, Burlingame, CA) in PBS containing 1% bovine serum albumin (BSA) and 0.1% Triton X-100 (PBS-T). For immunofluorescence staining and confocal microscopy, we used the following antibodies: anti-Iba1 (Wako), PE-conjugated rat anti-CD68 (Serotec). Unconjugated primary antibodies were revealed by the following secondary antibodies: AlexaFluor488 donkey anti-rabbit and AlexaFluor546 goat anti-rat (Molecular Probes). PE-conjugated rat antibodies were either visualized directly (when used in combination with other rat antibodies) or revealed by secondary AlexaFluor546 goat anti-rat antibodies. Concentrations of antibodies and detailed information on immunofluorescence staining protocols will be available upon request. Nuclei were stained by TO-PRO-3 (Molecular Probes). Confocal microscopy used an Axioskop 2 plus direct microscope (Zeiss) equipped with a Radiance 2100 three-laser confocal device (BioRad, Segrate, Italy). Axioskop 2 microscope used Zeiss W-PI 10×/0.23 or Zeiss Plan-Neofluor 20×/0.5 numerical aperture objective lens. Fluorescent signals from the individual fluorophores were sequentially acquired from single optical sections and analyzed by ImageJ software.

**Western Blotting**

Protein samples were obtained from cell pellets after two rinse of wash in ice-cold PBS and then lysed immediately or, alternatively,

stored as dry pellets at –80°C. Cell lysis was achieved by resuspending cell pellets in RIPA buffer (Tris-HCl 20 mM, NaCl 150 mM, EDTA 5mM, 1%, Triton 0.5%) supplemented with CompleteMini protease inhibitor cocktail (Roche). Membranes were incubated with the following primary antibodies: rabbit monoclonal anti-PU.1 (Cell Signaling #2258, 1:1000), mouse monoclonal anti-p84/THOC-1 (Abcam, Cambridge, MA; 1:2000) and mouse anti-GAPDH (1:10.000, Sigma). Secondary HRP-conjugated anti-mouse or anti-rabbit IgG (Sigma) were utilized and bands were visualized by Western Blotting Analysis System (GE Healthcare) on Amersham Hyperfilm$^{TM}$ (GE Healthcare). Densitometric analysis of scanned films was performed using ImageJ. Normalized fold-change (NFC) was calculated as the ratio between two normalized band intensities, each one obtained by dividing the optical density value of that band for the optical density of the loading control band below.

**Genomic DNA isolation and VCN**

To measure the lentiviral vector copy number (VCN) in transgenic/transduced cells, we purified genomic DNA from either RAW 264.7 cells or BM hematopoietic cells using a Maxwell-16 instrument (Promega) and performed qPCR using custom TaqMan assays specific for the *βactin*, HIV sequences (Applied Biosystems). Standard curves for the HIV sequence were obtained from a transgenic mice with 1 copy of LV. The VCN of genomic DNA standard curves was determined using custom TaqMan assays specific

for LVs (Applied Biosystems). All reactions were carried in out in triplicate.

**miRNA expression**

miRNA expression was analyzed as described (Gentner et al., 2008). Briefly, small RNAs were extracted using miRNeasy mini kit (Qiagen) and miRNA expression levels were determined by the Applied Biosystems Taqman® microRNA Assay system. Reactions were carried out in triplicate in an ABI Prism 7900HT (Applied Biosystems, Foster City, CA). miRNA expression was normalized to Let7a or miR-16.

**Quantitative *Real-Time*® PCR for gene expression analysis**

Literature-validated microRNA natural target genes were assayed at the RNA level by a gene expression analysis using made-to-order Taqman® Gene Expression Assays™. Total RNA was extracted from cells in culture using Qiagen miRNeasy RNA extraction kit and following manufacturer's instructions. Retrotranscription of total RNA for gene expression analysis was performed using Invitrogen Superscript III First Strand Synthesis™ System for RT-PCR, by loading a maximum of 500 ng of total RNA per reaction. Taqman® gene expression analysis was performed using the following primer/probe sets: PU.1 (Mm00488142_m1), SHIP1 (Mm00494987_m1), Beta2 microglobulin (B2M) (Mm00437762_m1). Reactions were carried out in triplicate in an

ABI Prism 7900 by using a standard amplification protocol, according to manufacturer's instructions. Gene expression was calculated by the $2^{-\Delta Ct}$ or by the $2^{-\Delta\Delta Ct}$ method, with calibrator samples indicated for each experiment.

**TaqMan Low Density Array**

*Freshly isolated Mrc1$^{+}$ TEMs, Inflammatory TAMs, CD4$^{+}$ T cells*

After sorting, cells were washed in low-protein buffer, and total mRNA purified following RNeasy Micro/Mini kit guidelines (Qiagen). RNA was quantified with a NanoDrop ND-1000 and retrotranscribed with SuperScript III (Vilo kit, Invitrogen). All qPCR analyses were performed with TaqMan probes from Applied Biosystems on 3 independent experiments. We used a custom TaqMan low density arrays, measuring the expression of 96 genes (Table 2) in 2 technical replicates. One hundred ng − 1 μg of cDNA was loaded on each array. qPCR was run for 40 cycles in standard mode using an ABI7900HT apparatus (Applied Biosystems).

The SDS 2.2.1 software was used to extract raw data. The difference between the threshold cycle (CT) of each gene and that of the endogenous controls b*2m* (DCT) was used to determine gene expression. The lower the DCT, the higher the gene expression level.

To calculate gene expression, we implemented in R (http://www.R-project.org) a multivariate regression model to compute over the whole dataset and estimate the fold-change in gene expression for each single target gene. This model jointly evaluates the role of

different variables of interest providing for: (i) statistical significance of the observed differences in expression level across the whole set of experimental samples; (ii) identifying the experimental variables that contribute to each individual measurement; (iii) subtracting experimentally introduced biases to obtain a stringent estimate of the actual biological differences (Pucci et al., 2009).

The multiple regression formula reads as follows:

$$C_T = \beta_0 + \beta_1 \cdot X_{Experiment} + \beta_2 \cdot X_{Gene \bullet Treatment} + \varepsilon.$$

In the regression formulas above, $C_T$ is the threshold cycle, $\beta_i$ are the coefficients calculated by the model that represents the impact of the respective qualitative variable $X_j$, with j being each of the covariates, and ε the residual error. The implemented model leads to a procedure equivalent to test the $\Delta\Delta C_T$. A detailed explanation of this equivalence can be found in (Pucci et al., 2009). The advantage of this procedure with respect to two-by-two t-test comparisons lies on the joint nature of the modeling of all covariates, which allows minimizing type I errors (false positive results). Estimation technique is based on Likelihood Ratio Test. The model is implemented in R-statistical software (version 2.6.1; see http://www.R-project.org). Significance level is chosen at $\alpha = 0.05$. We selected *B2m* and *Bact* as the most stable reference genes (according to GeNorm analysis; data not shown).

**Table 2**

**TaqMan low-density array (List of genes)**

| **Normalizer** | **miR-155 direct/indirect targets** | **Other genes** |
|---|---|---|
| Actb | SOCS1 | Stat1 |
| B2m | ASK1 (MAP3K5) | Stat3 |
| HPRT1 | CCR7 | Ctla4 |
| **Proinflammatory cytokines (Th1)** | CXCR3 | Il2ra |
| IL-1a | CCR6 | Tbx21 |
| IL-1b | PU.1 (SFPI1) | Cd28 |
| IL-6 | c-myc | H2-Ea |
| IL-12a | c-fes | Hmox1 |
| IL-12b | CD115 (M-CSF receptor) | Lta |
| IL-17 | GATA-1 (TF) | Cd40 |
| IL-18 | Flt3 (FMS-like tyrosin kinase) | Nfkb1 |
| IFNg | CDK6 | Cd40lg |
| TNFa | CEBPb | Icos |
| **Antinflammatory cytokines (Th2)** | CEBPd | Fasl |
| IL-4 | COX-2 (Ptgs2) | Cd80 |
| IL-5 | SHIP1 (inpp5d) | Cd86 |
| IL-10 | IFN-b | Ikbkb |
| IL-13 | Fli-1 | c-MAF |
| IL-23 | JARID2 | IL6R |
| **Others cytokines** | Bach 1 | MMD2 |
| IL-2 | Ikbke | MYADM |
| IL-3 | **Type I IFN-inducible genes** | ARG2 |
| IL-7 | CXCL10 (IP-10) | IL22Ra1 |
| IL-9 | IFN-4a | ITK |
| IL-15 | p48; ISGF3 IRF-9 | GATA-3 |

| | | |
|---|---|---|
| CSF-1 (M-CSF) | ISG15 | |
| CSF-2 (GM-CSF) | IRF-1 | |
| CSF-3 (G-CSF) | ICSBP (IRF8) | |
| CCL3 (MIP-1a) | mig (CXCL9) | |
| TGF-b1 | TRAIL (TNSF10) | |
| IL-21 | OAS | |
| **Chemokines/Chemokine Receptors** | PKR | |
| CCL19 | iNOS | |
| CXCL11 | AGTR2 | |
| CCL2 (MCP-1) | FAS-R | |
| CCL5 | Gbp-1, mag-1 | |
| CCR2 | Sca-1 | |
| CCR4 | | |

**Statistical analysis**

In all studies, values are expressed as mean ± standard error (SEM). Statistical analyses were performed by unpaired Student's *t*-test, or Mann-Whitney test, as indicated. Differences were considered statistically significant at $p < 0.05$.

## Supplementary Figures

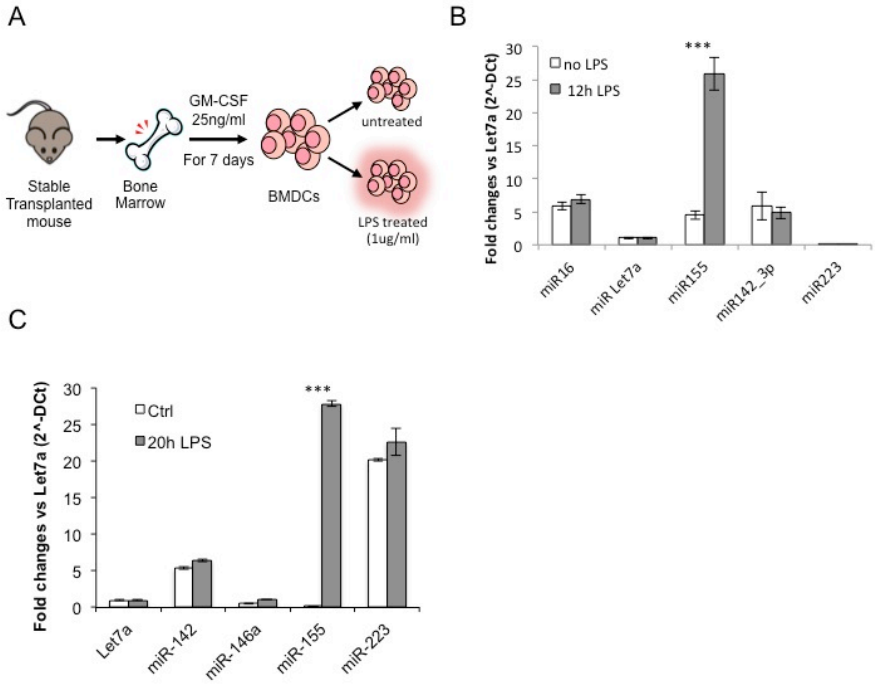


**Supplementary Figure S1.**

**Expression of miR-155 in primary BMDC and RAW264.7 monocytic cell line.**

***A:*** *Scheme of bone-marrow derived dendritic cell (BMDCs) differentiation protocol.*

***B:*** *qPCR of selected miRNAs in BMDCs treated or not with LPS for 12 hours. The data show relative abundance of each miRNA (mean values ± SEM vs. Let7a; n = 3 biological samples). Statistical analysis*

*of the data was performed on actual $\Delta C_t$ values by unpaired Student's t-test. ***: $p < 0.001$.*

***C:** qPCR of selected miRNAs in Raw 264.7 cells treated or not with LPS for 20 hours. The data show relative abundance of each miRNA (mean values ± SEM vs. Let7a; n = 3 biological samples). Statistical analysis of the data was performed on actual $\Delta C_t$ values by unpaired Student's t-test. ***: $p < 0.001$.*

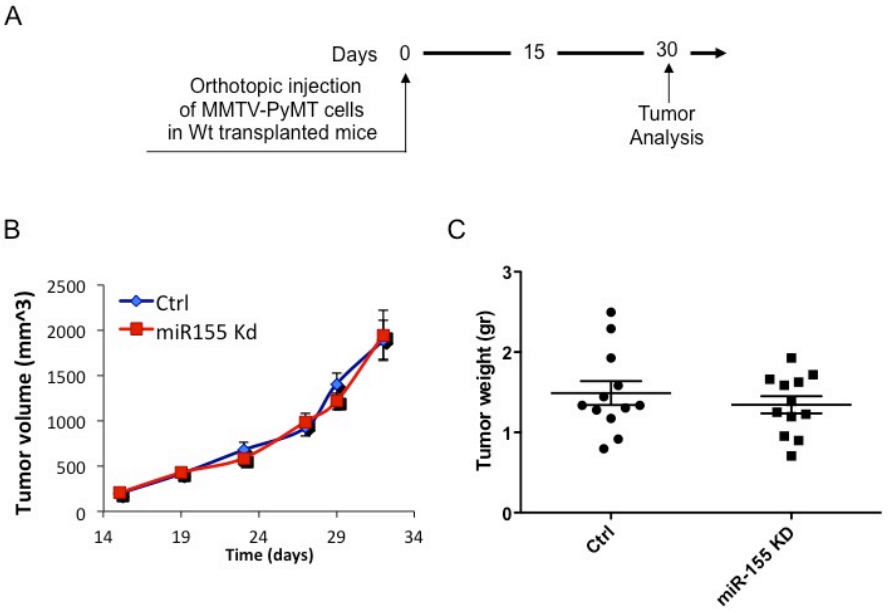


**Supplementary Figure S2.**

**Effect on the growth of established mammary carcinomas of the miR-155 KD.**

***A:** Tumor growth in mice carrying orthotopic, late-stage MMTV-PyMT mammary tumors. Schematics of experiment design.*

***B:*** *Tumor growth (mean tumor volume ± SEM; n=6 mice/group).*

***C:*** *Tumor weight (mean tumor weight ± SEM; n=6 mice/group). Each dot in the plot corresponds to one mouse. Statistical analysis was performed by Mann-Whitney U test.*

# References


Amendola, M., Passerini, L., Pucci, F., Gentner, B., Bacchetta, R., and Naldini, L. (2009). Regulated and multiple miRNA and siRNA delivery into primary cells by a lentiviral platform. Molecular therapy : the journal of the American Society of Gene Therapy *17*, 1039-1052.

Androulidaki, A., Iliopoulos, D., Arranz, A., Doxaki, C., Schworer, S., Zacharioudaki, V., Margioris, A.N., Tsichlis, P.N., and Tsatsanis, C. (2009). The kinase Akt1 controls macrophage response to lipopolysaccharide by regulating microRNAs. Immunity *31*, 220-231.

Baltimore, D., Boldin, M.P., O'Connell, R.M., Rao, D.S., and Taganov, K.D. (2008). MicroRNAs: new regulators of immune cell development and function. Nat Immunol *9*, 839-845.

Bartel, D.P. (2004). MicroRNAs: genomics, biogenesis, mechanism, and function. Cell *116*, 281-297.

Brown, B.D., Gentner, B., Cantore, A., Colleoni, S., Amendola, M., Zingale, A., Baccarini, A., Lazzari, G., Galli, C., and Naldini, L. (2007). Endogenous microRNA can be broadly exploited to regulate transgene expression according to tissue, lineage and differentiation state. Nat Biotechnol *25*, 1457-1467.

Costinean, S., Sandhu, S.K., Pedersen, I.M., Tili, E., Trotta, R., Perrotti, D., Ciarlariello, D., Neviani, P., Harb, J., Kauffman, L.R.*, et al.* (2009). Src homology 2 domain-containing inositol-5-phosphatase and CCAAT enhancer-binding protein beta are targeted by miR-155 in B cells of Emicro-MiR-155 transgenic mice. Blood *114*, 1374-1382.

Cubillos-Ruiz, J.R., Baird, J.R., Tesone, A.J., Rutkowski, M.R., Scarlett, U.K., Camposeco-Jacobs, A.L., Anadon-Arnillas, J., Harwood, N.M., Korc, M., Fiering, S.N.*, et al.* (2012). Reprogramming tumor-associated dendritic cells in vivo using microRNA mimetics triggers protective immunity against ovarian cancer. Cancer Res.

Dagan, L.N., Jiang, X., Bhatt, S., Cubedo, E., Rajewsky, K., and Lossos, I.S. (2012). miR-155 regulates HGAL expression and increases lymphoma cell motility. Blood *119*, 513-520.

De Palma, M., Mazzieri, R., Politi, L.S., Pucci, F., Zonari, E., Sitia, G., Mazzoleni, S., Moi, D., Venneri, M.A., Indraccolo, S., *et al.* (2008). Tumor-targeted interferon-alpha delivery by Tie2-expressing monocytes inhibits tumor growth and metastasis. Cancer Cell *14*, 299-311.

Eis, P.S., Tam, W., Sun, L., Chadburn, A., Li, Z., Gomez, M.F., Lund, E., and Dahlberg, J.E. (2005). Accumulation of miR-155 and BIC RNA in human B cell lymphomas. Proc Natl Acad Sci U S A *102*, 3627-3632.

Esquela-Kerscher, A., and Slack, F.J. (2006). Oncomirs - microRNAs with a role in cancer. Nat Rev Cancer *6*, 259-269.

Gambari, R., Fabbri, E., Borgatti, M., Lampronti, I., Finotti, A., Brognara, E., Bianchi, N., Manicardi, A., Marchelli, R., and Corradini, R. (2011). Targeting microRNAs involved in human diseases: a novel approach for modification of gene expression and drug development. Biochem Pharmacol *82*, 1416-1429.

Gentner, B., Schira, G., Giustacchini, A., Amendola, M., Brown, B.D., Ponzoni, M., and Naldini, L. (2009). Stable knockdown of microRNA in vivo by lentiviral vectors. Nat Methods *6*, 63-66.

Hu, Y.L., Fong, S., Largman, C., and Shen, W.F. (2010). HOXA9 regulates miR-155 in hematopoietic cells. Nucleic Acids Res *38*, 5472-5478.

Iorio, M.V., Casalini, P., Piovan, C., Braccioli, L., and Tagliabue, E. (2011). Breast cancer and microRNAs: therapeutic impact. Breast *20 Suppl 3*, S63-70.

Iorio, M.V., and Croce, C.M. (2012). MicroRNA dysregulation in cancer: diagnostics, monitoring and therapeutics. A comprehensive review. EMBO Mol Med.

Iorio, M.V., Ferracin, M., Liu, C.G., Veronese, A., Spizzo, R., Sabbioni, S., Magri, E., Pedriali, M., Fabbri, M., Campiglio, M., *et al.* (2005). MicroRNA gene expression deregulation in human breast cancer. Cancer Res *65*, 7065-7070.

Jay, C., Nemunaitis, J., Chen, P., Fulgham, P., and Tong, A.W. (2007). miRNA profiling for diagnosis and prognosis of human cancer. DNA Cell Biol *26*, 293-300.

Jiang, S., Zhang, L.F., Zhang, H.W., Hu, S., Lu, M.H., Liang, S., Li, B., Li, Y., Li, D., Wang, E.D*., et al.* (2012). A novel miR-155/miR-143 cascade controls glycolysis by regulating hexokinase 2 in breast cancer cells. Embo J.

Kluiver, J., Poppema, S., de Jong, D., Blokzijl, T., Harms, G., Jacobs, S., Kroesen, B.J., and van den Berg, A. (2005). BIC and miR-155 are highly expressed in Hodgkin, primary mediastinal and diffuse large B cell lymphomas. J Pathol *207*, 243-249.

Kohlhaas, S., Garden, O.A., Scudamore, C., Turner, M., Okkenhaug, K., and Vigorito, E. (2009). Cutting edge: the Foxp3 target miR-155 contributes to the development of regulatory T cells. J Immunol *182*, 2578-2582.

Lee, D.W., Futami, M., Carroll, M., Feng, Y., Wang, Z., Fernandez, M., Whichard, Z., Chen, Y., Kornblau, S., Shpall, E.J*., et al.* (2012). Loss of SHIP-1 protein expression in high-risk myelodysplastic syndromes is associated with miR-210 and miR-155. Oncogene.

Lee, E.J., Gusev, Y., Jiang, J., Nuovo, G.J., Lerner, M.R., Frankel, W.L., Morgan, D.L., Postier, R.G., Brackett, D.J., and Schmittgen, T.D. (2007). Expression profiling identifies microRNA signature in pancreatic cancer. Int J Cancer *120*, 1046-1054.

Lindsay, M.A. (2008). microRNAs and the immune response. Trends Immunol *29*, 343-351.

Lodish, H.F., Zhou, B., Liu, G., and Chen, C.Z. (2008). Micromanagement of the immune system by microRNAs. Nat Rev Immunol *8*, 120-130.

Lovat, F., Valeri, N., and Croce, C.M. (2011). MicroRNAs in the pathogenesis of cancer. Semin Oncol *38*, 724-733.

Lu, L.F., Thai, T.H., Calado, D.P., Chaudhry, A., Kubo, M., Tanaka, K., Loeb, G.B., Lee, H., Yoshimura, A., Rajewsky, K*., et al.* (2009). Foxp3-dependent microRNA155 confers competitive fitness to regulatory T cells by targeting SOCS1 protein. Immunity *30*, 80-91.

Mann, M., Barad, O., Agami, R., Geiger, B., and Hornstein, E. (2010). miRNA-based mechanism for the commitment of multipotent progenitors to a single cellular fate. Proc Natl Acad Sci U S A *107*, 15804-15809.

Mazzieri, R., Pucci, F., Moi, D., Zonari, E., Ranghetti, A., Berti, A., Politi, L.S., Gentner, B., Brown, J.L., Naldini, L.*, et al.* (2011). Targeting the ANG2/TIE2 axis inhibits tumor growth and metastasis by impairing angiogenesis and disabling rebounds of proangiogenic myeloid cells. Cancer Cell *19*, 512-526.

Nikiforova, M.N., Tseng, G.C., Steward, D., Diorio, D., and Nikiforov, Y.E. (2008). MicroRNA expression profiling of thyroid tumors: biological significance and diagnostic utility. J Clin Endocrinol Metab *93*, 1600-1608.

O'Connell, R.M., Kahn, D., Gibson, W.S., Round, J.L., Scholz, R.L., Chaudhuri, A.A., Kahn, M.E., Rao, D.S., and Baltimore, D. (2010a). MicroRNA-155 promotes autoimmune inflammation by enhancing inflammatory T cell development. Immunity *33*, 607-619.

O'Connell, R.M., Rao, D.S., Chaudhuri, A.A., and Baltimore, D. (2010b). Physiological and pathological roles for microRNAs in the immune system. Nat Rev Immunol *10*, 111-122.

O'Connell, R.M., Rao, D.S., Chaudhuri, A.A., Boldin, M.P., Taganov, K.D., Nicoll, J., Paquette, R.L., and Baltimore, D. (2008). Sustained expression of microRNA-155 in hematopoietic stem cells causes a myeloproliferative disorder. J Exp Med *205*, 585-594.

O'Connell, R.M., Taganov, K.D., Boldin, M.P., Cheng, G., and Baltimore, D. (2007). MicroRNA-155 is induced during the macrophage inflammatory response. Proc Natl Acad Sci U S A *104*, 1604-1609.

Parsa, K.V., Ganesan, L.P., Rajaram, M.V., Gavrilin, M.A., Balagopal, A., Mohapatra, N.P., Wewers, M.D., Schlesinger, L.S., Gunn, J.S., and Tridandapani, S. (2006). Macrophage pro-inflammatory response to Francisella novicida infection is regulated by SHIP. PLoS Pathog *2*, e71.

Pucci, F., Venneri, M.A., Biziato, D., Nonis, A., Moi, D., Sica, A., Di Serio, C., Naldini, L., and De Palma, M. (2009). A distinguishing gene signature shared by tumor-infiltrating Tie2-expressing monocytes, blood "resident" monocytes, and embryonic macrophages suggests common functions and developmental relationships. Blood *114*, 901-914.

Rajaram, M.V., Butchar, J.P., Parsa, K.V., Cremer, T.J., Amer, A., Schlesinger, L.S., and Tridandapani, S. (2009). Akt and SHIP modulate

Francisella escape from the phagosome and induction of the Fas-mediated death pathway. PLoS One *4*, e7919.

Rodriguez, A., Vigorito, E., Clare, S., Warren, M.V., Couttet, P., Soond, D.R., van Dongen, S., Grocock, R.J., Das, P.P., Miska, E.A.*, et al.* (2007). Requirement of bic/microRNA-155 for normal immune function. Science *316*, 608-611.

Schreiber, R.D., Old, L.J., and Smyth, M.J. (2011). Cancer immunoediting: integrating immunity's roles in cancer suppression and promotion. Science *331*, 1565-1570.

Shojaei, F., Zhong, C., Wu, X., Yu, L., and Ferrara, N. (2008). Role of myeloid cells in tumor angiogenesis and growth. Trends Cell Biol *18*, 372-378.

Sica, A., and Bronte, V. (2007). Altered macrophage differentiation and immune dysfunction in tumor development. J Clin Invest *117*, 1155-1166.

Stahl, H.F., Fauti, T., Ullrich, N., Bopp, T., Kubach, J., Rust, W., Labhart, P., Alexiadis, V., Becker, C., Hafner, M.*, et al.* (2009). miR-155 inhibition sensitizes CD4+ Th cells for TREG mediated suppression. PLoS One *4*, e7158.

Szafranska, A.E., Davison, T.S., John, J., Cannon, T., Sipos, B., Maghnouj, A., Labourier, E., and Hahn, S.A. (2007). MicroRNA expression alterations are linked to tumorigenesis and non-neoplastic processes in pancreatic ductal adenocarcinoma. Oncogene *26*, 4442-4452.

Thai, T.H., Calado, D.P., Casola, S., Ansel, K.M., Xiao, C., Xue, Y., Murphy, A., Frendewey, D., Valenzuela, D., Kutok, J.L.*, et al.* (2007). Regulation of the germinal center response by microRNA-155. Science *316*, 604-608.

Tili, E., Michaille, J.J., Cimino, A., Costinean, S., Dumitru, C.D., Adair, B., Fabbri, M., Alder, H., Liu, C.G., Calin, G.A.*, et al.* (2007). Modulation of miR-155 and miR-125b levels following lipopolysaccharide/TNF-alpha stimulation and their possible roles in regulating the response to endotoxin shock. J Immunol *179*, 5082-5089.

Tili, E., Michaille, J.J., Wernicke, D., Alder, H., Costinean, S., Volinia, S., and Croce, C.M. (2011). Mutator activity induced by microRNA-155 (miR-

155) links inflammation and cancer. Proc Natl Acad Sci U S A *108*, 4908-4913.

Vargova, K., Curik, N., Burda, P., Basova, P., Kulvait, V., Pospisil, V., Savvulidi, F., Kokavec, J., Necas, E., Berkova, A.*, et al.* (2011). MYB transcriptionally regulates the miR-155 host gene in chronic lymphocytic leukemia. Blood *117*, 3816-3825.

Vigorito, E., Perks, K.L., Abreu-Goodger, C., Bunting, S., Xiang, Z., Kohlhaas, S., Das, P.P., Miska, E.A., Rodriguez, A., Bradley, A.*, et al.* (2007). microRNA-155 regulates the generation of immunoglobulin class-switched plasma cells. Immunity *27*, 847-859.

Volinia, S., Calin, G.A., Liu, C.G., Ambs, S., Cimmino, A., Petrocca, F., Visone, R., Iorio, M., Roldo, C., Ferracin, M.*, et al.* (2006). A microRNA expression signature of human solid tumors defines cancer gene targets. Proc Natl Acad Sci U S A *103*, 2257-2261.

Wang, X., Tang, S., Le, S.Y., Lu, R., Rader, J.S., Meyers, C., and Zheng, Z.M. (2008). Aberrant expression of oncogenic and tumor-suppressive microRNAs in cervical cancer is required for cancer cell growth. PLoS One *3*, e2557.

Willimsky, G., and Blankenstein, T. (2007). The adaptive immune response to sporadic cancer. Immunol Rev *220*, 102-112.

Xia, Q.S., Ishigaki, Y., Sun, L., Chen, R., and Motoo, Y. (2010). [Effect of anti-cancer drugs on the expression of BIC/miR-155 in human pancreatic cancer PANC-1 cells]. Zhonghua Yi Xue Za Zhi *90*, 123-127.

Xiao, C., and Rajewsky, K. (2009). MicroRNA control in the immune system: basic principles. Cell *136*, 26-36.

Yamanaka, Y., Tagawa, H., Takahashi, N., Watanabe, A., Guo, Y.M., Iwamoto, K., Yamashita, J., Saitoh, H., Kameoka, Y., Shimizu, N.*, et al.* (2009). Aberrant overexpression of microRNAs activate AKT signaling via down-regulation of tumor suppressors in natural killer-cell lymphoma/leukemia. Blood *114*, 3265-3275.

Yanaihara, N., Caplen, N., Bowman, E., Seike, M., Kumamoto, K., Yi, M., Stephens, R.M., Okamoto, A., Yokota, J., Tanaka, T.*, et al.* (2006). Unique

microRNA molecular profiles in lung cancer diagnosis and prognosis. Cancer Cell *9*, 189-198.

Yang, L., DeBusk, L.M., Fukuda, K., Fingleton, B., Green-Jarvis, B., Shyr, Y., Matrisian, L.M., Carbone, D.P., and Lin, P.C. (2004). Expansion of myeloid immune suppressor Gr+CD11b+ cells in tumor-bearing host directly promotes tumor angiogenesis. Cancer Cell *6*, 409-421.

Yang, Z.F., Ho, D.W., Ngai, P., Lau, C.K., Zhao, Y., Poon, R.T., and Fan, S.T. (2007). Antiinflammatory properties of IL-10 rescue small-for-size liver grafts. Liver Transpl *13*, 558-565.

Zanesi, N., Pekarsky, Y., Trapasso, F., Calin, G., and Croce, C.M. (2010). MicroRNAs in mouse models of lymphoid malignancies. J Nucleic Acids Investig *1*, 36-40.

Zhou, X., He, Z., Henegar, J., Allen, B., and Bigler, S. (2011). Expression of allograft inflammatory factor-1 (AIF-1) in acute cellular rejection of cardiac allografts. Cardiovasc Pathol *20*, e177-184.

# CHAPTER 4

# Final Discussion

## Molecular and Clinical Consideration

### Summary

The Ph.D. project in which I was engaged has been carried out at the San Raffaele Telethon Institute for Gene Therapy (HSR-TIGET). The research project focused on the study of the tumor microenvironment with the ultimate goal of translating our basic and applied results into therapeutic advances. In particular, we worked on the characterization and targeting of a subset of tumor-infiltrating myeloid cells, which play a predominant role in tumor development and progression.

We previously reported (De Palma et al., 2008; De Palma et al., 2005; De Palma et al., 2003) that a specific Tumor-Associated Macrophage (TAM) subpopulation, the TIE2-Expressing Macrophages (TEMs), play a non-redundant role in the promotion of tumor angiogenesis. These findings have received much attention from the scientific community. An increasing number of groups have confirmed and extended our findings; they recently reported that the enhanced recruitment of these $TIE2^{+}$ TAM cells is associated with tumor re-vascularization and relapse following radiation therapy.

**Aim 1: Targeting the Tie2/Ang2 pathway**. In Chapter 2, I present new findings on the role of the ANG2/TIE2 pathway in the

proangiogenic activity of TEMs in tumors. Our data support a model wherein the ANG2-TIE2 signalling axis mediates juxtacrine interactions between TAMs and endothelial cells required for tumor angiogenesis. Indeed, blocking the ANG2/TIE2 signaling pathway with a fully humanized anti-ANG2 monoclonal antibody induced tumor vessel regression and tumor growth inhibition in multiple tumor models (including late-stage, spontaneous and metastatic breast cancer). We also show, for the first time, that ANG2 blockade – at variance with other antiangiogenic treatments – potently limits the metastatic dissemination of primary tumors and constrains the outgrowth of established metastases. Importantly, by developing a conditional *Tie2* gene knock-down strategy in bone marrow-derived cells, we demonstrate that targeting TIE2 also disables the proangiogenic activity of $TIE2^{+}$ macrophages recruited *de novo* to the tumor vasculature. In conclusion, targeting the Tie2/Ang2 pathway may represent a dual target therapy (TEMs and ECs) able to overcome the emergence of evasive resistance to antiangiogenic therapy.

**Aim 2: To study the role of miRNAs in TAM functions.** In Chapter 3 of this thesis, I show new findings on the role of miR-155 in TAMs, and on how this miRNA modulates the proinflammatory activity of these cells in tumors. These studies were possible due to the expertise of the laboratory in stable miRNA knockdown technologies (Gentner et al., 2009). Our data show how the specific knockdown of miR-155 in myeloid cells causes an acceleration of tumor growth in a

spontaneous breast cancer model but not in established breast carcinoma, thus indicating a prominent role of miR-155 in immunosurveillance during the early phases of tumor development. We provide evidence for attenuated transduction of proinflammatory signals in macrophages, a decrease in the expression of the macrophage activation marker "Iba1" in TAMs and a Th2 skewed tumor microenvironment upon myeloid-specific miR-155 knockdown.

**Conclusions and future perspectives**

- The finding that targeting the ANG2-TIE2 pathway in TAMs inhibits tumor angiogenesis and progression represents a new concept in vascular biology, since the ANG2/TIE2 signaling axis has historically been linked to regulation of endothelial cells in the process of angiogenesis. These findings are particularly relevant in light of the emerging concept that tumor-infiltrating myeloid cells, such as TAMs or subsets of these cells, convey proangiogenic programs that counteract the efficacy of antiangiogenic therapies targeting the VEGF pathway. Blocking ANG2 thus surpasses the efficacy of current antiangiogenic therapies by concomitantly targeting tumor blood vessels and disabling rebounds of proangiogenic myeloid cells. Moreover, from a mechanistic standpoint, we propose that TIE2 expression by TEMs regulates blood vessel formation in tumors by a non-canonical angiogenic mechanism, which involves cell-to-cell adhesive interactions between

TEMs and endothelial cells. These interactions are likely to be crucial to facilitate the navigation of endothelial sprouts through the dense extracellular matrix, eventually enabling the fusion of nascent blood vessels in angiogenic tissues. Specifically targeting ANG2 may thus provide an effective antiangiogenic therapy that targets tumor blood vessels while concomitantly disabling rebounds of proangiogenic myeloid cells.

- Among several miRNAs that have been identified to regulate immune cell functions (O'Connell et al., 2010), little is known about their role in the modulation of TAMs. Here we describe for the first time the *in vivo* role of miR-155 in the context of tumor-associated hematopoietic cells. The evidences that, constitutive miR-155 expression in the hematopoietic compartment causes hematologic malignancies have motivated the development of anti- miR-155 drugs as potential anticancer therapeutics (Gambari et al., 2011; Iorio et al., 2011; Iorio and Croce, 2012; Xia et al., 2010). Our data expand the role of miR-155 to myeloid cell mediated anti-tumoral responses, since blocking its physiological upregulation in these cells accelerated tumor development. In our spontaneous breast cancer model, miR-155 expression in hematopoietic cells might boost anti-tumor immunity, suggesting that miR-155 is, first of all, an "immunomiR". On the other hand, it has been

reported that constitutive miR-155 expression drives oncogenesis, which granted miR-155 the designation "oncomiR". Given the data provided here, care must be taken when applying anti-miR-155 drugs as a therapeutic strategy against cancer since these very same drugs will likely impair immune responses which can result in infectious complications and, paradoxically, in a facilitation of tumor development by disabling immunosurveillance by innate immune cells. It needs to be determined whether there is a therapeutic window for anti-miR-155 treatments, balancing its potential benefits (i.e., reduction in tumor cell autonomous growth) against side effects.

# References

De Palma, M., Mazzieri, R., Politi, L.S., Pucci, F., Zonari, E., Sitia, G., Mazzoleni, S., Moi, D., Venneri, M.A., Indraccolo, S.*, et al.* (2008). Tumor-targeted interferon-alpha delivery by Tie2-expressing monocytes inhibits tumor growth and metastasis. Cancer Cell *14*, 299-311.

De Palma, M., Venneri, M.A., Galli, R., Sergi Sergi, L., Politi, L.S., Sampaolesi, M., and Naldini, L. (2005). Tie2 identifies a hematopoietic lineage of proangiogenic monocytes required for tumor vessel formation and a mesenchymal population of pericyte progenitors. Cancer Cell *8*, 211-226.

De Palma, M., Venneri, M.A., Roca, C., and Naldini, L. (2003). Targeting exogenous genes to tumor angiogenesis by transplantation of genetically modified hematopoietic stem cells. Nat Med *9*, 789-795.

Gambari, R., Fabbri, E., Borgatti, M., Lampronti, I., Finotti, A., Brognara, E., Bianchi, N., Manicardi, A., Marchelli, R., and Corradini, R. (2011). Targeting microRNAs involved in human diseases: a novel approach for modification of gene expression and drug development. Biochem Pharmacol *82*, 1416-1429.

Gentner, B., Schira, G., Giustacchini, A., Amendola, M., Brown, B.D., Ponzoni, M., and Naldini, L. (2009). Stable knockdown of microRNA in vivo by lentiviral vectors. Nat Methods *6*, 63-66.

Iorio, M.V., Casalini, P., Piovan, C., Braccioli, L., and Tagliabue, E. (2011). Breast cancer and microRNAs: therapeutic impact. Breast *20 Suppl 3*, S63-70.

Iorio, M.V., and Croce, C.M. (2012). MicroRNA dysregulation in cancer: diagnostics, monitoring and therapeutics. A comprehensive review. EMBO Mol Med.

O'Connell, R.M., Rao, D.S., Chaudhuri, A.A., and Baltimore, D. (2010). Physiological and pathological roles for microRNAs in the immune system. Nat Rev Immunol *10*, 111-122.

Xia, Q.S., Ishigaki, Y., Sun, L., Chen, R., and Motoo, Y. (2010). [Effect of anti-cancer drugs on the expression of BIC/miR-155 in human pancreatic cancer PANC-1 cells]. Zhonghua Yi Xue Za Zhi *90*, 123-127.

# Publications

**Zonari E**, Pucci F., Saini M., Mazzieri R., Politi L., Gentner B., and Naldini L.
A role of miR-155 in enabling tumor-infiltrating innate immune cells to mount effective anti-tumor responses. *Manuscript in preparation.*

Mazzieri R*, Pucci F*, Moi D, **Zonari E**, Ranghetti A, Berti A, Politi LS, Gentner B, Brown JL, Naldini L, De Palma M.
Targeting the Angiopoietin-2/TIE2 axis inhibits tumor progression and metastasis by impairing angiogenesis and disabling rebounds of pro-angiogenic myeloid cells. **Cancer Cell. 2011** Apr 12;19(4):512-26. Cited: 10.

De Palma M*, Mazzieri R*, Politi LS, Pucci F, **Zonari E**, Sitia G, Mazzoleni S, Moi D, Venneri MA, Indraccolo S, Falini A, Guidotti LG, Galli R, Naldini L.
Tumor-targeted interferon-alpha delivery by Tie2-expressing monocytes inhibits tumor growth and metastasis. **Cancer Cell. 2008** Oct 7;14(4):299-311. Cited: 58.

Venneri MA, De Palma M, Ponzoni M, Pucci F, Scielzo C, **Zonari E**, Mazzieri R, Doglioni C, Naldini L.
Identification of proangiogenic TIE2-expressing monocytes (TEMs) in human peripheral blood and cancer. **Blood. 2007** Jun 15;109(12):5276-85. Cited: 104.

R. Mazzieri*, F. Furlan*, S. D'Alessio, **E. Zonari**, F. Talotta, P. Verde and F. Blasi "A direct link between expression of urokinase plasminogen activator receptor, growth rate and oncogenic transformation in mouse embryonic fibroblasts" **Oncogene. 2007**, 26 (5) 725-32. Cited: 7

# Acknowledgments

First, I thank Prof. Luigi Naldini, director of the Telethon Institute for Gene Therapy (TIGET), for giving me the opportunity to do my PhD in his excellent laboratory, where I have been involved in very interesting and challenging projects.

Chronologically, I express my gratitude to Roberta Mazzieri, for teaching me how to work accurately and for always believing in me; Michele De Palma and Bernhard Gentner, whose expertise and understanding added considerably to my experience. I appreciated all their contributions of time, ideas, and funding to make my Ph.D. experience productive and stimulating. Thank you for contributing to my professional growth.

I cannot forget all the collaborators who participated in the miRNA project: Massimo Saini performed Western blot and phosphoflow analysis; Giulia Schira helped with HS/PC transplantation; Ferdinando Pucci helped with TaqMan array, cell sorting and discussion of the work and for his friendship.

Special thank to Alice, not only for BMT but also for her discretion, her support, her peculiar sympathy and for her friendship that although recent I do hope will be present in my future.

I would also like to thank all the people working in the Angiogenesis unit, my first home, in particular Daniela for all the times that she said “my room is your home” and Mario for unforgettable fights. Thanks also to Davide, Silvia and Mary.

My sincere gratitude also goes to all the people in the lab in particular Lucia for her helpfulness, Alessio, Tiziano, Francesco, Daniela C, Marco and all other people. Thanks also to Matteo for informatics support and for daily smile. Luca Libelli for the kindness and helpfulness. I acknowledge a 3 years fellowship from FIRC.

I thank all those people I met on my path, who have shared moments with me, who have taught me important things to grow and improve.

Last but not least, I thank my family for all their love and encouragement. My parents, Albano and Mary, who encouraged me and let me do what I most like. Big hug to my nephew, Sofia, who has eased last months of my life.

And most of all, my faithful, encouraging, loving and patient husband Rocco, for supporting me during the final stages of my Ph.D. and for the last 7 years spent together. Thank you!

*"...Your time is limited, so don't waste it living someone else's life. Don't be trapped by dogma — which is living with the results of other people's thinking. Don't let the noise of others' opinions drown out your own inner voice. And most important, have the courage to follow your heart and intuition. They somehow already know what you truly want to become. Everything else is secondary."*

*Steve Jobs*